Development of Techniques and Applications for CIL LC-MS Based Sweat Metabolomics

By

Kevin Hooton

A thesis submitted in partial fulfillment of the requirements for the degree of

Master of Science

Department of Chemistry

University of Alberta

Abstract

The most often used biofluids in metabolomics and disease biomarker discovery studies in the literature include urine, processed blood (serum or plasma), and cerebral spinal fluid. While investigations using these biofluids have led to numerous innovations in the field of metabolomics, little attention has been given to the possible clinical relevance of sweat. Very few studies have attempted to perform global sweat metabolomics with high sensitivity, coverage, and accurate quantification. The goal of this thesis work was to develop robust, sensitive, and accurate analytical workflows to use sweat in CIL LC-MS global metabolomics.

In Chapter 2, we profiled the metabolome of pure liquid sweat collected using an occlusive style sweat patch during 3 time points of moderate to intense exercise. Over 2707 unique metabolites were detected across 54 sweat samples collected from six individuals. We were able to positively identify 83 metabolites using a dansyl standard library, many of them never being reported as a part of the sweat metabolome. We observed significant metabolome differences in early vs. late exercise sweat samples, as well as between genders. This study demonstrated that CIL LC-MS can be used to detect metabolic changes in the sweat metabolome between comparative samples, justifying the use of sweat for future quantitative metabolomics research.

Chapter 3 describes an improved sweat metabolomics workflow that uses sweat collected using a non-occlusive patch. After analyzing sweat samples collected from forearm, neck, and lower back areas, a total of 3140 sweat metabolites were detected across 342 LC-MS runs with 84 metabolites positively identified using a dansyl standard library. We see a location dependence characteristic of sweat composition, as well as significant metabolome differences between male

and female sweat. This work showed the applicability of non-occlusive sample collection and CIL-LC-MS to study phenotypic differences as well as mapping locations on the skin.

Chapter 4 demonstrates the use of non-occlusive sweat collection combined with CIL LC-MS to study lymphedema in a real world clinical application. Sweat was collected from diseased and healthy areas of lymphedema patients, and preliminary data revealed metabolome differences between these collection areas which were not present in the same areas of healthy individuals. This project is currently being expanded to include more lymphedema patients in order to confirm the sweat metabolome trends observed.

Preface

Chapter 2 was published as "Comprehensive and Quantitative Profiling of the Human Sweat Submetabolome Using High-performance Chemical Isotope Labeling LC-MS" Hooton, K.; Han, W.; Li, L. *Anal. Chem.* **2016**, 88, 7378– 7386. My mentor, Wei Han, assisted me early on in this project with my experimental technique and provided valuable advice through the data processing portion of this work. Professor Liang Li contributed to the project design, concept discussion, and editing the manuscript.

Chapter 3 was published as "Non-occlusive Sweat Collection Combined with Chemical Isotope Labeling LC-MS for Human Sweat Metabolomics and Mapping the Sweat Metabolomes at Different Skin Locations" Hooton, K.; Li, L. *Anal. Chem*, **2017**, 89, 7847-7851. I designed and tested the non-occlusive sweat patch, collected the samples, performed all experimental work, processed and analyzed the data. Professor Liang Li contributed to the project design, concept discussion, and editing the manuscript.

Chapter 4 was done in collaboration with Ian Soles, President of the Salutaris Centre for Lymphatic and Massage Therapy. Patient volunteers who graciously donated their sweat for this study were clients of the Salutaris Centre. I collected the samples, performed all experimental work, processed and analyzed the data. Ian Soles recruited all of the patient volunteers for this study. Professor Liang Li contributed to the project design, concept discussion, and editing the manuscript.

All supplementary information referred to in these chapters are stored at Professor Liang Li's laboratory and are available from Professor Liang Li. This includes supplemental text, supplemental figures, and supplemental tables.

Acknowledgements

Table of Contents

List of Tables

List of Figures

List of Abbreviations

ACN   Acetonitrile

APCI   Atmospheric pressure chemical ionization

CF   Cystic fibrosis

CFTR   Cystic fibrosis transmembrane conductance regulator

CIL   Chemical isotope labeling

cm   Centimeter

CSF   Cerebral spinal fluid

CSV   Comma separated value

Da   Dalton

DmPa   p-dimethylaminophenacyl

DnsCl   Dansyl chloride

DnsID   Dansyl identification library

EI   Electron ionization

EML   Evidence based metabolome library

ESI   Electrospray ionization

FC   Fold change

FT-ICR   Fourier transform ion cyclotron resonance

GC/MS	Gas chromatography mass spectrometry
H_2O	Water
HMDB	Human metabolome database
HPLC	High performance liquid chromatography
h	Hours
ID	Identification
in.	Inches
IPA	Isopropyl alcohol
L	Liters
LC	Liquid chromatography
LC-MS	Liquid chromatography mass spectrometry
LC-UV	Liquid chromatography ultra violet
M	Molarity (mols/litre)
MALDI	Matrix assisted laser desorption ionization
MCID	MyCompoundID
MeOH	Methanol
min	Minutes
mM	Millimolar (millimols/litre)

mm	Millimeters
mL	Millilitres
MS	Mass spectrometry
MS/MS	Tandem mass spectrometry
nmol	Nanomols
NMR	Nuclear magnetic resonance
PCA	Principal component analysis
PDA	Photodiode array
PLS-DA	Partial least squares discriminant analysis
ppm	Parts per million
Q-TOF	Quadrupole time-of-flight
rpm	revolutions per minute
s	seconds
UPLC	Ultra performance liquid chromatography
UV	Ultra Violet
VOC	Volatile organic compoind

List of Symbols

°C	Degree centigrade
m/z	Mass to charge ratio
S/N	Signal to noise ratio
T1	Time 1 (10-20 minutes of exercise)
T2	Time 2 (20-30 minutes of exercise)
T3	Time 3 (30-40 minutes of exercise)
μL	Microliter
μm	Micron
v/v	Volume per volume

Chapter 1: Introduction

1.1 Mass Spectrometry Instrumentation

A mass spectrometer is an analytical instrument that measures the masses of ions in a sample of interest. The basic components of a mass spectrometer include sample introduction, ionization method, mass analyzer, and ion detector. Ionization methods are used to transform the molecules in a sample into ions. These ions are then introduced into the mass analyzer, where they are manipulated using electromagnetic fields so their mass to charge ratio (m/z) can be measured. Common ionization methods include Electron Ionization (EI), Electrospray Ionization (ESI), Atmospheric Pressure Chemical Ionization (APCI), and Matrix Assisted Laser Desorption Ionization (MALDI). Common mass analyzers include Quadrupole Time-of-Flight (Q-TOF), Fourier Transform Ion Cyclotron Resonance (FT-ICR), Triple Quadupole, and Ion Trap. Mass spectrometry (MS) is a versatile analytical tool that is applicable to all chemical research that requires identity confirmation, structural elucidation, and quantification of both small (MW < 1000 Da) and large molecules.[1]

Separation techniques such as liquid chromatography (LC) can be coupled to MS in order to analyze biological samples with complex matrices. This coupling is commonly referred to as LC-MS. In global metabolomics studies, LC separation is required before sample introduction into the mass spectrometer in order to generate maximum metabolome coverage and mitigate ionization suppression. Downstream from LC separation, an ESI source coupled to a Q-TOF mass analyzer is a common mass spectrometer configuration for studying metabolomics. Reasons for this include the soft ionization capabilities of ESI, combined with the high resolution and mass spectral recording speed of a Q-TOF. ESI is considered a soft ionization method that prevents in-

source fragmentation of molecular ions, which is a crucial feature required to detect fully intact metabolites. The fast spectral recording speed of a Q-TOF mass analyzer allows for the detection of metabolites in lower abundance with very narrow chromatographic peak widths.[1] This configuration is used most often in this thesis work.
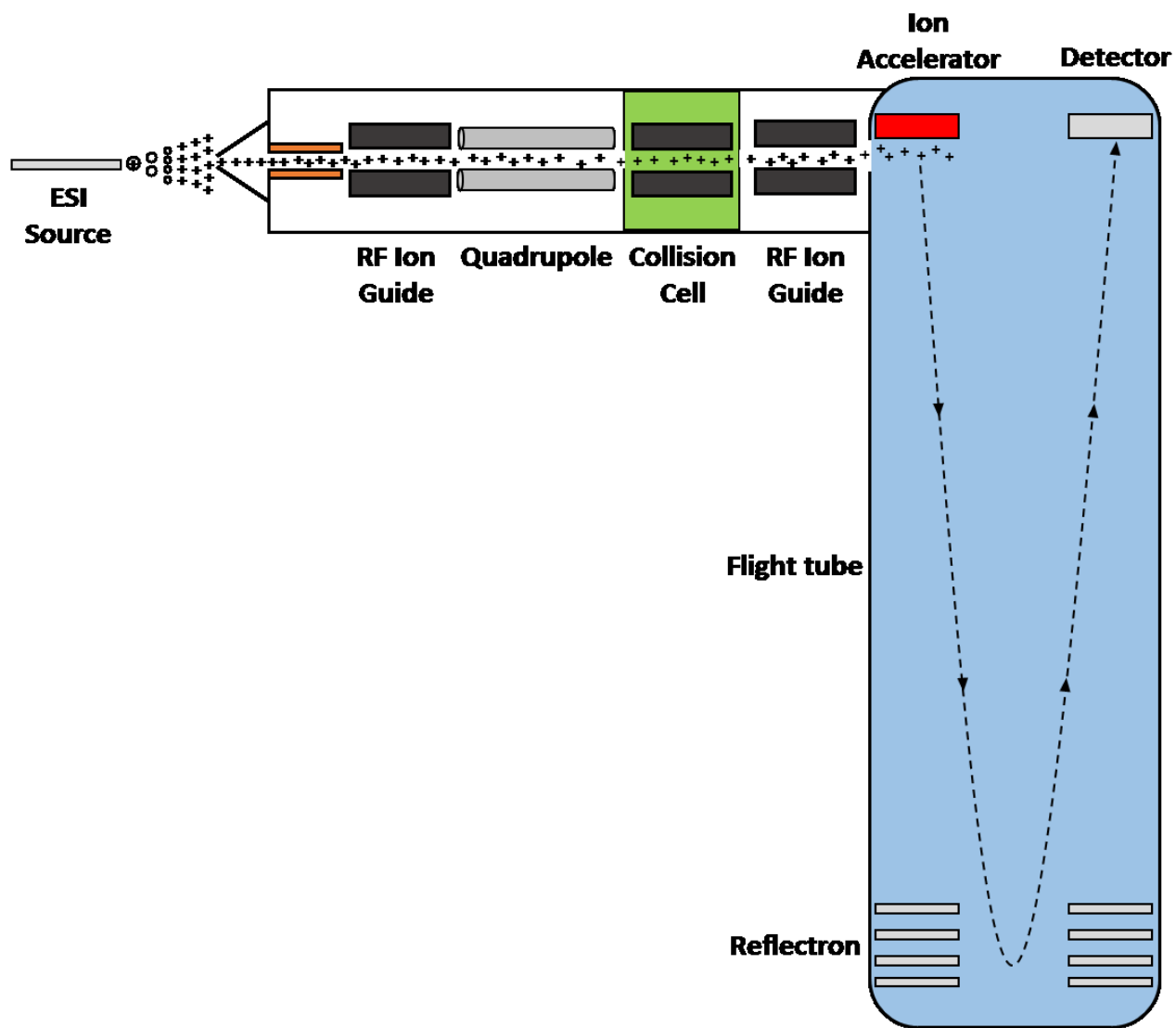
Figure 1.1. Diagram of ESI-QTOF mass spectrometer configuration.

1.2 Metabolomics

Metabolomics uses modern analytical techniques to study small molecules in biological systems. These small molecules are referred to as metabolites, and monitoring their changes in abundance in response to external stimuli can provide clues to metabolic changes occurring in the host.[2] Comparing the metabolite composition of biofluids collected from diseased groups and healthy groups may reveal unique metabolites or metabolite levels that are characteristic for a particular disease, known as biomarkers. MS is often used for disease biomarker discovery due to its high sensitivity, allowing the detection of the low abundance metabolites that may be overlooked by less sensitive techniques like Nuclear Magnetic Resonance (NMR).[3] Examples of metabolites include small molecules, sugars, lipids, and electrolytes. It is estimated that there are >3,500 unique human metabolites compared with the larger number of genes >30,000, however the exact number remains to be definitively determined.[4] The reasoning behind using metabolomics data as an alternative to proteomics, transcriptomics, and genomics data is the presumption that small changes in the transcriptome and resulting proteome may lead to amplified changes in the metabolome as it is more downstream. With amplified changes as well as fewer metabolites to analyze than genes, metabolomics has great potential to become the most promising way to discover disease biomarkers and monitor health states.[5]

Metabolites can be further classified into endogenous and exogenous metabolites. Endogenous metabolites are naturally occurring and are synthesized within the body. They are key components in crucial metabolic processes such as the citric acid cycle, amino acid synthesis, and lipid synthesis to name a few. Exogenous metabolites are sourced from outside the body though consumption, inhaling, or absorption. These metabolites include various drugs, xenobiotics, and nutrients from food sources.[6] Exogenous metabolites also encompasses the natural metabolic by-

products from these exogenous sources (eg. Theophylline, although not consumed directly, is a metabolic byproduct of caffeine metabolism and is considered an exogenous metabolite).[7] The Human Metabolome Database (HMDB) contains a growing list of endogenous metabolites, drugs, and food compounds that can be found in the human body.[8] This database freely accessible (http://www.hmdb.ca/) and is often used in this thesis to putatively identify metabolites based on accurate mass.

1.3 Targeted and Untargeted Profiling

There are two different conceptual approaches to metabolomics which include targeted and untargeted (global). Target metabolomics involves quantifying and monitoring one or a select few known metabolites that are involved in a particular pathway of interest. This type of metabolomics is most common in the clinical laboratory tests when monitoring a particular disease state. Untargeted or global metabolomics involves profiling all metabolites, both known and unknown, in order to discover interesting metabolites that may be related to a particular disease state. Untargeted metabolomics is most common in disease biomarker discovery investigations, where the researchers are initially unaware of what metabolites may be implicated in the disease being studied. By profiling the entire metabolome, researchers increase their odds of finding metabolites with significant changes between diseased and healthy samples.[5] In global metabolomics, researchers aim to discover a "metabolic fingerprint" consistent with a particular disease state. Once this "diseased fingerprint" has been discovered, individual metabolites that differentiate this fingerprint from a "healthy fingerprint" can be elucidated and their biological relevance can be further investigated.

1.4 Chemical Isotope Labeling Metabolomics

Chemical isotope labeling (CIL) metabolomics involves utilizing a stable isotope labeling reagent in order to introduce a "tag" into a class of biological compounds with particular functional groups. CIL can improve the metabolome coverage, sensitivity, and quantification capabilities of metabolomics workflows depending on the type of chemical reagent used. To perform CIL, a biological sample may be labeled with the stable isotope reagent containing deuterium (^{2}H) or carbon thirteen (^{13}C) isotopes to introduce a "heavy" tag, or hydrogen (^{1}H) or carbon twelve (^{12}C) for a "light" tag. By labeling comparative samples with a light tag, a pooled standard with a heavy tag, then mixing heavy and light tagged samples in equal molar amounts, it is possible compare relative concentrations of individual metabolites between comparative samples by comparing the relative signal intensities of the "light" peaks compared to the "heavy" peaks.

The Li group uses dansyl-chloride[9], ρ-dimethylaminophenacyl (DmPA) bromide[10], and dansyl-hydrazine[11], in order to target multiple sub-metabolomes in a "divide and conquer" approach. These high-performance labeling reagents have many advantages over other standard labeling reagents that only improve quantification capabilities using light and heavy tags. Along with light and heavy isotope capabilities, the Li group labeling reagents each contain a hydrophobic benzyl group that improves separation with reverse phase liquid chromatography and a tertiary amine group that improves ionization efficiency in positive-ion mode LC-MS.

1.5 Metabolite Identification

In disease biomarker discovery studies, the first step is to discover metabolites with significant differences in signal between comparative samples. Once these features are discovered the next step is to positively identify them with high confidence, which is crucial to understanding

the biological relevance of the metabolite within a disease pathway. MS is often used for disease biomarker discovery due to its high sensitivity, allowing the detection of the low abundance metabolites that may be overlooked by less sensitive techniques like NMR.[3] The advantage of using NMR is its capability to elucidate molecular connectivity, making it easier to positively identify individual metabolites. MS is capable of structural elucidation as long as the appropriate standards are available. An unknown metabolite must be matched to a previously analyzed standard using an MS/MS spectrum, accurate mass, and retention time. Confidence of the identification is increased as each of these three characteristics of the metabolite is matched to the library values.

The Li group uses in-house developed software which is available for free at http://www.mycompoundid.org [12,13] in order to identify metabolites of interest. This library contains accurate mass, retention time, and MS/MS spectral information of 275 dansyl-labeled amine/phenol, 188 DmPA-labeled organic acid, 78 dansyl-labeled aldehyde/ketone, and 85 dansyl-labeled hydroxyl metabolites. In our workflow, features with significant differences between comparative samples are first discovered, then the accurate mass and retention time information of these features are matched to the appropriate library of standards. During this process, retention times of the input features are calibrated to the library of standards based on retention times of amino acid standards.

1.6 The Biology of Sweat

Sweating or "perspiring" is the body's response to heat, stress, or physical exertion in order to regulate internal body temperature. This is accomplished through the continuous secretion of an odourless fluid by eccrine sweat glands, followed by subsequent evaporation and dissipation of excess heat. In periods of prolonged physical exercise or heat stress, failure of this mechanism can

ultimately lead to hyperthermia. There are up to 4.0 million eccrine sweat glands distributed thoughout the entire body except the lips, external ear canal, and female genitalia. The largest density of glands in humans are located on the palms of the hands and the soles of the feet.[14] Sweating is controlled by the hypothalamus which responds changes in core body temperature, physical activity, emotions, and hormones.[15] Although the mechanism of how the brain communicates with the sweat gland is not entirely understood, it is thought that signals from the pre-optic hypothalamus travel to peripheral nerve fibres that are wrapped around the tissue of eccrine sweat glands.[14,16]

Eccrine sweat glands are tubular epithelium systems which contain both a secretory coil portion located within the deep dermis, as well as a dermal duct that connects the coil to the skin's surface. Each gland is a single tubule and ranges from 4-8 mm in length.[17] Sweat secretion begins by the movement of fluid into the secretory coil, which then moves to the skins surface via the duct. As sweat moves from the secretory coil, through the duct and to the skins surface, sodium channels within the duct reabsorb sodium in order to conserve electrolytes. This mechanism of sweating leads to a hypotonic sweat. For eccrine sweat the major neurotransmitter involved is acetylcholine.[17] The composition of eccrine sweat has shown to be influenced by health state, collection location, hydration state, and exercise.[18-22] While eccrine sweat consists of 99% H_2O, smaller amounts of other constituents are present including sodium, chloride, potassium, bicarbonate, lactate, urea, ammonia, glucose, and amino acids.[14]

Apocrine sweat glands differ from eccrine sweat glands in a number of ways. Their location is always associated with hair follicles, and they secrete a viscous, protein-rich fluid containing a number of odorous compounds. Compounds in this thick fluid are further decomposed by bacteria and lead to the strong odours that are typically associated with body odour. These sweat glands

7

appear in largest densities in the auxilla (underarm) and genitals.[14] Unlike eccrine sweat glands whose main responsibility is thermoregulation in response to heat or exercise, apocrine glands respond more to emotional stimuli such as pain, anxiety, sexual arousal, and are considered the pheromone/odour producing glands.

The apoeccrine gland contains features from both apocrine and eccrine sweat glands and were first described in 1987.[23] Like apocrine glands, apoeccrine glands can also be found in the anogenital region. These sweat glands secrete fluid continuously akin to eccrine glands, and since their morphology and secretion method is more similar to eccrine glands it is thought that their sweat compositions are also similar. However, their overall sweat rate is greater than that of eccrine or apocrine glands which suggests they contribute a great amount to sweating.[23]

1.7 Sweat as a Biofluid for Metabolomics Applications

The most common use of sweat as a biological fluid for diagnostic purposes is its use in the chloride test for cystic fibrosis (CF) in newborns. This test uses a sweat collection technique called pilocarpine iontophoresis. The chloride channel cystic fibrosis transmembrane conductance regulator (CFTR) is a major component in the regulation of chloride electrical conductance throughout the body. It is also a highly expressed protein in the reabsorptive duct within the sweat gland. Mutations in the CFTR gene lead to CF, where ductal electrolyte reabsorption in the sweat gland is also impaired leading to high sweat chloride levels.[24,25] This is an example of how ones disease state can alter their sweat metabolome, demonstrating how sweat can possibly be used to monitor an individual's health state for a range of other diseases and conditions. Additionally sweat collection is used to monitor drugs of abuse[26,27] and more recently an indicator test has been developed to detect peripheral neuropathy in diabetic foot sweat.[28]

Besides the previously mentioned targeted metabolomics applications, sweat has overall been overlooked as a potential source of new, lucrative disease biomarkers and metabolites that can monitor one's health state. The lack of sweat metabolomics research can partially be attributed to its relatively low concentration of metabolites compared to urine and blood, and expensive equipment required to achieve sufficient sample amounts (pilocarpine iontophoresis). Lack of standardized sample collection methods also make it difficult to compare and validate results from competing studies.

1.8 Sweat Collection Methods

There are a number of methods for collecting sweat induced through heat or exercise. These methods include total body wash down[29], occlusive[21] and non-occlusive patch[30] methods like the ones used in this thesis, polypropylene copolymer bag and adhesive rubber[31], glass rollers[32], and special pipettes with reverse capillaries to collect sweat droplets from the skin.[32] It is also possible to collect sweat instantaneously using pilocarpine iontophoresis.[33,34] This technique is used in the sweat chloride test for CF in newborns.

The lack of a standardized protocol for collecting sweat is partially due to large variations between individuals in the amounts and location of sweating. For example, it may be possible to collect pure liquid sweat from a subjects who sweats profusely during light exercise by simply pipetting droplets off the skin. In contrast to an individual who does not sweat copious amounts and may require an occlusive or non-occlusive sweat patch, or a newborn who is incapable of undergoing the heat or physical exercise required and requires pilocarpine iontophoresis.

Each of these techniques has their own advantages and disadvantages, and results in either a pure liquid sweat that can be used directly in downstream workflows, or a dried sweat that must

be extracted prior. Occlusive patches, pilocarpine iontophoresis, droplet pipetting, and copolymer bag methods result in the collection of pure liquid sweat. One obvious advantage to collecting a pure liquid sweat is the possibility to perform absolute quantification of the metabolites, a requirement for the sweat chloride test for CF.[35] A disadvantage to occlusive patches, droplet pipetting, and copolymer bag techniques include difficulty in acquiring sufficient amounts of sample from individuals who don't sweat excessively. A disadvantage to pilocarpine ionophoresis is the need for specialized equipment, training, expense, and lack of portability. Non-occlusive patches result in a dried sweat that must be extracted from the patch using an optimal extraction protocol. The glass roller method is a hybrid method that involves rolling the device across the skin and washing the sweat off of the roller. A disadvantage to these two techniques are the difficulties in performing absolute quantification, as one cannot know the volume of sweat collected. However, there are studies that have attempted to normalize sweat volume based on the absolute amounts of particular solutes.[31,36] Advantages to these techniques include the ease and portability of the non-occlusive patch, and their applicability to individuals who don't sweat enough to collect droplets for both methods.

The end goal of this work was to design sweat metabolomics workflows that can be used in future disease biomarker discovery investigations, as well as a feasible clinical diagnostic device that can collect sweat easily with minimal sample preparation and at low cost to the consumer. Methods that require special equipment such as the polypropylene copolymer bag and adhesive rubber, glass rollers, and pilocarpine iontophoresis techniques are ill-suited for our goals. While each technique has its own advantages and disadvantages, occlusive and non-occlusive patch collection methods were chosen for this thesis work due to their low cost, simplicity, and ease of application and removal. It is even possible for individuals to apply, remove, extract, and store

their own sweat samples using a non-occlusive patch. Construction and demonstration of a non-occlusive sweat collection kit to study Lymphedema described in Chapter 4.

1.9 Novel Aspect of Thesis

The objectives of this research is to develop CIL LC-MS based sweat metabolomics workflows using a variety of sweat collection methods. Chapter 2 describes the first time CIL LC-MS has been used to profile the sweat metabolome to detect changes in sweat metabolite levels during different periods of exercise. Pure liquid sweat collected during exercise using an occlusive sweat patch was used for all work in Chapter 2. Chapter 3 describes an improved procedure for collecting sweat using a non-occlusive sweat patch, and describes the method development procedures that went into designing the device. Chapter 4 outlines the use of the non-occlusive sweat patch in a clinical study of lymphedema. A pilot study was first conducted, prompting the development of a non-occlusive sweat patch kit that is being used in an expanded study of lymphedema.

1.10 Literature Cited

1) Dettmer, K.; Aronov, P. A.; Hammock, B. D. *Mass Spectrom. Rev.* **2007**, *26*, 51-78.

2) Courant, F.; Antignac, J. P.; Dervilly-Pinel, G.; Le Bizec, B. *Proteomics* **2014**, *14*, 2369-2388.

3) Mena-Bravo, A.; De Castro, M. L. *J. Pharmaceut. Biomed.* **2014**, *90*, 139-147.

4) Emwas, A.-H. M.; Salek, R. M.; Griffin, J. L.; Merzaban, J. *Metabolomics* **2013**, *9*, 1048-1072.

5) Hussain, J. N.; Mantri, N.; Cohen, M. M. *Clin. Biochem. Rev.* **2017**, *38*, 13.

6) Vulimiri, S. V.; Berger, A.; Sonawane, B. *Mutat. Res. Genet. Toxicol. Environ. Mutagen.* **2011**, *722*, 147-153.

7) Martínez-López, S.; Sarriá, B.; Gómez-Juaristi, M.; Goya, L.; Mateos, R.; Bravo-Clemente, L. *Food Res.Int.* **2014**, *63*, 446-455.

8) Wishart, D. S.; Jewison, T.; Guo, A. C.; Wilson, M.; Knox, C.; Liu, Y.; Djoumbou, Y.; Mandal, R.; Aziat, F.; Dong, E. *Nucleic Acids Res.* **2012**, *41*, D801-D807.

9) Guo, K.; Li, L. *Anal. Chem.* **2009**, *81*, 3919-3932.

10) Guo, K.; Li, L. *Anal. Chem.* **2010**, *82*, 8789-8793.

11) Zhao, S.; Dawe, M.; Guo, K.; Li, L. *Anal. Chem.* **2017**.

12) Huan, T.; Tang, C.; Li, R.; Shi, Y.; Lin, G.; Li, L. *Anal. Chem.* **2015**, *87*, 10619-10626.

13) Li, L.; Li, R.; Zhou, J.; Zuniga, A.; Stanislaus, A. E.; Wu, Y.; Huan, T.; Zheng, J.; Shi, Y.; Wishart, D. S. *Anal. Chem.* **2013**, *85*, 3401-3408.

14) Sato, K.; Kang, W. H.; Saga, K.; Sato, K. T. *J. Am. Acad. Dermatol.* **1989**, *20*, 537-563.

15) Hölzle, E. In *Hyperhidrosis and Botulinum Toxin in Dermatology*; Karger Publishers, 2002, pp 10-22.

16) Uno, H. *J. Invest. Dermatol.* **1977**, *69*, 112-120.

17) Wilke, K.; Martin, A.; Terstegen, L.; Biel, S. *Int. J. Cosmetic Sci.* **2007**, *29*, 169-179.

18) Morgan, R.; Patterson, M.; Nimmo, M. *Acta Physiol.* **2004**, *182*, 37-43.

19) Mitsubayashi, K.; Suzuki, M.; Tamiya, E.; Karube, I. *Anal. Chim. Acta* **1994**, *289*, 27-34.

20) Patterson, M. J.; Galloway, S. D.; Nimmo, M. A. *Exp. Physiol.* **2000**, *85*, 869-875.

21) Hooton, K.; Han, W.; Li, L. *Anal. Chem.* **2016**, *88*, 7378-7386.

22) Hooton, K.; Li, L. *Anal. Chem.* **2017**.

23) Sato, K.; Leidal, R.; Sato, F. *Am. J. Physiol-Reg. I.* **1987**, *252*, R166-R180.

24) Ready, M.; Quinton, P. *J. Membrane Biol.* **1994**, *140*, 57-67.

25) LeGrys, V. A. *Arch. Pathol. Lab. Med.* **2001**, *125*, 1420-1424.

26) Kintz, P. *Ther. Drug Monit.* **1996**, *18*, 450-455.

27) Huestis, M. A.; Oyler, J. M.; Cone, E. J.; Wstadik, A. T.; Schoendorfer, D.; Joseph, R. E. *J. Chromatogr. B* **1999**, *733*, 247-264.

28) Quattrini, C.; Jeziorska, M.; Tavakoli, M.; Begum, P.; Boulton, A.; Malik, R. *Diabetologia* **2008**, *51*, 1046-1050.

29) Shirreffs, S.; Maughan, R. *J. Appl. Physiol.* **1997**, *82*, 336-341.

30) Jadoon, S.; Karim, S.; Akram, M. R.; Kalsoom Khan, A.; Zia, M. A.; Siddiqi, A. R.; Murtaza, G. *Int. J. Anal. Chem.* **2015**, *2015*.

31) Appenzeller, B. M.; Schummer, C.; Rodrigues, S. B.; Wennig, R. *J. Chromatogr. B* **2007**, *852*, 333-337.

32) Kutyshenko, V. P.; Molchanov, M.; Beskaravayny, P.; Uversky, V. N.; Timchenko, M. A. *PLoS One* **2011**, *6*, e28824.

33) Calderón-Santiago, M.; Priego-Capote, F.; Jurado-Gámez, B.; de Castro, M. L. *J. Chromatogr. A* **2014**, *1333*, 70-78.

34) Calderón-Santiago, M.; Priego-Capote, F.; Turck, N.; Robin, X.; Jurado-Gámez, B.; Sanchez, J. C.; De Castro, M. D. L. *Anal. Bioanal. Chem.* **2015**, *407*, 5381-5392.

35) DeMarco, M. L.; Dietzen, D. J.; Brown, S. M. *Clin. Biochem.* **2015**, *48*, 443-447.

36) Myint, K. T.; Aoshima, K.; Tanaka, S.; Nakamura, T.; Oda, Y. *Anal. Chem.* **2009**, *81*, 1121-1129.

Chapter 2: Comprehensive and Quantitative Profiling of the Human Sweat Submetabolome Using High-Performance Chemical Isotope Labeling LC-MS

2.1 Introduction

Sweat is a colorless, hypotonic biofluid produced by both eccrine and aprocrine sweat glands in the epidermis. Its main function is the thermoregulation of internal body temperature through evaporative cooling in response to heat or physical exercise. The main constituents of sweat include water, electrolytes (sodium, potassium, and chloride), urea, pyruvate, lactate, and amino acids; but other molecules such as proteins, peptides, drugs, and other xenobiotics can also be detected.[1] It has been shown that the eccrine sweat proteome is significantly different than the serum proteome, suggesting that sweat components are not simply a diffused fluid from the plasma but may be representative of surround[1]ing tissues and cellular processes.[2] Thus, sweat can serve as another important biofluid for omics-based biomarker discovery research. Since the majority of sweat constituents are small molecules (<1000 Da), it is a prime candidate for metabolomics applications.[3] Currently, human urine and blood, as well as cerebrospinal fluid (CSF) and saliva, are more commonly used for metabolomics. Compared to collecting these biofluids, sweat sampling is attractive because it is a noninvasive procedure that can be conveniently collected on regular intervals or on a continuous basis.[4] For example, wearable sensors for monitoring a few sweat components (glucose, pH, Na, and K) have been recently reported.[5] Since there are a total of 1.6–4.0 million sweat glands located on the majority of the epidermis,[6] sweat has enormous potential to become the perfect source of biomarkers for imaging the body's surface.

Sweat is already used as a clinical sample in a test for sweat chloride concentration to aid in the diagnosis of cystic fibrosis.[7] Certain drugs in sweat are detectable by mass spectrometry (MS), and sweat drug testing provides an alternative or complementary means of detecting substance abuse.[8] Despite these applications, this biofluid has been overlooked as a biospecimen in most clinical analysis due to low concentration of endogenous metabolites and lack of research relating pathological states to sweat metabolite composition. However, with recent advances in the development of sensitive analytical techniques for metabolite detection, metabolomic profiling of sweat may provide a means of searching for potential biomarkers of health state using sweat samples. Indeed, a few studies of profiling sweat metabolites using NMR,[9,10] gas chromatography mass spectrometry (GC/MS),[11, 12] and electrospray ionization (ESI)-MS, or liquid chromatography–mass spectrometry (LC–MS)[13-15] have been reported. However, the overall metabolite coverage with current techniques is low (i.e., tens of metabolites detectable).[3] In a related work, GC/MS analysis of volatile organic compounds (VOC) collected from human skin including sweat[16] from 200 individuals detected a combined list of 373 peaks.[17] Aside from limited coverage, due to large variations of total metabolite concentrations in sweat, sample amount normalization is a major challenge for quantitative metabolomic profiling of individual sweat samples.

We report a sensitive LC–MS workflow for human sweat metabolomics with high coverage. Our method is based on the high-performance chemical isotope labeling (CIL) LC–MS platform for quantitative and in-depth submetabolome profiling.[18-21] High-performance CIL uses rationally designed labeling reagents to modify the metabolite's chemical and physical properties to such an extent that simultaneous improvement in separation, ionization, and quantification can be achieved in LC–MS. For example, 12C- and 13C-dansyl labeling LC–MS can be used for

relative quantification of the amine/phenol submetabolome with high sensitivity.[18] This labeling technique has been applied to metabolomics studies using serum, CSF,[22] urine,[23] saliva,[24] and human feces.[25] In a recent study comparing the number of metabolites detectable by nanoflow LC–MS and microflow LC–MS, human urine and sweat droplets were used as testing samples.[26] In this report, the entire workflow for human sweat metabolomics is described and the analytical performance of this method is demonstrated in metabolomic profiling of sweat samples collected at different time points during exercise. It is shown that a large number of metabolites could be readily profiled using CIL LC–MS. Thus, sweat can be used as an important biofluid for comprehensive and quantitative metabolomics research.

2.2 Experimental
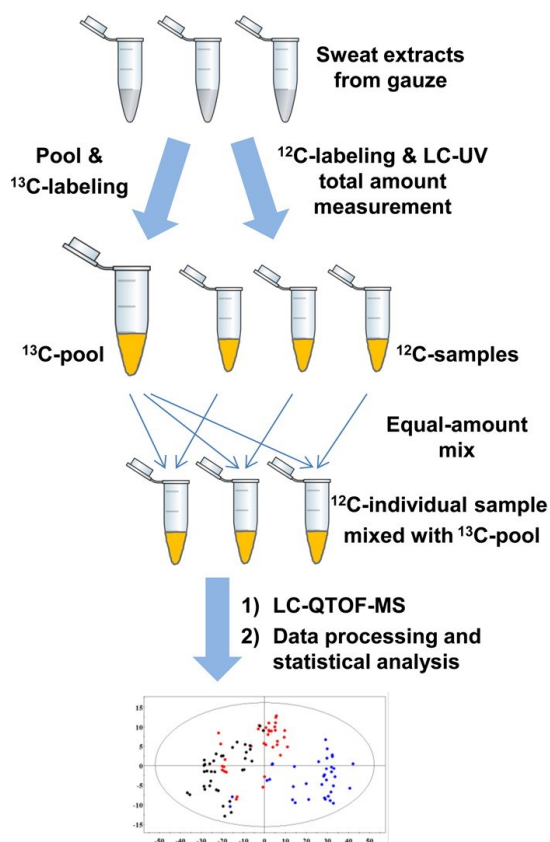
Figure 2.1. Workflow for sweat metabolomics using a high performance CIL LC-MS method.

16

2.2.1 Sweat Sample Collection and Extraction

A total of 54 sweat samples were collected from both men (n = 3) and women (n = 3) with ethics approval from the University of Alberta. Volunteers were instructed to refrain from consuming alcohol 24 h prior and coffee the day of sweat collection. Samples were obtained on three separate days from each volunteer. On each day, sweat was collected from the proximal forearm for 10 min during three separate time periods of moderate to intense exercise using a patch method.[27] To collect the sweat, a gauze sponge sweat patch was constructed in-house and utilized. The proximal forearm collection area was first cleansed with 70% isopropyl alcohol and distilled water, followed by the application of a 10-layer, 5 cm × 5 cm gauze pad (Safe Cross First Aid Ltd.); no cleansing was done between time intervals. Gauze was covered with a Teflon sheet (13/1000 in.), previously cleansed by sonicating in a mixture of organic solvents composed of acetonitrile, methanol, isopropyl alcohol, and water, and secured with medical tape. Commercial plastic wrap (Glad Cling Wrap) was wrapped around the forearm to prevent lifting of the tape. This was found to be an optimal method for collecting pure sweat, as the use of the Teflon sheet shortens the time that sweat is exposed to the air during exercise, thereby minimizing environmental contamination. For method blank, water-spiked gauze was sandwiched between two pieces of Teflon and then attached with the fixation tape.

We note that the use of the occlusive patch for a short period of time during exercise does not cause skin irritation. This simple and inexpensive "classical" method works for this type of application. We could collect droplets of sweat directly, but it is not easy and convenient, as we wanted to collect sweat cumulated over a period time (10–20, 20–30, and 30–40 min) to measure the averaged metabolite level changes in these three periods. Other methods such as using semipermeable patches were not explored in this study. One concern with using semipermeable

17

patches is that any atmospheric chemicals surrounding a patch in a gym or outdoor area might contaminate the sweat collected in the patch. However, using semipermeable patches is likely to be a better option for collecting sweat over a long period of time, as it reduces skin irritation. In the future, we will study the use of this option for sweat collection for metabolomics.

In this study, volunteers were asked to lightly jog around an indoor track for 40 min, and sweat was collected during 10–20 (T1), 20–30 (T2), and 30–40 (T3) min of exercise. Samples were kept on ice until extraction via centrifugation at 14 000 rpm for 10 min. Extracted sweat was stored at −80 °C until dansylation labeling. A total of 54 sweat samples were collected (6 volunteers × 3 time intervals × 3 separate days). A diagram of the sample collection is depicted Appendix Figure A2.1.

2.2.2 Dansylation Labeling

Frozen sweat samples were thawed at 4 °C, vortexed to dissolve precipitates, then centrifuged at 14 000 rpm for 10 min before aliquoting 12.5 μL of sweat for labeling. We did not study how sample freezing could affect the sweat metabolome and could not find any report of such a study, although sample freezing is not an issue for other biospecimens such as urine and serum. Future research of examining the sample storage issue on sweat metabolome is warranted. In this work, the labeling method was adapted from a protocol previously described.[8] Supporting Materials Supplemental Note S1 provides the detailed information on dansylation labeling.

2.2.3 LC–UV Sample Normalization

Sample amount was normalized using a protocol previously described based on LC–UV measurement of the total concentration of dansyl-labeled metabolites in a sample.[28] A Waters ACQUITY UPLC system with photodiode array (PDA) detector was used to quantify the amount

of labeled metabolites in the sweat samples. Labeled sweat was diluted 3-fold, and 4 μL of sample was injected onto a Phenomenex Kinetex C18 column (50 mm × 2.1 mm, 1.7 μm particle size, 100 Å pore size) for a fast step-gradient run to elute out all labeled metabolites together using a high percentage of organic solvent (See Supporting Materials Supplemental Note S1. for running conditions used). The total peak areas of the labeled metabolites measured at 338 nm were used for sample quantification.

2.2.4 LC–QTOF-MS

Labeled sweat samples were analyzed using a Bruker HD Impact quadrupole time-of-flight (QTOF) mass spectrometer (Billerica, MA, U.S.A.) with ESI linked to an Agilent 1100 series HPLC system (Palo Alto, CA, U.S.A.) with an Agilent eclipse plus C18 column (100 mm × 2.1 mm, 1.8 μm particle size). Supporting Materials Supplemental Note S1 provides the experimental conditions used.

2.2.5 Data Processing and Statistical Analysis

After LC–QTOF-MS analysis, entire peak lists were exported from Bruker Data Analysis software with a signal-to-noise threshold of 3. IsoMS software was used for peak-pair picking, peak-pair filtering, and peak-pair intensity ratio calculations.[29] The program eliminates false-positive peaks such as dimers and common adducts. All 108 peak-pair lists were aligned to produce a CSV file highlighting peak pairs shared between samples, as well as their accurate mass, retention time, and peak-pair ratios relative to the control. A zero-fill program developed in-house was used to fill in missing values in the CSV file by searching the raw data file for missed peaks.[30] Peak pairs were reconstructed and their chromatographic peak ratios were determined using IsoMS-Quant (m/z tolerance = 5 ppm, retention time tolerance = 30 s).[31]

Multivariate analysis was conducted using SIMCA-P+ (version 12.0) software. Volcano plots were constructed using Microsoft Excel and OriginPro 8.5 (OriginLab). To calculate the fold change between groups (male vs. female and different exercise times), the average peak-pair ratio of all the injections in one group was calculated, then divided by the average peak-pair ratio of all the injections in the other group. The p-value was calculated using a Student's t test. Peak pairs with a significant fold change had a fold change ≥ 1.5, or ≤ 0.67, with $p \leq 0.05$. The multiple-testing-corrected p-value (q-value) was calculated using R and BioConductor (www.bioconductor.org).[32]

2.2.6 Metabolite Identification

Positive metabolite identification was performed based on mass and retention time match to the dansyl standard library containing 273 unique amines/phenols using DnsID.[33] In our previous publication,[33] we have already shown that the combined information on accurate mass and retention time is sufficient for positive metabolite identification and there is no need of performing or using MS/MS information. Putative metabolite identification was done based on accurate mass match to the metabolites in the human metabolome database (HMDB) (8021 known human endogenous metabolites) and the evidence-based metabolome library (EML) (375 809 predicted human metabolites with one reaction) using MyCompoundID (MCID).[34] The mass accuracy tolerance window was set at 5 ppm for database search.

2.3 Results and Discussion

2.3.1 Sample Amount Normalization

When comparing individual metabolites present in different samples, it is crucial to normalize the total sample amount of these samples before performing metabolomic profiling. Electrolyte concentration in sweat has been found to increase in the event of dehydration compared

to euhydration,[35] and it is possible that the concentration of metabolites may also vary depending on sweat rate and hydration levels. Sample normalization has been considered to be a major challenge in clinical sweat analysis.[8] However, normalizing the total amount of labeled metabolites in sweat samples is possible since dansyl labeling allows for the quantification of labeled metabolites using LC–UV.[28]

We applied the dansylation LC–UV method to quantify the sweat metabolites, and Figure 2.2A shows a representative LC–UV chromatogram. The average concentrations of labeled metabolites in the 10–20, 20–30, and 30–40 min sweat were determined to be 1.25 ± 0.40, 0.60 ± 0.09, and 0.38 ± 0.07 mM, respectively. Thus, there was more than 2-fold increase in concentration of labeled metabolites in sweat collected during early exercise (10–20 min) compared to late exercise (20–30 and 30–40 min). Greater volumes of sweat were obtained in samples collected from later exercise than earlier exercise. Sweat solute concentration was reported to be influenced by sweat rate,[36] which explains why the greater yield of sweat collected during late exercise was more dilute than sweat collected during early exercise. There was also larger variance in labeled metabolite concentration for the 10–20 min samples, compared to the 20–30 and 30–40 min samples (see Figure 2.2B). The larger variance in the 10–20 min sweat could be explained by differences in the fatigue of volunteers in early stages of exercise. During 10–20 min of exercise, some volunteers might experience fatigue more than others, resulting in larger amounts of sweating and more dilute sweat. In later stages of exercise, all volunteers were experiencing heavy fatigue and were sweating at a relatively more consistent rate, resulting in a plateauing of sweat concentration. The large concentration differences found in sweat samples strongly suggest that sample amount normalization is required prior to quantitative metabolomic analysis. Note that, compared to a sample, the peak area of the blank is relatively small (i.e., 3–

7%) (see Figure 2.2, parts A and B), and thus during sample normalization the peak area of a blank was not subtracted.
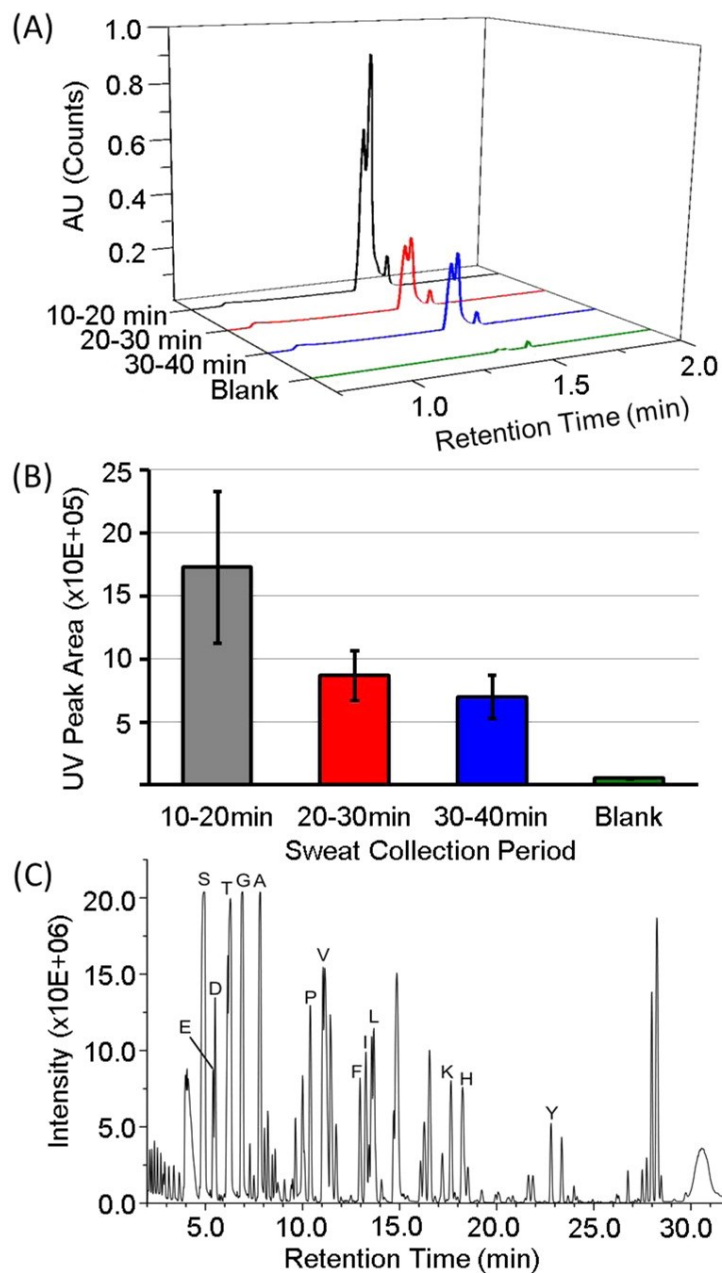
Figure 2.2 (A) Overlaid UV chromatograms of labeled sweat samples collected after 10–20, 20–30, and 30–40 min of exercise and labeled method blank. (B) Average peak areas of labeled sweat collected from all volunteers at different times during exercise and labeled method blank. Error bars represent standard deviation ($N = 36$ for samples and $N = 3$ for blank). (C) LC–MS base-peak chromatogram from a 20 nmol injection of dansyl-labeled sweat. Amino acids are indicated by their single letter code.

2.3.2 Metabolite Detection

In order to demonstrate the performance of the developed method for comparative sweat metabolomics, we analyzed the amine/phenol submetabolome of sweat collected from six volunteers at three different days with three time points during exercise in each day. In total, 108 ^{12}C-/^{13}C-mixtures were analyzed from duplicate ^{12}C-labeling experiments of 54 sweat samples referencing to ^{13}C-labeled sweat pool. Amount of labeled metabolites injected onto the LC–MS can have an effect on the number of metabolites detected in a sample. Therefore, injection amount was first optimized by injecting increasing volumes of a sweat sample with a known concentration of labeled metabolites that was determined using LC–UV. It was found that injecting 20 nmol of labeled metabolites generated the maximum number of peak pairs without sample carryover into subsequent injections; the sample amount was determined from the injection volume and the concentration of labeled sample measured by LC–UV. Thus, all sweat samples were analyzed using LC–MS with 20 nmol injection for each run. Figure 2.2C shows a representative base-peak ion chromatogram of dansyl-labeled sweat.

From the 108 LC–MS runs, a total of 3130 different peak pairs were detected with an average of 2002 ± 165 peak pairs per run. In order to differentiate the peak pairs resulting from the sweat samples and the background peak pairs resulting from the method, a method blank was studied. A new gauze pad of the same style was spiked with a small volume of water, followed by extracting and labeling the water using the same protocol as sweat labeling. The same volume of labeled blank sample (30 μL) as the labeled sample was injected onto the LC–MS for analysis. A total of 423 peak pairs were shared between the sweat samples and the method blank (see Supplemental Table S2.1 for the lists of putatively identified features from the method blanks). While it is possible that some of the 423 peak pairs from the blank may belong to the same

compounds as those of sweat metabolites, we conservatively left all of them out and only counted the remaining pairs, i.e., 2707 unique pairs, as the sweat metabolites.

We note that the process of sweat collection can introduce background chemicals from multiple sources including chemical residuals remaining on the skin after cleaning, the gauze pad, and extraction solvents. We have conducted a separate investigation of the peak pairs detected from a gauze pad without sweat, sweat collected in a gauze pad, and a sweat droplet itself. Sweat collection was conducted on the forehead, instead of forearm, as a sweat droplet can be readily collected from the forehead after exercise. The results are described in Supporting Materials Supplemental Note S2, from which we conclude that the metabolites detected in sweat samples collected in a gauze pad were mainly from sweat (>90%).

2.3.3 Human Sweat Submetabolome

To identify the 2707 peak pairs unique to sweat, a dansyl-library search based on accurate mass and retention time was conducted against 315 entries from 273 unique dansylated metabolite standards. We were able to identify 83 metabolites with high confidence (see Appendix Table A2.1 or Supplemental Table S2.2). Some of these metabolites such as amino acids are the same as those identified in sweat using other techniques.[9-15] We also searched the human metabolites in the HMDB library and the predicted human metabolites with one metabolic reaction in the MCID library using accurate masses of the peak pairs found. We matched 1025 metabolites to HMDB and 1386 metabolites to MCID (Supplemental Table S2.2). Thus, out of the 2707 peak pairs detected, we could match a total of 2494 metabolites (92%). To our knowledge, this is the largest human sweat submetabolome ever reported. Our results indicate that the sweat metabolome is much more diverse than once thought, and its constituents extends past the categories of electrolytes, amino acids, peptides, urea, and pyruvate.[1]

In all LC–MS runs, amino acids generated the strongest peak intensities compared to other metabolites (see Figure 2.2C). All common amino acids except histidine and a large number of dipeptides were also identified in sweat using dansyl-library search. Histidine was identified putatively using HMDB. Although lactate and urea were reported to have high abundance in sweat,[1] they could not be labeled by dansyl chloride due to their lack of primary or secondary amine or phenol group, and thus were not detected in our analysis. Note that the same workflow shown in Figure 2.1 should be applicable to other high-performance CIL experiments targeting different chemical-group-based submetabolomes. For example, *p*-dimethylaminophenacyl bromide (DmPA) has been shown to be useful for profiling the carboxyl acid submetabolome with high coverage.[19] Thus, we envisage that using multiple labeling of sweat will increase the metabolomic coverage even further.

2.3.4 Quantitative Metabolomics

While having high metabolomic coverage is certainly important to ensure that a large number of metabolites are examined, being able to quantify their changes in comparative samples with high accuracy and precision is also critical, particularly for revealing subtle differences. In the CIL LC–MS method, a pooled sample from mixing aliquots of individual sweat samples was labeled with ^{13}C-dansylation, which served as a global internal standard or control for analyzing all the ^{12}C-labeled individual samples (See Figure 2.1). Using the pooled sample as a reference mitigated the matrix effect and ion suppression effect on metabolite detection,[37] as a ^{12}C-labeled metabolite from a sample and its corresponding ^{13}C-labeled counterpart from the pool experienced the same labeling, separation, ionization, and detection processes with constant efficiencies. Thus, the peak ratio of the ^{12}C-/^{13}C-labeled metabolite shown as a peak pair in MS reflected the relative concentration of the metabolite in the sample versus that in the pool. Since all the individual

samples were spiked with the same pooled sample, the peak ratio values of a given metabolite found in all the samples provided the measurement of concentration changes of the metabolites in these samples.

Another important issue in quantitative metabolomics is related to the missing data in the metabolite-intensity table containing sample/metabolite IDs and their corresponding metabolite peak ratios. Missing data can affect the performance of multivariate analysis including principal component analysis (PCA) and partial least squares discriminant analysis (PLS-DA). In our work, we chose a stringent criterion to retain the metabolites for statistical analysis: metabolites must have peak ratio values in at least 80% of the samples in a comparative group. With this criterion, a total of 1262 peak pairs were used for multivariate analysis in comparing the sweat samples collected from males and females, and 1387 peak pairs were used to compare the three exercise intervals. When comparing sweat samples collected between individuals, metabolites must be present in 80% of all the injections. These three comparisons are described below to illustrate that the CIL LC–MS method is useful for quantitative sweat metabolomics.

2.3.5 Metabolomic Comparison of Individuals

Multivariate analysis was performed to compare time-dependent metabolomic changes in a series of samples collected from six individuals; three samples per day for three different days were collected from each individual. Figure 2.3 shows the PLS-DA plot of the metabolomic data set. Overall, higher interindividual variability in the sweat metabolome was observed between subjects, which is consistent with previous studies involving sweat.[10] Sweat collected from individuals cluster together on the plot with $R^2X = 0.869$, $R^2Y = 0.961$, and $Q^2 = 0.931$, despite sample collection on three separate days without any diet control. The model was validated using a permutations test (see Appendix Figure A2.2). This clustering indicates that an individual's

genetics and environment (i.e., microbiome) are stronger determinants than diet on the sweat metabolome profile. Although an extensive study using more subjects and collecting more samples over a larger time frame is still needed to confirm this finding, this finding is not surprising considering that, even in plasma and urine collected from individuals with standardized meals, large interindividual variability of the metabolomes has been observed.[38]
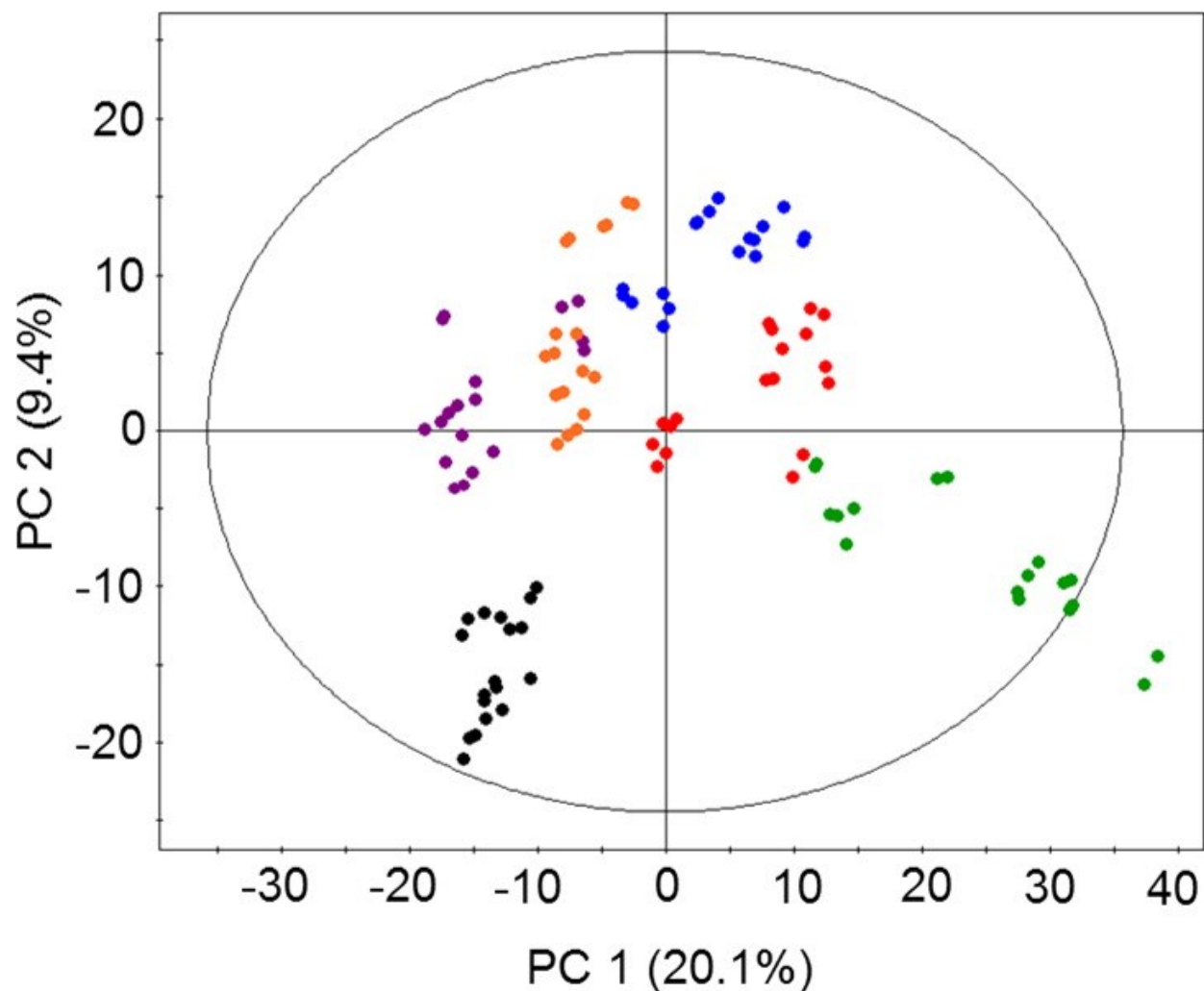
Figure 2.3. PLS-DA plot of sweat samples from different individuals. Each color represents a different individual's sweat. There are 18 data points for each individual (3 samples × 3 days × duplicate labeling). $R^2X = 0.869$, $R^2Y = 0.961$, and $Q^2 = 0.931$.

2.3.6 Metabolomic Comparison of Male and Female

There have been a number of studies investigating the effects of gender on the urine and plasma metabolome using either human or mouse models.[39-43] Studying the effects of gender, along with age, ethnicity, and environment, on the human metabolome can assist in our understanding of the normal physiology of healthy individuals and help eliminate artifacts when conducting disease biomarker discovery investigations. We applied dansylation LC–MS to sweat samples collected from male and female individuals in order to determine whether this method is sufficiently sensitive and quantitative to detect metabolomic differences between genders. Figure 2.4A shows the PCA plot, and a clear separation between male and female sweat is visible on the second principal component. A separation is also observed mainly on the first principal component of the PLS-DA plot shown in Figure 2.4B, with $R^2X = 0.647$, $R^2Y = 0.973$, and $Q^2 = 0.960$. The model was validated using permutations test (see Appendix Figure A2.2).
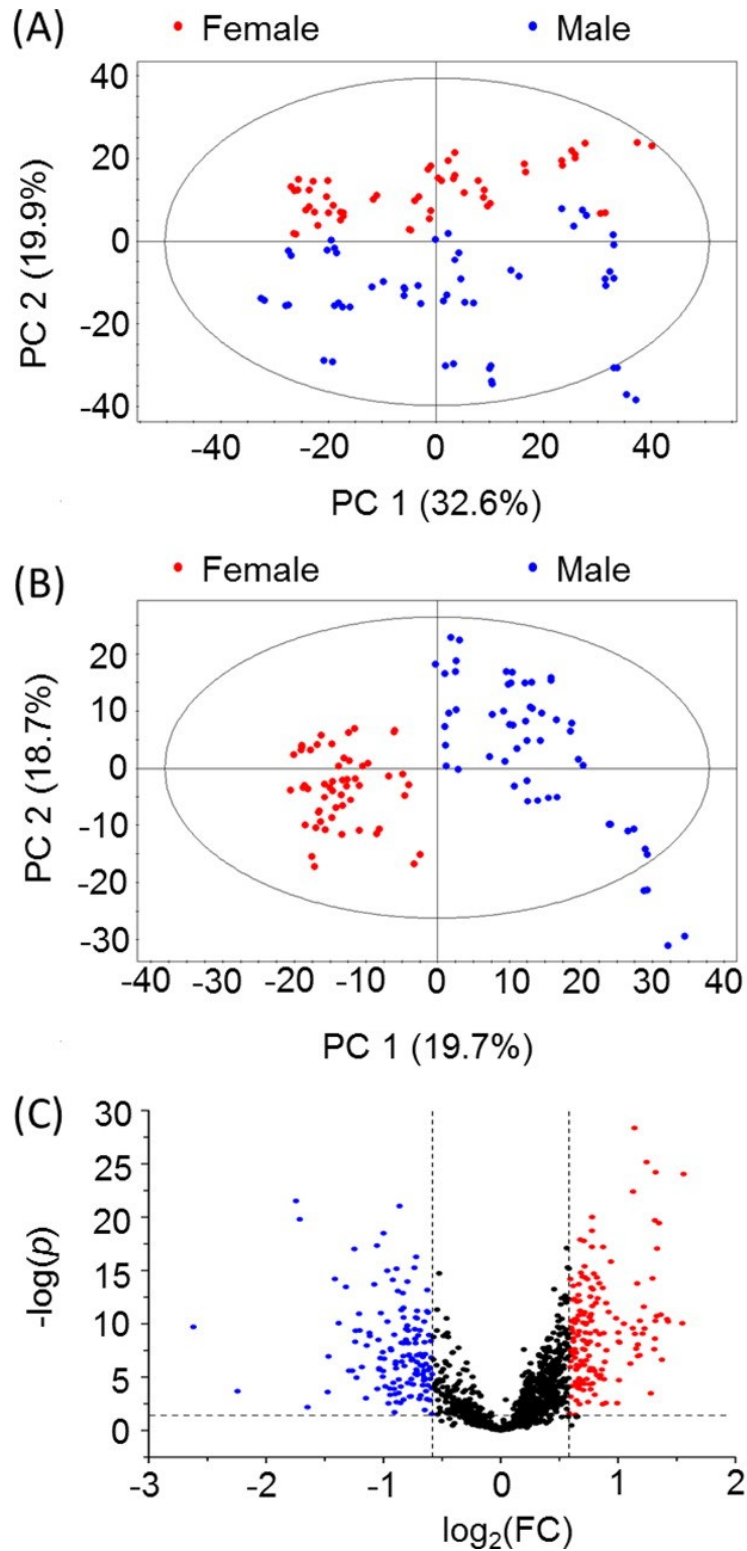
Figure 2.4. (A) PCA plot and (B) PLS-DA plot of sweat samples from males and females ($R^2X =$ 0.647, $R^2Y = 0.973$, and $Q^2 = 0.960$). (C) Volcano plot with highlighted features fitting the criteria of $0.67 \geq$ fold change (FC) ≥ 1.5 and $p \leq 0.05$.

The same data set was also subjected to univariate analysis to determine the significant metabolites that contribute to the separation between male and female sweat. In Figure 2.4C, a volcano plot highlights the significant metabolites with a fold change of ≥ 1.5 or ≤ 0.67 and a p-value ≤ 0.05. In total, 161 peak pairs had an increase in concentration and 142 peak pairs had a decrease in concentration in females compared to males. Among the 303 significant peak pairs, 14 of them were positively identified using the dansyl standard library (Appendix Table A2.2), and 276 were putatively identified using accurate mass search against the HMDB and MCID libraries (See Supplemental Table S2.3 for the lists). To gauge the false discovery rate, q-values were calculated for 1262 differentiating metabolites (Supplemental Table S2.4). Using a cutoff of $p < 0.05$, before multiple-testing correction, we expect a total number of 63 false positives with a $p < 0.05$. There should be far less false positives in the volcano plot since we also have the fold-change filter to determine the significant metabolites. The corresponding q-value for $p = 0.049907$ was 0.012406, meaning that 1.24% of metabolites with $p < 0.05$ were likely false positives. Thus, the false discovery rate in this comparison is low.

Because there is no report of quantitative sweat metabolomics with this high coverage, direct comparison of our results to other sweat analyses could not be made. However, some of the metabolic changes found in our work are worth noting to indicate that sweat metabolomics is a largely untapped research field and our method allows investigating the sweat metabolome for biological and biomarker research. For example, previous research has shown an increase in hydroxyphenyllactic acid in male serum,[43] which is consistent with what we observed in male sweat. The L-form of this compound is found in higher concentrations in the urine and CSF of patients exhibiting phenylketonuria and tyrosinemia, while the D-form is only produced by bacteria and is found in patients with abnormal gut microbiota.[44] To our knowledge, this is the first instance

of hydroxyphenyllactic acid being positively identified in human sweat, and this finding may encourage future work on discovering noninvasive biomarkers in sweat to aid in diagnosing these diseases. While some of the metabolites can be readily measured in blood test (e.g., for determining phenylketonuria), one could use sweat as an alternative media for measuring these metabolites if the levels of these metabolites need to be monitored over a period of time. Multiple sample collections is in favor of sweat, as it is more convenient and less stress and risk to collect sweat than blood.

Another example is on the observation of a 1.57-fold change for 6-hydroxynicotinic acid whose identity was confirmed using the dansyl standard library in female sweat compared to male sweat. This compound has been previously identified in rat and human urine after oral administration of nicotinic acid.[45, 46] The metabolite is supposedly a downstream metabolite of nicotinic acid metabolism in *Pseudomonas aeruginosa*, and is used to identify *P. aeruginosa* in urinary tract infections.[47] *P. aeruginosa* is common bacteria of the natural human microbiome, and these results may be a reflection of female microbial flora compared to male. Although it is well-known that the gut microbiome strongly influences the host's metabolic phenotype,[48, 49] to our knowledge, no studies have observed a significant gender difference in *P. aeruginosa* abundance. Future research in this direction, including direct analysis of microbes to determine the extent of microbe metabolite contribution to the human sweat metabolome, is warranted.

A third example is on the decreased levels of theophylline found in female sweat compared to male. Theophylline, whose identity was confirmed using the dansyl standard library, is a metabolic byproduct of caffeine, which accounts for $3.7 \pm 1.3\%$ of caffeine demethylation.[50] It can also be demethylated by Cyp1A2, an enzyme with higher activity in men than in women.[51] The decreased level of theophylline in females may indicate lower levels of enzyme activities in

females compared to males. It might also be possible that the females in this study consumed less caffeinated beverages by chance than the males. A large population-based study of sweat, in conjunction with other biospecimens such as blood, should be able to answer these questions.

The above results show that sweat metabolome differences between genders can be observed using dansylation LC–MS. Future work of using a larger sample size is needed to investigate and compare the sweat metabolomes of healthy individuals as baseline information for disease biomarker discovery research.

2.3.7 Metabolomic Comparison of Different Exercise Times

We envisage that quantitative sweat metabolomics with high coverage will play an important role in studying the relationship between exercise and human health; sweat can be readily collected during exercise. We were curious as to whether our method can be used to differentiate sweat collected during early exercise and late exercise. We thus compared sweat collected during 10–20 min (T1, early), 20–30 min (T2, middle), and 30–40 min (T3, late) of exercise and the results are shown in Figure 2.5. The PCA plot (Figure 2.5A) shows a gradual separation from early, middle, and late exercise. The PLS-DA plot (Figure 2.5B) shows a clear separation between the early and late exercise, but the separation between the middle and late exercise is not as clear ($R^2X = 0.865$, $R^2Y = 0.978$, $Q^2 = 0.701$). The model was validated using a permutations test (see Appendix Figure A2.2).
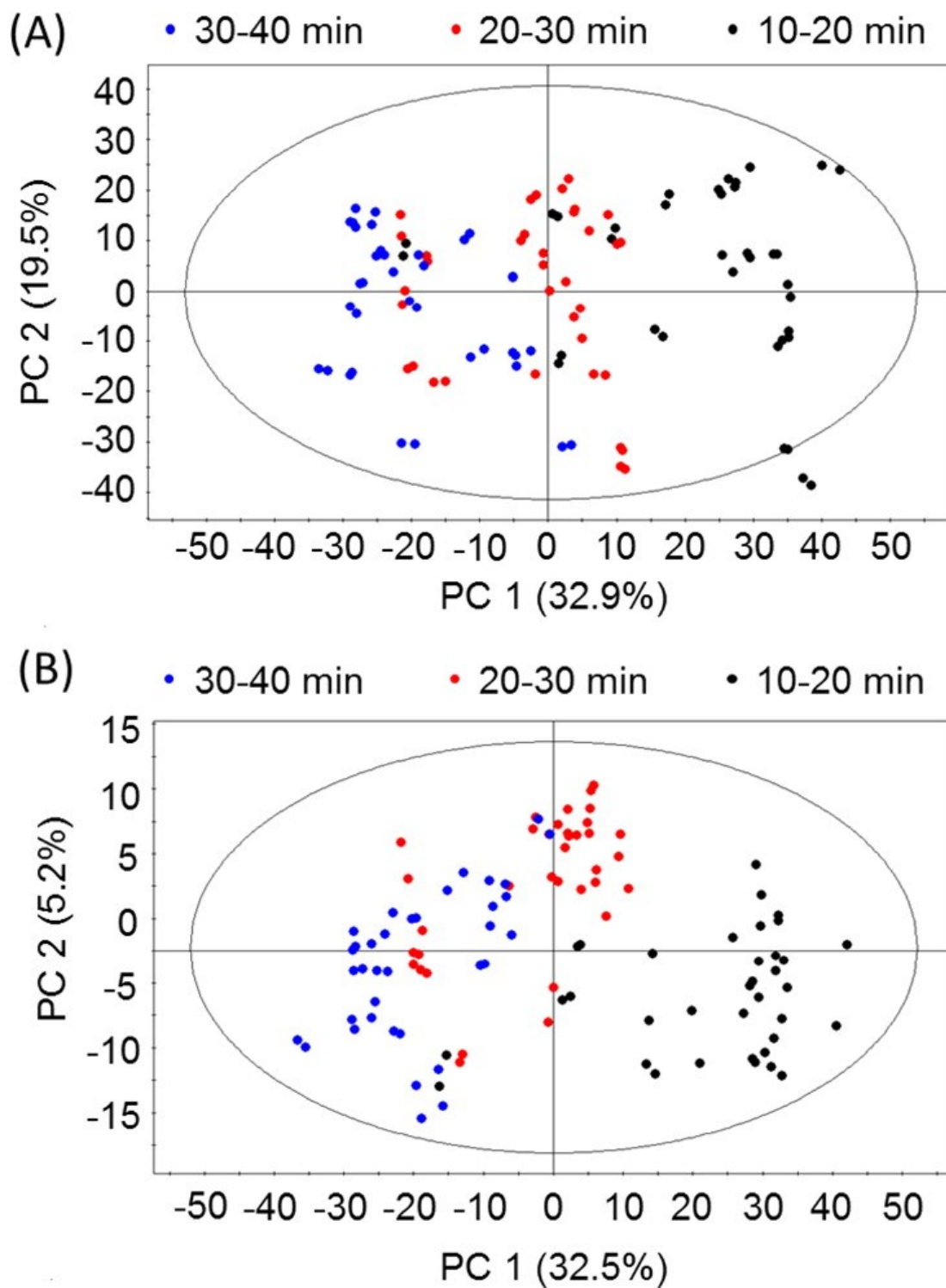
Figure 2.5. (A) PCA plot and (B) PLS-DA plots of sweat samples collected after different exercise times ($R^2X = 0.865$, $R^2Y = 0.978$, $Q^2 = 0.701$).

Univariate analyses were also performed on the same data set. Volcano plots (Figure 2.6) compare the metabolite composition of sweat collected during different periods of exercise. Significant metabolites with a fold change of ≥ 1.5 or ≤ 0.67 and p-value ≤ 0.05 are highlighted. When comparing the composition of T1 versus T2, 160 metabolites had an increase in concentration and 99 had a decrease in concentration in T2. When comparing the composition of T2 versus T3, only 31 metabolites had a decrease in concentration in T3. When comparing the composition of T1 versus T3, 299 metabolites had an increase in concentration and 411 had a decrease in concentration in T3. Of the 717 significant metabolites detected, 99% of them were detected when comparing T1 versus T3. To gauge the false discovery rate, q-values of 1387 metabolites were calculated (Supplemental Table S2.5). Using a cutoff of $p < 0.05$, before multiple-testing correction, we expect a total number of 69 false positives with a $p < 0.05$. Like the male versus female sweat comparison, there should be far less false positives that we call significant after applying the fold-change filter. The corresponding q-value for $p < 0.047831$ was 0.006568, meaning that 0.66% of metabolites with $p < 0.05$ were likely false positives. Thus, the false discovery rate in this comparison is also low.
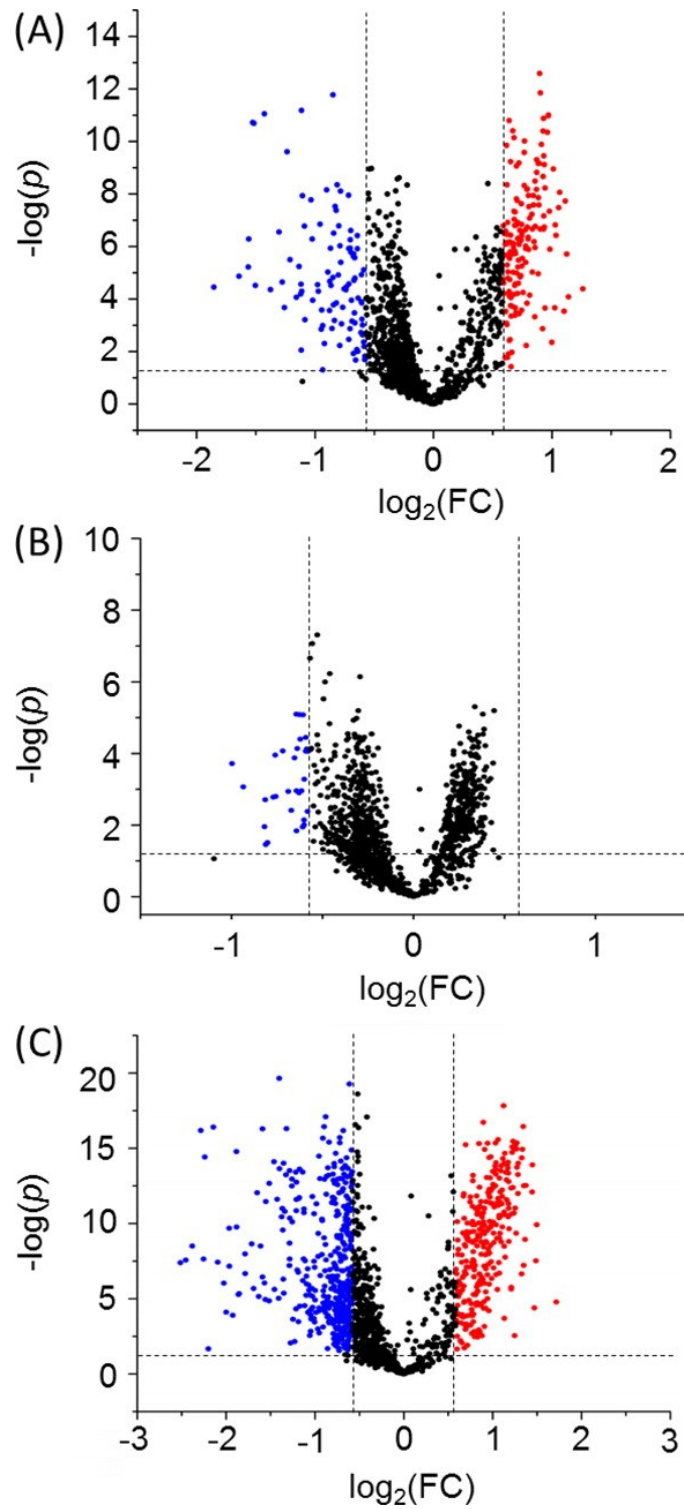
Figure 2.6. Volcano plots of sweat collected after different exercise times: (A) T1 vs T2, (B) T2 vs T3, and (C) T1 vs T3. The fold change represents the average ratio of the later exercise period divided by that of the earlier exercise period. Highlighted features fit the criteria of $0.67 \geq FC \geq 1.5$ and $p \leq 0.05$.

Taken together, the results of both multivariate and univariate analyses indicate that larger metabolic changes are occurring between early exercise and late exercise and smaller, indistinguishable changes in sweat composition occur once extreme fatigue has already set in. These metabolomic changes appear to be well-correlated to the shift of aerobic metabolism to anaerobic metabolism during exercise.[52] Because our technique can quantify many metabolite changes, it should be possible to design future experiments to study how this aerobic-to-anaerobic translation affects the overall metabolism in a time resolution that cannot be done using blood. For example, we could collect sweat samples frequently (e.g., by minutes) to observe the sweat metabolite changes with fast turnover rates. One potential application of frequent sampling of sweat may be to monitor the metabolomic composition changes as a function of exercise time as a way of gauging health state of an individual.

Among the 710 significant metabolites separating T1 and T3, we positively identified 25 metabolites using the dansyl standard library (Appendix Table A2.3) and putatively identified 644 metabolites using HMDB and MCID database search (See Supplemental Table S2.6 for the list). The majority of the 25 identified metabolites with a significant fold change after prolonged exercise are amino acids and dipeptides, and they seem to show a decrease in concentration during late exercise. Our findings are consistent with other studies that report a decrease in overall amino acid concentration in the plasma after prolonged periods of exercise, mainly due to their catabolism to produce energy during anaerobic metabolism.[53, 54]

One of our interesting findings is related to imidazoleacetic acid, a common metabolite in the brain that is thought to be derived from the oxidation of histamine. This compound was found to have a decrease in concentration in T3 (late exercise) compared to T1 (early exercise). This observation may suggest a decrease in histamine metabolism or decrease in histamine release in

late exercise under heavy fatigue. Imidazoleacetic acid has been shown to have neurophysiological, cardiovascular, and behavioral effects. While its mechanism of action and receptor site has been disputed, it has been repeatedly shown that introducing this compound into animal models causes a dose-dependent reduction in blood pressure.[55] It is possible that the body works to decrease imidazoleacetic acid abundance during late exercise in order to regulate blood pressure. Histamine was also detected with a fold change of 0.50 in T3 compared to T1. In future studies, we will compare the sweat metabolome to those of other biofluids directly within the same individuals in order to gauge their differences.

2.4 Conclusion

We have developed a high-performance CIL LC–MS method for quantitative human sweat metabolome profiling with high coverage. Using dansylation LC–MS targeting the amine/phenol submetabolome, a total of 2707 unique metabolites were detected across 54 sweat samples from six individuals with an average of 2002 ± 165 metabolites detected per sample from 108 LC–MS runs. We have detected many metabolites that have never been associated with human sweat, indicating that the human sweat metabolome is much more complex than previously thought. Because our technique is able to detect many metabolites, it opens the venue for future research in designing biological or clinical experiments, including population-based study, instead of a limited number of subjects used in this study, to investigate their significances for biological or clinical applications. We conclude that, using CIL LC–MS, sweat can be used as another important human biofluid for in-depth and quantitative metabolomics research. Future work on improving detection sensitivity and sweat collection method may allow metabolomic monitoring of sweat using a small volume of sample at a short interval.

2.5 Literature Cited

1) Sato, K.; Kang, W. H.; Saga, K.; Sato, K. T. *J. Am. Acad. Dermatol.* **1989**, 20, 537– 563

2) Raiszadeh, M. M.; Ross, M. M.; Russo, P. S.; Schaepper, M. A.; Zhou, W.; Deng, J.; Ng, D.; Dickson, A.;Dickson, C.; Strom, M.*J. Proteome Res.* **2012**, 11, 2127– 2139

3) Mena-Bravo, A.; Luque de Castro, M. D. *J. Pharm. Biomed. Anal.* **2014**, 90, 139– 147

4) Bandodkar, A. J.; Wang, J. *Trends Biotechnol.* **2014**, 32, 363– 371

5) Gao, W.; Emaminejad, S.; Nyein, H. Y. Y.; Challa, S.; Chen, K.; Peck, A.; Fahad, H. M.; Ota, H.; Shiraki, H.;Kiriya, D.*Nature* **2016**, 529, 509– 514

6) Farrell, P. M.; Rosenstein, B. J.; White, T. B.; Accurso, F. J.; Castellani, C.; Cutting, G. R.; Durie, P. R.;Legrys, V. A.; Massie, J.; Parad, R. B.*J. Pediatr.* **2008**, 153, S4– S14

7) Collie, J. T. B.; Massie, R. J.; Jones, O. A. H.; LeGrys, V. A.; Greaves, R. F. *Pediatr Pulmonol* **2014**, 49,106– 117

8) De Giovanni, N.; Fucci, N. *Curr. Med. Chem.* **2013**, 20, 545– 561

9) Kutyshenko, V. P.; Molchanov, M.; Beskaravayny, P.; Uversky, V. N.; Timchenko, M. A. *PLoS One* **2011**, 6,e28824

10) Harker, M.; Coulson, H.; Fairweather, I.; Taylor, D.; Daykin, C. A. *Metabolomics* **2006**, 2, 105– 112

11) Mark, H.; Harding, C. R. *Int. J. Cosmet. Sci.* **2013**, 35, 163– 168

12) Nunome, Y.; Tsuda, T.; Kitagawa, K. *Anal. Sci.* **2010**, 26, 917– 919

13) Calderon-Santiago, M.; Priego-Capote, F.; Jurado-Gamez, B.; Luque de Castro, M. D. *J. Chromatogr., A***2014**, 1333, 70– 78

14) Calderon-Santiago, M.; Priego-Capote, F.; Turck, N.; Robin, X.; Jurado-Gamez, B.; Sanchez, J. C.;Luque de Castro, M. D. *Anal. Bioanal. Chem.* **2015**, 407, 5381– 5392

15) Dutkiewicz, E. P.; Lin, J. D.; Tseng, T. W.; Wang, Y. S.; Urban, P. L. *Anal. Chem.* **2014**, 86, 2337– 2344

16) Soini, H. A.; Bruce, K. E.; Klouckova, I.; Brereton, R. G.; Penn, D. J.; Novotny, M. V. *Anal. Chem.* **2006**, 78,7161– 7168

17) Xu, Y.; Gong, F.; Dixon, S. J.; Brereton, R. G.; Soini, H. A.; Novotny, M. V.; Oberzaucher, E.; Grammer, K.;Penn, D. J. *Anal. Chem.* **2007**, 79, 5633– 5641

18) Guo, K.; Li, L. *Anal. Chem.* **2009**, 81, 3919– 3932

19) Guo, K.; Li, L. *Anal. Chem.* **2010**, 82, 8789– 8793

20) Zhou, R.; Huan, T.; Li, L. *Anal. Chim. Acta* **2015**, 881, 107– 116

21) Peng, J.; Li, L. *Anal. Chim. Acta* **2013**, 803, 97– 105

22) Guo, K.; Bamforth, F.; Li, L. *J. Am. Soc. Mass Spectrom.* **2011**, 22, 339– 347

23) Peng, J.; Chen, Y. T.; Chen, C. L.; Li, L. *Anal. Chem.* **2014**, 86, 6540– 6547

24) Zheng, J.; Dixon, R. A.; Li, L. *Anal. Chem.* **2012**, 84, 10802– 10811

25) Xu, W.; Chen, D.; Wang, N.; Zhang, T.; Zhou, R.; Huan, T.; Lu, Y.; Su, X.; Xie, Q.; Li, L.*Anal. Chem.***2015**, 87, 829– 836

26) Li, Z. D.; Tatlay, J.; Li, L. *Anal. Chem.* **2015**, 87, 11468– 11474

27) Verde, T.; Shephard, R. J.; Corey, P.; Moore, R. *J. Appl. Physiol.* **1982**, 53, 1540– 1545

28) Wu, Y.; Li, L. *Anal. Chem.* **2012**, 84, 10723– 10731

29) Zhou, R.; Tseng, C. L.; Huan, T.; Li, L. *Anal. Chem.* **2014**, 86, 4675– 4679

30) Huan, T.; Li, L. *Anal. Chem.* **2015**, 87, 1306– 1313

31) Huan, T.; Li, L. *Anal. Chem.* **2015**, 87, 7011– 7016

32) Gentleman, R. C.; Carey, V. J.; Bates, D. M.; Bolstad, B.; Dettling, M.; Dudoit, S.; Ellis, B.; Gautier, L.;Ge, Y. C.; Gentry, J.*Genome Biol.* **2004**, 5, R80

33) Huan, T.; Wu, Y. M.; Tang, C. Q.; Lin, G. H.; Li, L. *Anal. Chem.* **2015**, 87, 9838– 9845

34) Li, L.; Li, R. H.; Zhou, J. J.; Zuniga, A.; Stanislaus, A. E.; Wu, Y. M.; Huan, T.; Zheng, J. M.; Shi, Y.;Wishart, D. S.*Anal. Chem.* **2013**, 85, 3401– 3408

35) McLean, C.; Graham, T. E. *J. Appl. Physiol.* **2002**, 93, 1471– 1478

36) Mangos, J. *Am. J. Physiol.* **1973**, 224, 1235– 1240

37) Han, W.; Li, L. *Metabolomics* **2015**, 11, 1733– 1742

38) Kim, K.; Mall, C.; Taylor, S. L.; Hitchcock, S.; Zhang, C.; Wettersten, H. I.; Jones, A. D.; Chapman, A.;Weiss, R. H. *PLoS One* **2014**, 9, e86223

39) Slupsky, C. M.; Rankin, K. N.; Wagner, J.; Fu, H.; Chang, D.; Weljie, A. M.; Saude, E. J.; Lix, B.;Adamko, D. J.; Shah, S.*Anal. Chem.* **2007**, 79, 6995– 7004

40) Kochhar, S.; Jacobs, D. M.; Ramadan, Z.; Berruex, F.; Fuerholz, A.; Fay, L. B. *Anal. Biochem.* **2006**, 352,274– 281

41) Hodson, M. P.; Dear, G. J.; Roberts, A. D.; Haylock, C. L.; Ball, R. J.; Plumb, R. S.; Stumpf, C. L.;Griffin, J. L.; Haselden, J. N. *Anal. Biochem.* **2007**, 362, 182– 192

42) Plumb, R.; Granger, J.; Stumpf, C.; Wilson, I. D.; Evans, J. A.; Lenz, E. M. *Analyst* **2003**, 128, 819– 823

43) Dunn, W. B.; Lin, W.; Broadhurst, D.; Begley, P.; Brown, M.; Zelena, E.; Vaughan, A. A.; Halsall, A.; Harding, N.; Knowles, J. D.*Metabolomics* **2015**, 11, 9– 26

44) Spaapen, L. J.; Ketting, D.; Wadman, S. K.; Bruinvis, L.; Duran, M. *J. Inherited Metab. Dis.* **1987**, 10, 383–390

45) Iwaki, M.; Murakami, E.; Kikuchi, M.; Wada, A.; Ogiso, T.; Oda, Y.; Kubo, K.; Kakehi, K. *J. Chromatogr., Biomed. Appl.* **1998**, 716, 335– 342

46) Gronwald, W.; Klein, M. S.; Zeltner, R.; Schulze, B. D.; Reinhold, S. W.; Deutschmann, M.; Immervoll, A. K.;Boger, C. A.; Banas, B.; Eckardt, K. U.*Kidney Int.* **2011**, 79, 1244– 1253

47) Gupta, A.; Dwivedi, M.; Nagana Gowda, G. A.; Ayyagari, A.; Mahdi, A. A.; Bhandari, M.; Khetrapal, C. L.*NMR Biomed.* **2005**, 18, 293– 299

48) Li, M.; Wang, B.; Zhang, M.; Rantalainen, M.; Wang, S.; Zhou, H.; Zhang, Y.; Shen, J.; Pang, X.; Zhang, M.*Proc. Natl. Acad. Sci. U. S. A.* **2008**, 105, 2117– 2122

49) Nicholson, J. K.; Holmes, E.; Wilson, I. D. *Nat. Rev. Microbiol.* **2005**, 3, 431– 438

50) Lelo, A.; Miners, J. O.; Robson, R. A.; Birkett, D. J. *Br. J. Clin. Pharmacol.* **1986**, 22, 183– 186

51) Ou-Yang, D. S.; Huang, S. L.; Wang, W.; Xie, H. G.; Xu, Z. H.; Shu, Y.; Zhou, H. H. *Br. J. Clin. Pharmacol.***2000**, 49, 145– 151

52) De Feo, P.; Di Loreto, C.; Lucidi, P.; Murdolo, G.; Parlanti, N.; De Cicco, A.; Piccioni, F.; Santeusanio, F. *J. Endocrinol. Invest.* **2003**, 26, 851– 854

53) Haralambie, G.; Berg, A. *Eur. J. Appl. Physiol. Occup. Physiol.* **1976**, 36, 39– 48

54) Refsum, H. E.; Gjessing, L. R.; Strømme, S. B. *Scand. J. Clin. Lab. Invest.* **1979**, 39, 407– 413

55) Tunnicliff, G. *Gen. Pharmacol.* **1998**, 31, 503– 509

Chapter 3: Non-occlusive Sweat Collection Combined with Chemical Isotope Labeling LC-MS for Human Sweat Metabolomics and Mapping the Sweat Metabolomes at Different Skin Locations

3.1 Introduction

Sweat is an excellent candidate for metabolomics applications since a large portion of sweat solutes are small molecules (<1000 Da).[1-5] Compared to other biofluids, sweat collection is noninvasive and can be conveniently done on a regular basis for continuous monitoring (e.g., hourly or daily).[6, 7] In addition, sweat can serve as a media for detecting metabolic differences from skins with and without epidermal injuries or diseases (e.g.[2], soft tissue injury).[8, 9] While detecting low concentrations of sweat metabolites was a major challenge, recent advances in analytical techniques such as high-performance chemical isotope labeling LC–MS have made high-coverage metabolomic profiling possible.[4] However, to enable sweat metabolomics for various applications including discovering disease biomarkers and mapping metabolites of sweat from different skin locations of a subject, the use of a proper sweat collection method that can be conveniently administrated plays a crucial role.

Pilocarpine iontophoresis is a sweat collection technique used for the diagnosis of cystic fibrosis in newborns.[10] This method has also been used in untargeted sweat metabolomics studies.[11-13] However, it requires special equipment and caution to avoid any metabolite changes that may be induced by the applied chemical and the use of the device. Other sweat collection methods include the use of occlusive and nonocclusive patches. Occlusive sweat patches are ideal

for collecting pure liquid sweat over a short time interval (minutes).[4, 14, 15] This style of sweat collection uses exercise or heat to stimulate sweating, which is then collected into an absorbent material fixed to the skin by an impermeable barrier such as Teflon. This method is only suitable for short-term collection, as the skin is completely covered and unable to breathe during the collection time.

Nonocclusive style sweat patches are designed to be worn for longer periods of time (hours and days). For this style of collection, a semipermeable adhesive (e.g., Tegaderm) is used to fix an absorbent material to the skin which collects passive sweat over the collection period.[15, 16] Tegaderm allows the skin to breathe due to the semipermeable nature of the adhesive. Water vapor, oxygen, and carbon dioxide pass through while larger molecular weight, nonvolatile contaminants are prevented. Specially designed nonocclusive sweat patches are currently used for continuous monitoring of drug exposure (e.g., those from Pharmchek).[13, 17, 18] However, these patches are relatively expensive and have not been used for untargeted metabolomics studies where special care must be considered to avoid environmental contamination during sweat collection and sample loss during sweat extraction for downstream analysis. In this work, we report the development of a simple and inexpensive nonocclusive patch to collect passive sweat from different skin locations of a body and demonstrate its application and performance, in combination with chemical isotope labeling (CIL) LC–MS,[19, 20] for quantitative sweat metabolomics with high coverage.

3.2 Experimental

3.2.1 Nonocclusive Sweat Patch

Figure 3.1A shows a schematic diagram of the patch consisting of a Tegaderm film and two layers of Whatman filter paper. To apply the sweat patch to a skin (Figure 1B), the sampling

site was first cleansed by wiping the collection area with a Kimwipe soaked in 70% isopropyl alcohol in water. The area was left to air-dry. While waiting, the protective backing was removed from the Tegaderm (6 cm × 7 cm) which was then placed adhesive side up on a flat surface. Two clean 1.5 cm-diameter filter papers were adhered to the Tegaderm approximately 4 cm apart from one another. Two clean 1.27 cm-diameter filter papers were then carefully rested onto the collection area approximately 4 cm apart. The Tegaderm was secured overtop of the 1.27 cm filter papers on the collection area, making sure to line up the filter papers on the adhesive and the skin. The subject was asked to wear the patch for 24 h.
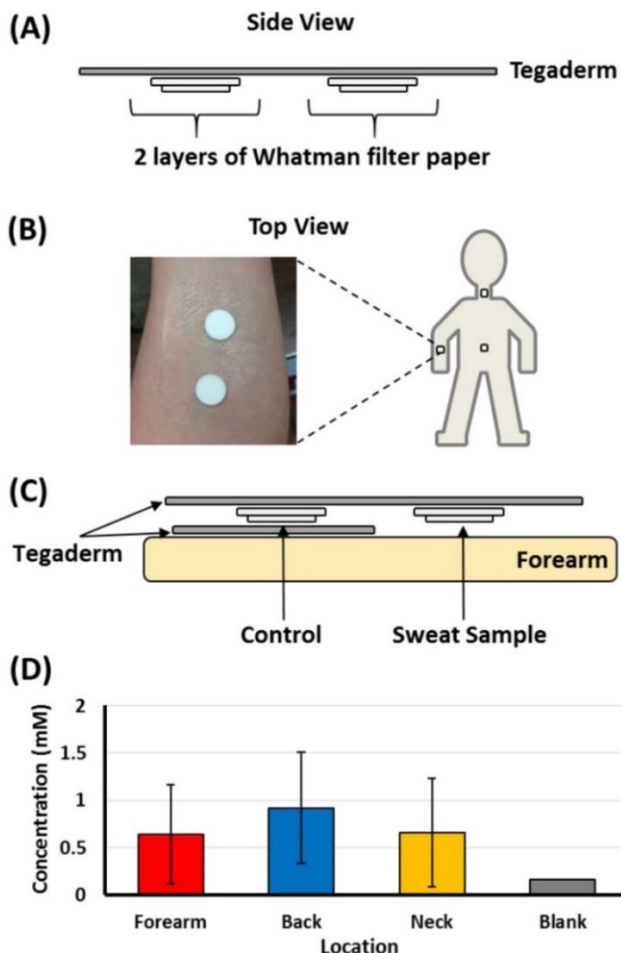
Figure 3.1. Side view (A) and top view (B) of a nonocclusive sweat patch design. (C) Side view of a special patch design for investigating environmental contaminations from wearing the patch. (D) Average concentrations of labeled metabolites measured by LC–UV in sweat and blank samples (error bar = 1 standard deviation).

3.2.2 Metabolite Extraction

Nonocclusive sweat collection resulted in a dried sweat in the filter paper. Water, 1:1 (v/v) acetonitrile–water, and acetonitrile (ACN), all compatible to dansylation labeling solvent (1:1 ACN–H2O), were tested as sweat extraction solvents. To examine the relative extraction efficiency, 40 µL of pure sweat was spiked in two cycles (20 µL each with a drying step in between to avoid saturation) onto a 1.27 cm filter paper. Pure sweat was collected from the proximal forearm of a single volunteer using a gauze sponge sweat patch method previously described.[4] After the final drying step, the filter paper was placed into a 1.5 mL microcentrifuge tube containing an insert with a fritted bottom. Sweat was then extracted by pipetting 40 µL of either water, 1:1 ACN–water, or ACN into the insert, incubating for 5 min at ambient temperature and centrifugation at 20 000g for 5 min. An aliquot (25 µL) of the extract was labeled with 12C-dansyl chloride (DnsCl),[19] and 2 µL of the labeled extract was injected into LC–UV to measure the peak area of labeled metabolites at 338 nm.[21] Extraction efficiency was calculated by comparing the total peak area of labeled sweat metabolites from the extraction to the total peak area after labeling 25 µL of pure sweat without filter paper spiking and extraction.

3.2.3 Environmental Contamination Testing

The sweat patch was worn over a period of time and thus environmental contamination may arise from the air, objects that may come in contact with the patch, bathing, etc. To study the sweat patch's ability to resist contamination, a modified sweat patch (Figure 3.1C) was constructed and worn on the left and right forearms of a volunteer for 24 h. The design of this sweat patch is similar to the normal patch; however, another layer of Tegaderm is placed between the filter paper and the skin on one of the two sampling sites. If the nonocclusive patch resists environmental contamination, then the labeled extract from the control filter paper worn between the 2 layers of

Tegaderm should be identical to an extract from a new filter paper. Detection of a large amount of unique metabolites present in this control sample compared to a new filter paper would signify a large amount of contamination from the environment or the patch itself. For LC–MS analysis, 10 nmol of labeled sweat was injected and an equivalent volume to 10 nmol injection was used for analyzing the control and new filter paper extracts. The peak pairs detected exclusively in filter paper in contact with the skin represents true sweat metabolites.

3.2.4 Study Design and Sweat Collection

Ten males and ten females were recruited to donate sweat for this study with Ethics Approval from the University of Alberta. For each recruit, sweat patches were placed on 3 sampling locations (left forearm, lower back, and back of neck) for 24 h. This procedure was repeated twice more for each recruit on separate days in 3 weeks. Each sweat patch contained 2 sampling spots for biological duplicates for a total of 360 sweat samples collected (20 recruits × 3 days × 3 locations × 2 replicates). After 24 h, patches were removed and sweat metabolites were extracted from the filter paper. Samples were stored at −80 °C until analysis.

3.2.5 Dansylation LC-UV and LC-MS Analysis

Section 3.5 Supplemental Note S1 describes the experimental details on preparing the control and blank samples, dansylation labeling, LC–UV for measuring the total concentration of labeled metabolites, LC–QTOF-MS setup, data processing,[22] statistical analysis, and metabolite identification.[23]

3.3 Results and Discussion

3.3.1 Sweat Extraction

Nonocclusive sample collection results in dried sweat due to the breathable nature of the patch. The sweat metabolites must be extracted from the absorbent collection material using a proper solvent and extraction technique in order to maximize metabolite detection sensitivity. To optimize the extraction process, three solvents, water, 1:1 water–ACN, and ACN, were investigated. They were chosen because the dansyl-labeling reaction takes place in 1:1 water–ACN and the use of one of these solvents can avoid a dry-down step.

To examine the extraction efficiency, a 1.27 cm filter paper spiked with pure sweat and left to dry was subjected to each solvent extraction, followed by dansyl labeling and LC–UV measurement of the labeled metabolites. Figure 3.2A shows the measured UV peak area for pure sweat, different extracts, and their controls (i.e., with water applied to the filter paper, instead of sweat), while Figure 3.2B shows the number of peak pairs detected in LC–MS for the corresponding samples. Similar results were observed for water and water–ACN with extraction efficiencies of >90% and good reproducibility, while ACN gave poor extraction. The peak number distribution shown in Figure 3.2C indicates that most metabolites were common between the water and water–ACN extracts. Water extraction produced a slightly lower number of background peak pairs (see Figure 3.2B for controls). These results are not surprising as sweat is approximately 99% H_2O, which suggests a mainly polar metabolome. Multiple extractions with smaller volumes were also attempted and produced similar results (Figure 3.2A,B, right side). On the basis of these results it was concluded that a single extraction with pure H_2O was optimal.
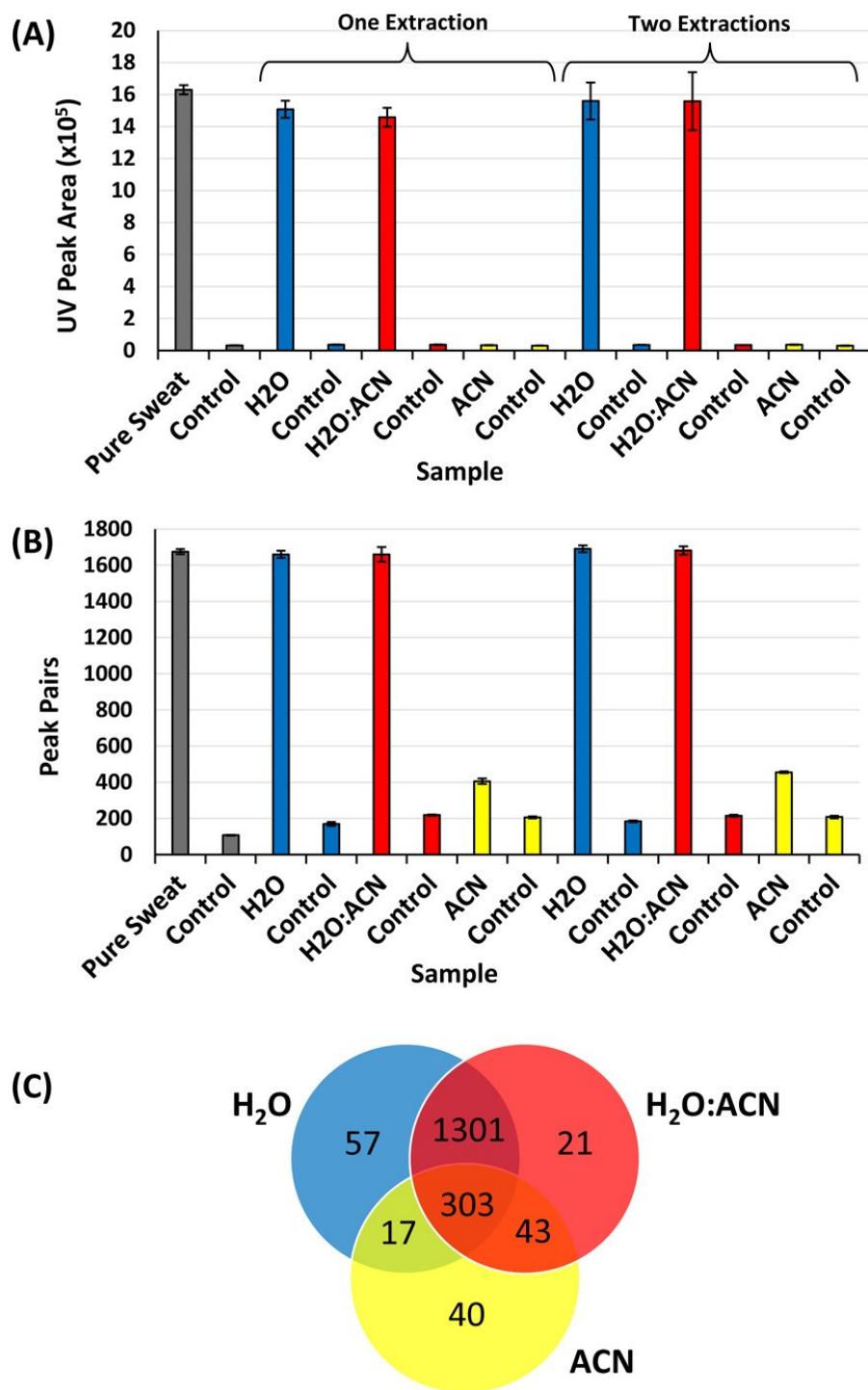
Figure 3.2. (A) UV peak areas of labeled metabolites from LC–UV analyses of labeled samples. (B) Peak pair numbers detected from LC–MS analyses of labeled samples. Pure sweat control was generated by labeling an equal volume of H2O. Control data for each solvent was generated by extracting a blank filter paper, labeling, and injecting the same volume as the experimental. Error bars represent standard deviation (n = 3). (C) Venn diagram of peak pairs detected using each solvent combination.

3.3.2 Resisting Environmental Contamination

In a real world, one would expect an individual wearing the sweat patch to undergo a variety of activities including sleeping and bathing. We tested the patch's ability to resist environmental contamination by comparing extracts of a clean filter paper with extracts from a filter paper worn for 24-h but not in contact with the skin (control) (Figure 3.1C). This experiment was performed in duplicate by placing the patch on the right and left forearm on a single volunteer. The volunteer was instructed to undergo their daily routine including bathing and sleeping as if the patches were not being worn. After extraction and dansyl-labeling, the UV peak areas of the control samples were almost identical to the blank filter paper samples (Appendix Figure A3.1 A). After injecting the same volume for LC–MS analysis (10 μL), total peak pair numbers were almost identical (Appendix Figure A3.1 B). The Venn diagrams of the peak pairs detected from left and right forearm experiments are shown in Appendix Figure A3.1 C,D, respectively. In both arms, only 11 unique metabolites were detected in the control sample. These 11 metabolites can be attributed to the method. Over 700 unique metabolites could be attributed to sweat secretion. Overall, these results demonstrated the selective nature of the patch for not allowing contaminants to pass, assuring that environmental contamination is not an issue during sample collection.

3.3.3 Sweat Submetabolome

A total of 365 peak pairs were detected in six method blank runs with an average of 310 ± 12 peak pairs per run (N = 6). A total of 201 peak pairs were shared between sweat samples and the method blank. Shared peak pairs were excluded from the sweat analysis if they were present in at least 50% of the method blank runs. While it is possible that these shared features are naturally occurring in sweat, we conservatively excluded them from the data analysis. After the background pairs were removed, a total of 3140 peak pairs were detected in all the sample runs. Dansyl library

search of these metabolites resulted in 84 definitive identifications (Appendix Table A3.1). Metabolites not identified were subjected to HMDB and EML searches based on accurate mass.[23] These searches resulted in 947 and 1769 putative IDs, respectively (Supplemental Table S3.1).

3.3.4 Metabolome Profiles at Different Skin Locations

Unlike other homogeneous biofluids such as urine, sweat can be collected at different skin locations and thus we examined whether collection location has any effect on the metabolome profiles. Concentrations of labeled metabolites in sweat extracts after dansyl labeling were determined by LC–UV, based on the total area of the LC peak produced from the elution of the labeled metabolites in high organic solvent of a step-gradient and a standard calibration curve of a labeled amino-acid-mixture.[21] Figure 3.1D shows the average concentrations of the labeled sweat samples with error bars depicting the standard deviation of each group. Lower back samples yielded the highest concentration of labeled metabolites on average. The large error bars for each of collection areas show just how variable the resulting concentrations were for each collection area. This was an expected result as concentration of an extract should correlate with how much an individual sweated through the collection period. Each individual performs different activities through the day and are expected to sweat different amounts depending on their level of activity.

Within a subject, the concentrations of individual metabolites in sweat samples collected from different locations can be different. This can be visualized using a heat map for the metabolome data set collected from lower back, forearm, and neck areas of an individual. Figure 3.3 shows two examples (see Appendix Figures A3.2-3.6 for the heat maps of other individuals). In these heat maps, only the 100 top-ranked metabolites with significant variations in three locations are shown. In Figure 3.3, for most metabolites shown, concentration variations in the 24-h sweat samples collected from the same location on three different days are small. However, the

concentrations of many of the metabolites are very different from one location to another. This location dependence characteristic is interesting from the perspective of mapping the metabolic differences in sweat samples collected from different locations to reveal metabolite distributions in different areas of skins. However, this location dependence also suggests that, to reveal biological variations among different groups of individuals, we need to take the collection site into consideration when comparing the metabolomes of different subjects (see below).
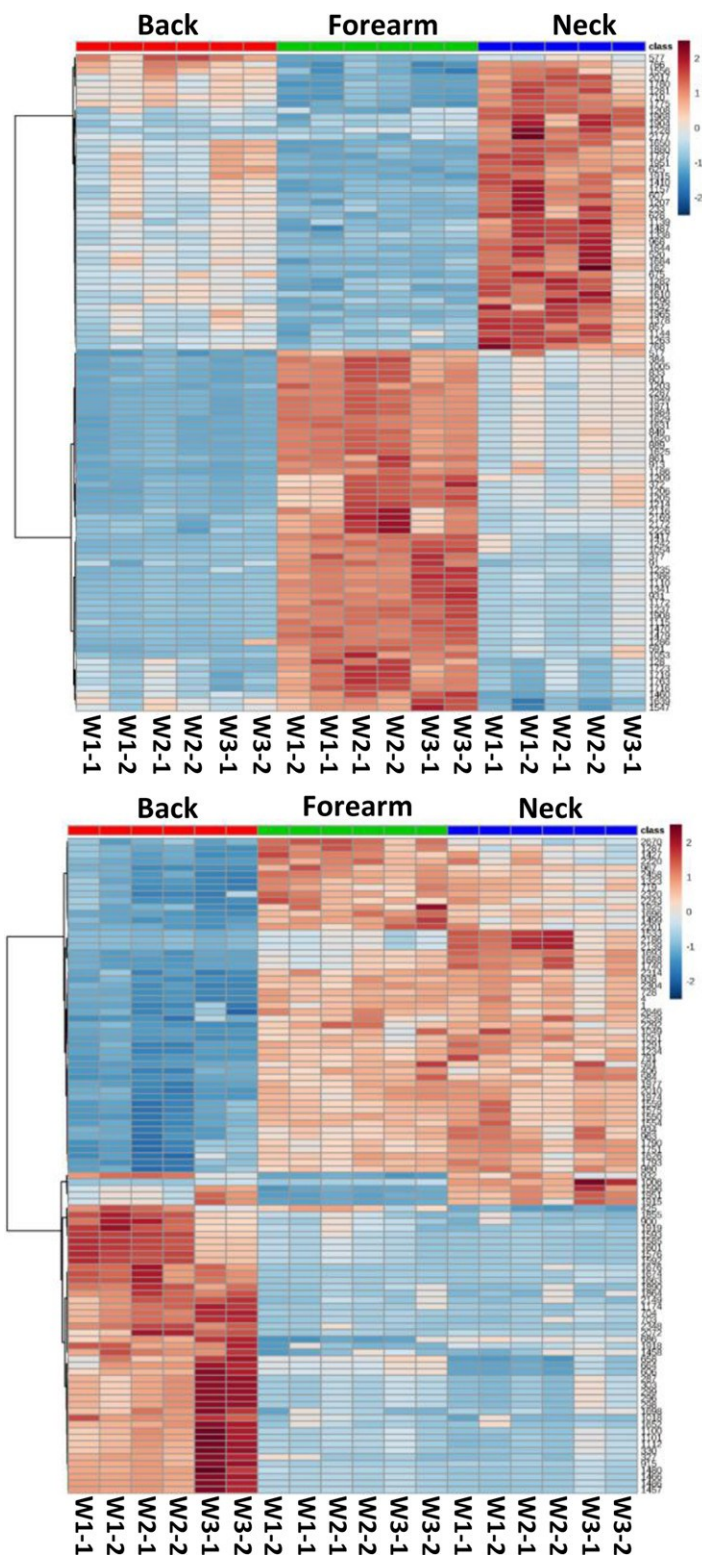
Figure 3.3. Heat maps of two individuals for the 100 top-ranked significant metabolites with varying concentrations in sweat samples collected from three locations. The bottom axis, Wx-y, refers to the replicate sample spot y collected from week x (e.g., W1-1 refers to the replicate sample spot 1 collected in week 1, while W1-2 refers to the replicate sample spot 2 collected in week 1).

3.3.5 Metabolomic Comparison of Male and Female

Figure 3.4 shows the PLS-DA plots for comparing the male and female sweat samples collected from all areas or different locations and Appendix Figures A3.7-3.10 show the corresponding permutations test results for model validation. Univariate analysis was performed to identify metabolites with significantly differing changes in abundance between sexes (Appendix Figure A3.11). Taking sex comparison from all sweat samples as an example (Figure 3.5A and Appendix Figure A3.11), multiple-testing correction was performed on the p-values from the t test to calculate q-values. On the basis of the table of q-values, in order to maintain a false discovery rate of $\leq 5\%$, a $p \leq 0.02$ must be used as a cutoff. Therefore, for this analysis, metabolite level changes were considered significantly different if the ratio had an FC $\geq$ 1.5 or ≤ 0.67 and a $p \leq$ 0.02. This criterion revealed 78 metabolites with significantly differing levels between sexes. The dansyl library search resulted in definitive identification of seven of these metabolites while HMDB and EML library searches based on accurate mass resulted in 22 and 42 matches, respectively (Supplemental Table S3.2). We note that we did not detect hormone/pheromone compounds in sweat in this work; they either could not be labeled by dansylation chemistry or, if labeled, had concentrations below the detection limit of the method. Future work of using other labeling chemistries in combination with concentrating the sweat samples may afford the detection of these compounds.
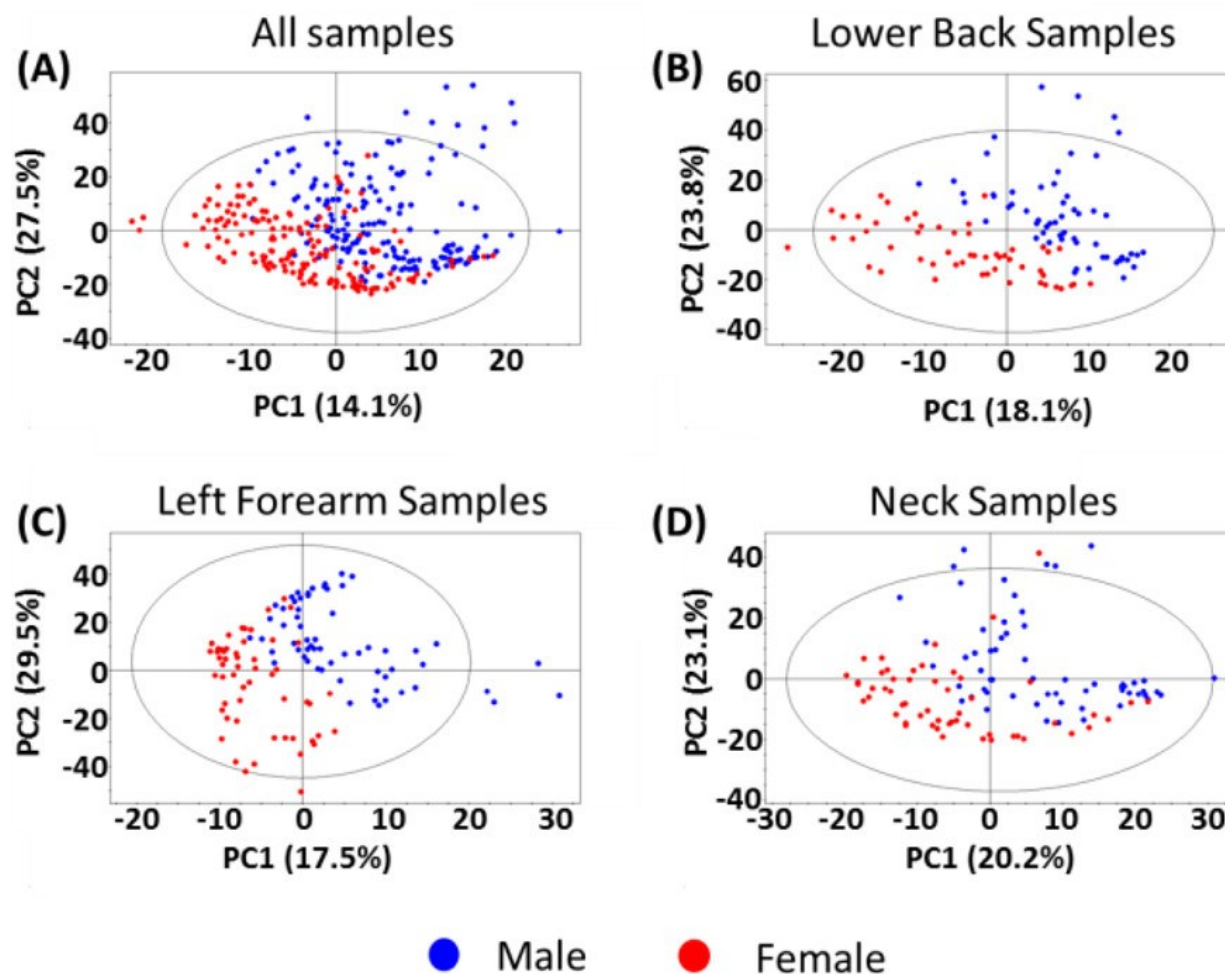
Figure 3.4. PLS-DA plots comparing sexes using sweat samples collected from (A) all areas (R2X = 0.590, R2Y = 0.905, Q2 = 0.770), (B) lower back (R2X = 0.582, R2Y = 0.965, Q2 = 0.844), (C) left forearm (R2X = 0.683, R2Y = 0.983, Q2 = 0.759), and (D) neck (R2X = 0.626, R2Y = 0.951, Q2 = 0.740).

Figure 3.4B–D shows the PLS-DA plots of the metabolome data from samples collected in three separate locations. Supplemental Note S2 describes the comparison results and significant metabolites detected to separate sexes from each comparison. Combining common dansyl library matches from each of the 3 collection areas, there were a total of 10 different metabolites with significantly differing levels between sexes, 9 of which are endogenous metabolites (see Section

Supplemental Note S2 for the discussion of these metabolites). Overall, a greater separation could be observed by using the metabolome data of samples collected from the same location.

3.4 Conclusions

We have developed a method to profile the sweat metabolome using nonocclusive sample collection and CIL LC–MS. Our results revealed the dynamic nature of the sweat metabolome and how important it is to consider sweat collection area when conducting metabolomic studies. This location dependence characteristic may also be explored further. For example, we are in the process of mapping the metabolomic profile differences in normal and affected areas of lymphedema patients for discovering potential metabolite biomarkers with diagnosis and prognosis values including measuring the severity of an affected area and guiding the management regimens (e.g., massaging areas and frequencies).

3.5 Literature Cited

1) Mena-Bravo, A.; de Castro, M. D. L. *J. Pharm. Biomed. Anal.* **2014**, 90, 139– 147

2) Calderón-Santiago, M.; Priego-Capote, F.; Turck, N.; Robin, X.; Jurado-Gámez, B.; Sanchez, J. C.;Luque de Castro, M. D. *Anal. Bioanal. Chem.* **2015**, 407, 5381– 5392

3) Delgado-Povedano, M. M.; Calderón-Santiago, M.; Priego-Capote, F.; Luque de Castro, M. D. *Anal. Chim. Acta* **2016**, 905, 115– 125

4) Hooton, K.; Han, W.; Li, L. *Anal. Chem.* **2016**, 88, 7378– 7386

5) Dutkiewicz, E. P.; Chiu, H. Y.; Urban, P. L. *Anal. Chem.* **2017**, 89, 2664– 2670

6) Imani, S.; Bandodkar, A. J.; Mohan, A. M. V.; Kumar, R.; Yu, S. F.; Wang, J.; Mercier, P. P. *Nat. Commun.***2016**, 7, 11650

7) Jia, W. Z.; Bandodkar, A. J.; Valdes-Ramirez, G.; Windmiller, J. R.; Yang, Z. J.; Ramirez, J.; Chan, G.;Wang, J. *Anal. Chem.* **2013**, 85, 6553– 6560

8) Polliack, A.; Taylor, R.; Bader, D. *J. Rehabil. Res. Dev.* **1993**, 30, 250– 259

9) Tur-Garcia, E. L.; Davis, F.; Collyer, S. D.; Holmes, J. L.; Barr, H.; Higson, S. P. J. *Sens. Actuators, B* **2017**,242, 502– 510

10) Farrell, P. M.; Rosenstein, B. J.; White, T. B.; Accurso, F. J.; Castellani, C.; Cutting, G. R.; Durie, P. R.;Legrys, V. A.; Massie, J.; Parad, R. B.*J. Pediatr.* **2008**, 153, S4– S14

11) Calderon-Santiago, M.; Priego-Capote, F.; Jurado-Gamez, B.; de Castro, M. D. L. *J. Chromatogr. A* **2014**,1333, 70– 78

12) Calderon-Santiago, M.; Priego-Capote, F.; Turck, N.; Robin, X.; Jurado-Gamez, B.; Sanchez, J. C.;de Castro, M. D. L. *Anal. Bioanal. Chem.* **2015**, 407, 5381– 5392

13) De Giovanni, N.; Fucci, N. *Curr. Med. Chem.* **2013**, 20, 545– 561

14) Huestis, M. A.; Oyler, J. M.; Cone, E. J.; Wstadik, A. T.; Schoendorfer, D.; Joseph, R. E., Jr *J. Chromatogr., Biomed. Appl.* **1999**, 733, 247– 264

15) Kintz, P.; Tracqui, A.; Mangin, P.; Edel, Y. *J. Anal. Toxicol.* **1996**, 20, 393– 397

16) Kintz, P.; Samyn, N. In *Handbook of Analytical Separations*; Maciej, J. B., Ed.; Elsevier Science B.V.: New York, **2000**; Vol. 2, pp 459– 488.

17) Barnes, A. J.; De Martinis, B. S.; Gorelick, D. A.; Goodwin, R. S.; Kolbrich, E. A.; Huestis, M. A. *Clin. Chem.***2009**, 55, 454– 462

18) Gambelunghe, C.; Fucci, N.; Aroni, K.; Bacci, M.; Marcelli, A.; Rossi, R. *Ther. Drug Monit.* **2016**, 38, 634–639

19) Guo, K.; Li, L. *Anal. Chem.* **2009**, 81, 3919– 3932

20) Huan, T.; Li, L. *Anal. Chem.* **2015**, 87, 7011– 7016

21) Wu, Y.; Li, L. *Anal. Chem.* **2012**, 84, 10723– 10731

22) Zhou, R.; Tseng, C. L.; Huan, T.; Li, L. *Anal. Chem.* **2014**, 86, 4675– 4679

23) Huan, T.; Li, L. *Anal. Chem.* **2015**, 87, 1306-1313

24) Huan, T.; Wu, Y.; Tang, C.; Lin, G.; Li, L. *Anal. Chem.* **2015**, 87, 9838– 9845

25) Li, L.; Li, R.; Zhou, J.; Zuniga, A.; Stanislaus, A. E.; Wu, Y.; Huan, T.; Zheng, J.; Shi, Y.; Wishart, D. S., et al. *Anal. Chem.* **2013**, 85, 3401-3408.

Chapter 4: Metabolic Profiling of Sweat Collected from Edema Affected and Healthy Areas of Lymphedema Patients Using A Non-Occlusive Sample Collection Kit and Chemical Isotope Labeling LC-MS

4.1 Introduction

Lymphedema is a progressive condition caused by a dysfunctional lymphatic transport system. In a healthy individual, the circulatory system is associated with a net fluid efflux from arterial capillaries to the interstitial space. The majority of this fluid is reabsorbed by venous capillaries, with the remaining fluid being subsequently drained by lymphatic vessels and redistributed to the bloodstream though the lymph nodes. In patients with lymphedema, their defective lymphatic system is unable to reabsorb and transport the entire net fluid efflux back into the bloodstream and results in a pooling of protein-rich interstitial fluid in extremities. The accumulation of this protein-rich fluid causes painful inflammation, adipose tissue hypertrophy, and fibrosis that may lead to serious infections of the affected area.[1,2]

There are two main classes of lymphatic dysfunction that lead to the progression of lymphedema. Primary lymphedema is used to describe patients with a congenitally defective lymphatic system. Secondary lymphedema manifests itself as a result of a damaged lymphatic system caused by a procedure or pre-existing condition. Human intervention such as surgery or radiation treatment in order to treat malignancy, as well as infection from the nematode Wuchereria bancrofti which dwell within lymphatic vessels can both cause lymphatic dysfunction. Most cases of secondary lymphedema in the United States are related to malignancy and its treatments, specifically surgery and radiation therapy of female breast cancer patients. Ordinary rates of

lymphedema after mastectomy are reported between 24% and 49%[3-7], yet there are few publication that attempt to understand the pathology of this common condition.

Current methods for diagnosing lymphedema are extremely limited and are normally made though clinical presentation and history. While diagnosis is easier in the later stages of the disease, it's reliance on visual clues make it difficult to differentiate early stage lymphedema from other causes of edema. A non-subjective molecular biomarker would greatly assist physicians in early stage diagnosis so treatment can begin early to improve the patient's quality of life. A reliable biomarker would also aid in monitoring disease progression, as documentation of lymphedema is normally done crudely though circumferential or volumetric measurements of the affected region.

Recently, chemical isotope labeling (CIL) combined with liquid chromatography-mass spectrometry (LC-MS) has been used to profile the metabolome of sweat collected from different areas of the skin with a non-occlusive device.[8] This study demonstrated a location dependence characteristic of the sweat metabolome, hinting at the possibility to conduct imagining studies of the skins surface. The feature of localized sample collection is a great benefit to studying lymphedema as sweat can be collected from both diseased and healthy areas from a single individual and analyzed for metabolome differences. Common metabolome trends between diseased and healthy areas may reveal possible biomarker candidates characteristic of lymphedema over other types of edema.

In this work, we used a previously described non-occlusive sweat patch method[8] to collect and analyze sweat from diseased and healthy areas of five primary lymphedema patients in a pilot study. The results of this pilot study are depicted in Supplementary Information for Chapter 4. The work described within the main body of this chapter describes the implementation of a new self-application non-occlusive sweat collection kit in an expanded study of lymphedema. In this

expanded clinical study, sweat metabolome differences between diseased and healthy areas are compared to the differences observed between the same areas of healthy volunteers.

4.2 Experimental

4.2.1 Development of the Nonocclusive Sweat Patch Kit

The positive results of the pilot study described in the Supplementary Information were convincing enough to pursue an expanded study using a greater number of lymphedema patients. For this work a self-application/removal/storage sweat collection kit was developed. The purpose of designing this kit was to eliminate scheduling issues that occurred during the pilot study, as the previous protocol required the volunteer and the analyst to meet twice per collection. A total of six meetings between the volunteer and the analyst were required for only 3 sample collections. By developing and distributing individual sweat collection kits to volunteers, an analyst would only have to meet with each volunteer once to distribute the kit and once to collect the kit. The reduction in required meetings also decreases the time required to collect a large number of samples, as all volunteers would be collecting their samples simultaneously.

The contents of the sweat collection kit mimic the same material used to collect sweat in Chapter 3 as well as the pilot study of lymphedema. The only notable changes are the sample collection tubes containing 500 µL of extraction solvent (Figure 4.1 A) and the Teflon lined box lid (Figure 4.1 B). Participants are to wear the sweat patch for 24-hours, then place the 1.5 cm filter paper containing the sweat metabolites into the appropriately labeled tube containing the extraction solvent. The purpose of the Teflon lined lid is to serve as a clean working service. Participants are first asked to clean the Teflon lined lid and tweezers with a provided alcohol wipe, then rest the sweat collection filter papers on the cleaned lid before sweat patch application. The

SOP for sweat patch application, removal, and metabolite extraction using the sweat collection kit is provided in the Supplementary information. The sweat collection kit contents are listed below.
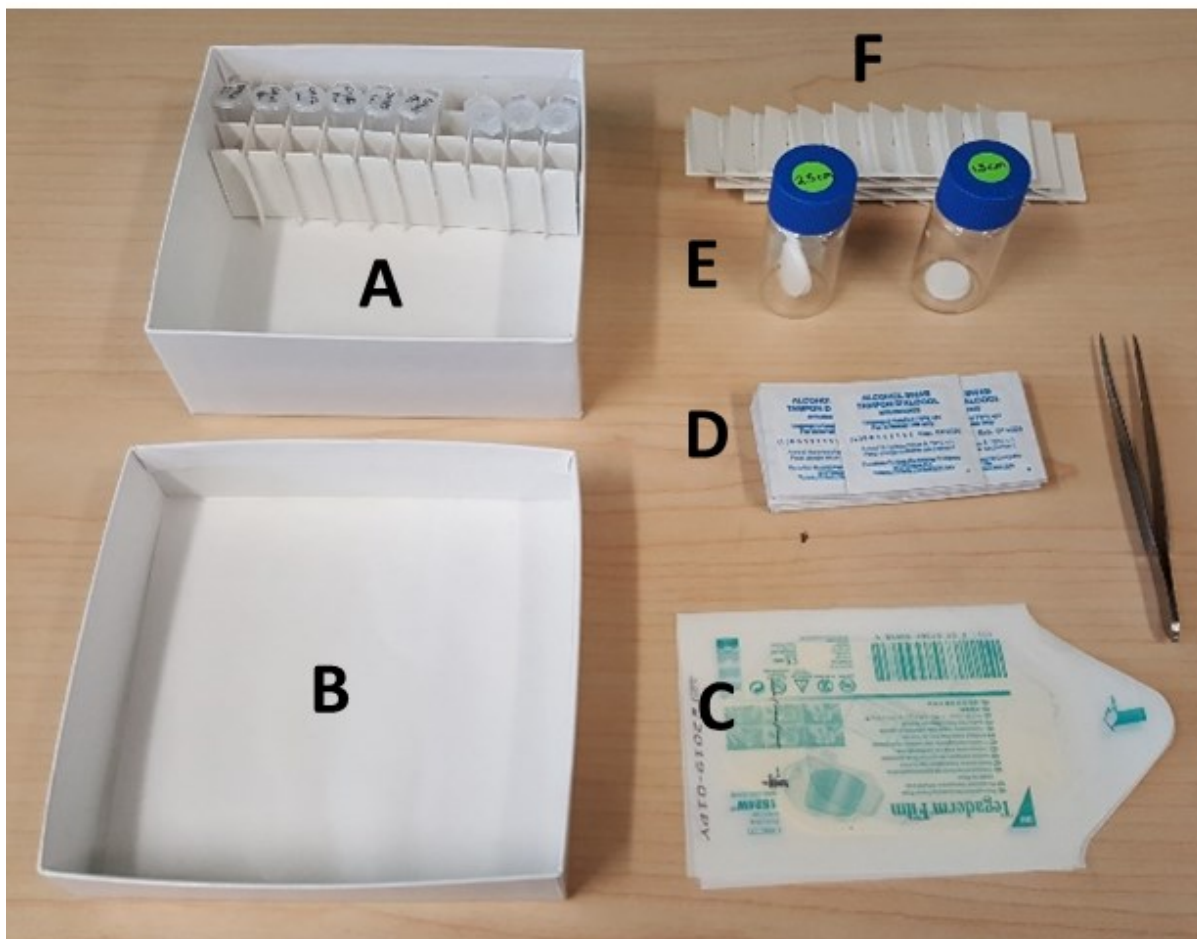
Figure 4.1. Sweat collection kit contents. Starting from the top left and moving counter-clockwise (A) Bottom half of sweat collection kit box with labeled sample collection tubes containing 50% isopropyl alcohol in water. (B) Sweat collection kit lid lined with thin sheet of Teflon plastic. (C) Tegaderm adhesives. (D) 70% Isopropyl alchohol wipes and stainless steel tweezers. (E) Glass vials containing 2.5 cm and 1.5cm diameter Whatman filter paper discs. (F) Additional cardboard sample collection tube stand.

The protocol for using the sweat collection kit is summarized as follows; (1) the sampling area is first cleaned with an isopropyl alcohol wipe, (2) the sweat patch is applied, (3) after 24-hours the sweat patch is removed, (4) the filter paper containing the sweat metabolites is placed in

the sample collection tubes where the extraction takes place, (4) the kit is stored in the volunteer's home freezer and returned to the analyst for sample processing once all samples have been collected.

4.2.2 Extraction Solvent Optimization

The optimal solvent combination for extracting sweat metabolites from filter paper was determined by comparing the total UV peak area of dansyl-labeled sweat extracts produced among three different solvent combinations. To test this, 10 µL of pure liquid sweat was spiked onto 1.5 cm Whatman filter papers and left to air dry. Next, the filter papers containing the dried sweat were placed in microcentrifuge tubes containing 500 µL of either 1:1 $ACN:H_2O$, $MeOH:H_2O$, or $IPA:H_2O$. The filter paper extractions were then left to sit overnight in the -20°C freezer. After 24-hours, filter papers were removed from the microcentrifuge tubes and the liquid containing the extracted sweat metabolites was dried down completely in a roto-evaporator. Dried down samples were then resuspended in 100 µL of water. All individual samples were labeled with ^{12}C dansyl chloride and a pooled sample was labeled with ^{13}C dansyl chloride. Since 10 µL of sweat was extracted from filter paper, dried down, then resuspended in 100 µL of water, sample loss during these procedures was quantified by comparing the UV peak areas of the extracts to labeling the same pure sweat sample diluted by 10x in water.

4.2.3 Sweat Sample Collection

Fifteen lymphedema patients (a combination of primary and secondary) were recruited for the expanded study. Of these 15 volunteers, 7 are considered having unilateral arm edema, 4 are considered having unilateral leg edema, and 4 are considered having bilateral leg edema. These recruits are clients of the Salutaris Massage Therapy Centre located in Edmonton, Alberta, Canada.

These patients were provided with the sweat collection kit and the SOP after being given a single demonstration of its use. Unilateral patients were instructed to apply the sweat patch to their diseased limb and opposite healthy limb (Eg. Diseased left leg and healthy right leg) in the same location on opposite sides. Bilateral patients were instructed to apply the sweat patch to their diseased left and right legs, as well as their right forearm. Each patient completed 3 separate sample collections on 3 different days. Unilateral patients generated 6 samples, and bilateral patients generated 9 samples upon completing their collections.

To make a proper binary comparison, samples from both diseased and healthy areas must be collected from each volunteer. For unilateral patients the edema was present in only one of their legs, with the alternate leg showing no signs of edema. In these cases, sweat was collected from both legs. Samples collected from the leg with edema served as the diseased area and samples collected from the unaffected leg served as the healthy control area. For bilateral patients the edema was present in both legs. In these cases, sweat was collected from both legs as well as the right forearm. The right forearm showed no signs of edema and hence served as a healthy control. Examples of sample collection locations for the lymphedema patients are depicted below.
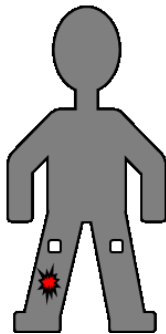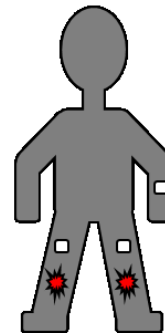
Figure 4.2. Sample collection locations for the patient volunteers based on their class of lymphedema. Red stars indicate diseased areas.

Ten healthy volunteers were also recruited for this study in order to investigate if sweat metabolome changes between left and right limbs, as well as between arms and legs are normally present in healthy people. For these healthy volunteers, samples were collected from both left and right forearms and legs. Each recruit completed 3 separate sample collections on 3 different days, generating 12 sweat samples each.

4.2.4 Sweat Sample Processing

Returned sweat patch kits were processed in order to concentrate the sweat samples and remove any filter paper fibres before chemical isotope labeling. The sample collection tubes were centrifuged at 20,000 g for 5 minutes to pellet any residual filter paper fibres. The solution was then transferred to a new microcentrifuge tube, dried down completely in a roto-evaporator, and resuspended in 70 µL of water. The sweat samples were stored at -80°C until dansyl-labeling.

4.2.5 Dansylation Labeling

Frozen sweat samples were thawed at 4°C, vortexed to dissolve precipitates, then centrifuged at 20,000 g for 5 minutes before aliquoting 50 µL for labeling. Aliquots of individual sweat extracts were combined with 25 µL each of acetonitrile and sodium carbonate/sodium bicarbonate buffer solution (0.5 mol/L, pH 9.5). These mixtures were labeled with 50 µL of 12C-dansyl chloride (DnsCl) solution (18 mg/mL in acetonitrile) at 40°C for 45 min. The reaction was quenched with 10 µL of sodium hydroxide (250 mmol/L) and incubating at 40°C for 10 min. Each reaction was acidified using 50 µL of formic acid (425 mmol/L in 1:1 ACN:H2O). A pooled sweat sample was created by combining equal volumes of all of the unlabeled individual sweat samples, and labeling with the above protocol and 13C-DnsCl solution (18 mg/mL). The 12C- and 13C-

labeled samples were vortexed and centrifuged 20,000 g for 5 min before performing LC-UV quantification.

4.2.6 LC-UV Sample Normalization

Sample amount was normalized based on LC-UV measurement of the total concentration of dansyl labeled metabolites in a sample.[9] A Waters ACQUITY UPLC system with photodiode array (PDA) detector was used to quantify the amount of labeled metabolites in the sweat samples. Dansyl-labeled samples were thawed in a 4ºC refrigerator and 4 µL of sample was injected onto an Agilent Eclipse Plus C18 column (100 x 2.1 mm, 1.8 µm). Solvent A was 0.1% (v/v) formic acid in 5% (v/v) acetonitrile, and solvent B was 0.1% (v/v) formic acid in acetonitrile. Previous work has shown that dansylated ammonia interferes with the LC-UV quantification of sweat, so a gradient was developed to separate dansylated ammonia from other metabolites. Initial flow rate was 180 µL/min. The chromatographic conditions were t = 0 min, 20% B; t = 3.5 min, 35% B; t = 5 min, 35% B; t = 5.1 min, 95% B. This solvent composition was held until t = 9 min to elute the rest of the labeled metabolites. The gradient was restored back to 20% B in 0.1 min and held at this position for 4 min. The total run time was 13 min. The total peak areas of the labeled metabolites other than ammonia measured at 338 nm were used for sample quantification.

4.2.7 LC-FTICR-MS Analysis

Labeled sweat samples were analyzed using a Bruker 9.4T Apex-Qe FT-ICR mass spectrometer (Billerica, MA, USA) with electrospray ionization (ESI) linked to an Agilent 1100 Series HPLC system. Samples were normalized so that 3 nmols of labeled metabolites were injected for each run. Samples were injected onto an Agilent Eclipse plus C18 column (100 × 2.1 mm, 1.8 µm particle size,) for reversed-phase separation. Solvent A was 0.1% (v/v) formic acid in

5% (v/v) acetonitrile, and solvent B was 0.1% (v/v) formic acid in acetonitrile. The chromatographic conditions were t = 0 min, 20% B; t = 3.5 min, 35% B; t = 18 min, 65% B; t = 24 min, 99% B, held until t = 32 min. The column was also cleaned and equilibrated in between runs. The chromatographic conditions were t = 0 min, 20% B; t = 4.5 min, 99.8% B; t = 5 min, 20% B, held until t = 15 min. Flow rate was 180 μL/min for all runs. A divert valve was used from t = 0-2 min to divert all non-retaining salts to waste. All MS spectra were obtained in positive ion mode. Quality control (QC) samples of 12C-/13C-labeled sweat were also analyzed every 20 runs to monitor the stability of the LC-MS runs.

4.2.8 Data Processing, Statistical Analysis, and Metabolite Identification

After LC-FTICR-MS analysis, Bruker database software was used to extract peaks with S/N greater than 3 from each LC-MS run, followed by IsoMS processing for peak-pair picking, peak-pair filtering, and peak-pair intensity ratio calculations,[10] Zero-filling for missed peaks,[11] IsoMS-Quant for calculating the chromatographic peak ratio for each pair.[12]

For statistical analysis, metabolites with peak ratio values detected in at least 80% of all the injections being compared were analyzed. Multivariate analysis was conducted using Metaboanalyst software.[13] Volcano plots were constructed using Microsoft Excel and OriginPro 8.5 (OriginLab). To calculate the fold-change between groups for univariate analyses, the average peak pair ratio of all the injections in one group was calculated, then divided by the average peak pair ratio of all the injections in the other group. The p-value was calculated using a Student's t-test.

Positive metabolite identification was performed based on mass and retention time match to the dansyl standard library containing 273 unique amines/phenols using DnsID.[14] Putative

metabolite identification was done based on accurate mass match to the metabolites in the human metabolome database (HMDB) (8,021 known human endogenous metabolites) and the Evidence-based Metabolome Library (EML) (375,809 predicted human metabolites with one reaction) using MyCompoundID.[15]

4.3 Results and Discussion

4.3.1 Extraction Solvent Optimization

Previous work has shown that pure H_2O is sufficient for extracting sweat metabolites, however in that work the sweat extracts were immediately frozen at -80°C until dansyl-labeling. Since subjects were to collect and store their samples in their own home, care must be taken to ensure individual sample storage conditions do not compromise the integrity of the sample. In order to prevent bacterial growth in the sample collection tube during sample storage, the addition of organic solvent to water should be sufficient. In addition, a larger volume of extraction solvent must be used in order to fully submerge the filter paper during the extraction and storage step. This larger volume of solvent required a dry-down step in order to concentrate the sweat metabolites before labeling. We tested 1:1 acetonitrile:H2O, isopropanol:H2O, and methanol:H2O for their extraction efficiencies by labeling each sweat extract and comparing their UV peak areas to a labeled pure sweat sample.
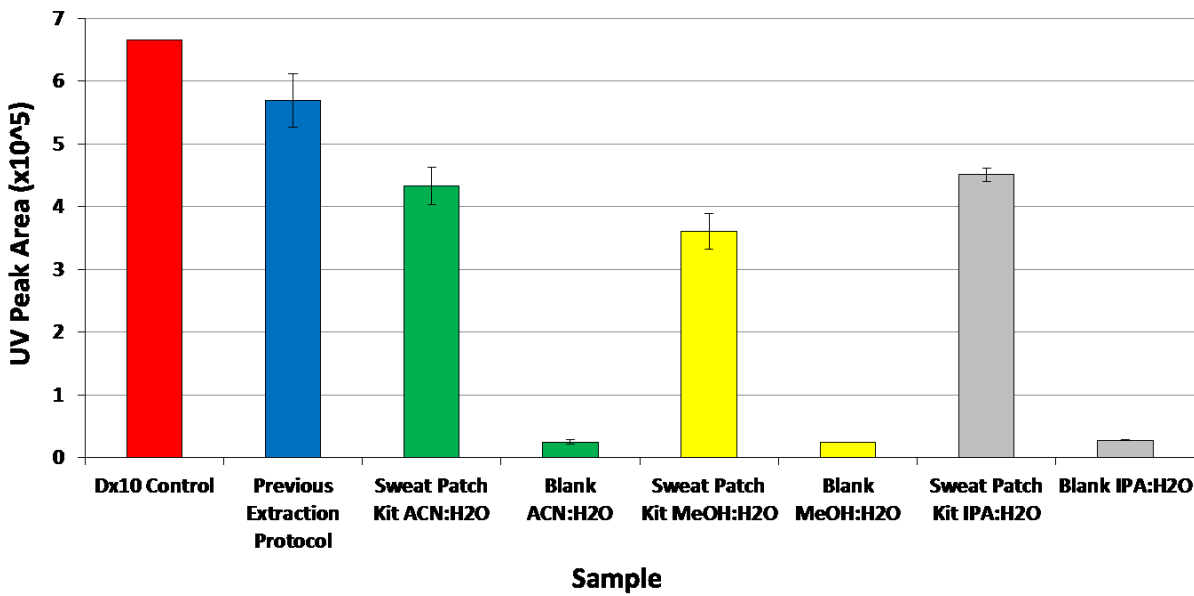
Figure 4.3. UV peak areas of sweat metabolites extracted from filter paper using different solvent combinations. ACN:H_2O (green), MeOH:H_2O (yellow), and IPA:H_2O (gray) extraction solvents were compared to labeling the same amount of pure sweat (red) and a previous extraction protocol using 100% H_2O.

After comparing the UV peak areas of labeled extracts from each solvent combination, it was found that ACN:H_2O and IPA:H_2O mixtures produced the highest efficiency. The latter was chosen as the optimal extraction solvent due to its practicality and similarity rubbing alcohol, as most subjects using the kit would be unfamiliar with acetonitrile. Each of the extraction solvents tested produced a lower peak area than the previous extraction method which used 100 µL of pure water. This reduction can be attributed to the loss of some volatile components during dry down step that is required to concentrate the sweat extracts before dansyl-labeling.

Since the reduced UV peak area of the sweat patch kit samples is indicative of some sample loss, the same volume of sample was analyzed using LC-QTOF-MS to investigate the number of metabolites that may be lost by using this particular method. Despite the lower concentration of metabolites in each sample, 86% of the metabolites detected in the pure sweat sample are also

detected in all three extraction conditions (Figure 4.4). This result shows that 86% (623/723) of

the metabolome is retained even after implementing this new sweat collection protocol.
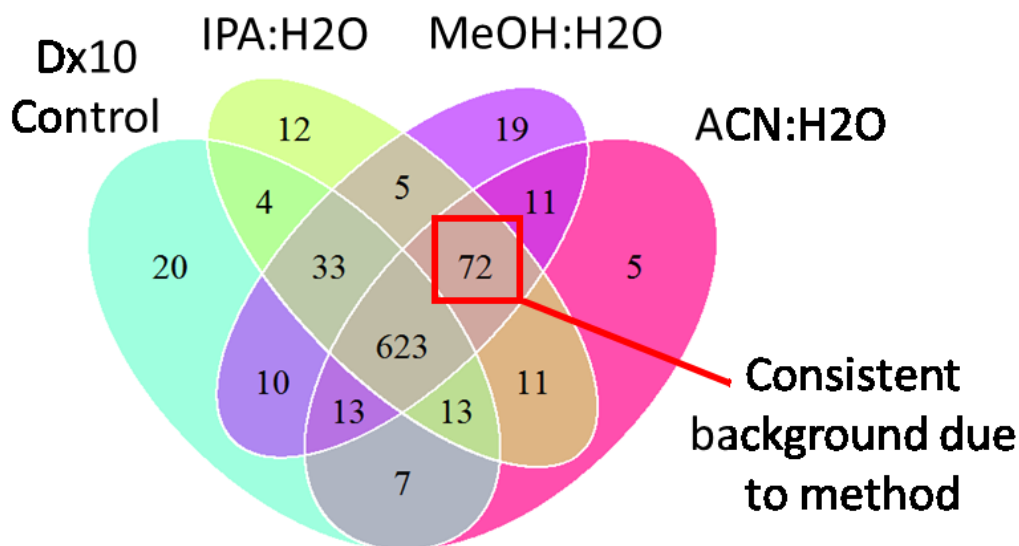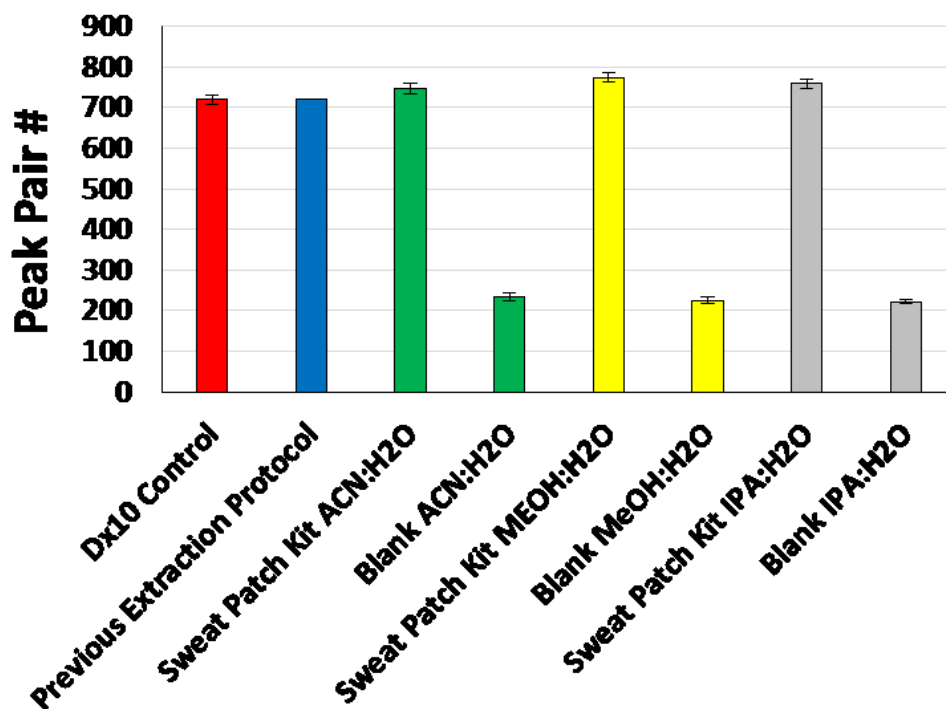
Figure 4.4. (Top) Resulting peak pair numbers after injecting the same volume (10 µL) for LC-QTOF-MS analysis. (Bottom) Venn diagram showing shared features between the Dx10 labeled pure sweat sample and sweat extracted from filter paper using various extraction solvents.

4.3.2 Sweat Metabolome Profiling of Legs and Arms of Healthy Individuals.

The end goal of this work is to find a biomarker of early stage lymphedema using a non-occlusive sample collection kit and CIL LC-MS. In order to search for potential biomarkers, proper controls must be analyzed in order to reduce the probability of false positive findings. In the case of unilateral lymphedema patients where the edema is asymmetric, we hypothesized that the healthy limb opposite to the diseased limb may serve as a source for a healthy control sample. In this case, the individual may serve as their own control. It has been shown that the effects of a non-standardized diet, gender, and age may create changes in the urine metabolome.[16,17] These trends may also be true for sweat. Sweat sampling has the advantage of allowing sampling of diseased and healthy areas of the same individual. By doing this, the control sample will theoretically have the same sample genetics, gender, age, and diet as the diseased sample, effectively eliminating artifacts due to inconsistencies between these factors. In order to show that the healthy limb may serve as a proper control for the diseased limb, we sought to show that there are no significant metabolome changes between left/right arms and left/right legs within the same individual in healthy people.

In-depth analysis was only performed for 4 of the 10 healthy recruits so far. The remaining healthy volunteers have yet to be analyzed as they had at least one very dilute sweat sample (<0.05 mM of labeled metabolites) that produced a low number of detected metabolites. Due to the analytical variation between the dilute and concentrated samples of these recruits, we instead focus on the 4 recruits where the same number of metabolites were detected across all of their collected sweat samples. In total, 1541 metabolites were detected across all the healthy individuals tested. We were able to identify 82 metabolites based on accurate mass and retention time using DnsID (See Appendix Table A4.1 for the list).[14] Figure 4.5 shows an example of results from a single

healthy volunteer. Figure 4.5 A1 and B1 shows multivariate analysis results comparing left and right limbs of the healthy individual, and no separation is observed. Figure 4.5 A2 and B2 depict univariate analysis results that show very few metabolites with FC greater than 1.5 or less than 0.67 and $p < 0.05$. This results demonstrates that there are little to no significant differences in the sweat metabolome between opposite limbs, meaning the opposite healthy limb can serve as a control for the diseased limb in this study. Examples of results from other volunteers are depicted in Appendix Figures A4.1-4.3, which show the same trends.

In the case of bilateral lymphedema, the edema is symmetric and affects either both arms or both legs. Because both limbs are affected, these individuals do not have the same opportunity to serve as their own control as unilateral patients. In order for these patients to provide their own healthy control sample, the healthy sample must be collected from another non-diseased area of the body. For patients with bilateral leg edema, we wished to use the forearm as a source for control sample. This location was chosen due to their ease of applying the sweat patch while seated. To demonstrate the suitability of these locations for control samples, we first had to prove that there is no significant difference between arm and leg sweat metabolomes of healthy individuals. Significant differences in the sweat metabolome between these locations in healthy people would suggests a high probability for false positive findings when comparing diseased legs vs. healthy forearm in bilateral lymphedema patients. In this case, we would have to consider comparing diseased samples in the lymphedema patients to the same areas in the healthy volunteers. Figure 4.5 C1 shows a distinct separation between leg and arm sweat metabolomes, while Figure 4.5 C2 reveals many significant metabolites with FC less than 0.67 or greater than 1.5 and $p \leq 0.05$. This results demonstrates that there are significant differences between the leg and arm sweat metabolomes, suggesting that sweat collected from a healthy forearm is not a suitable control when

69

comparing diseased and healthy areas for bilateral lymphedema patients. Sweat metabolome differences between legs and arms was an expected result, as we have previously demonstrated a location dependence of the sweat metabolome in Chapter 3.[8] Examples of results from other volunteers are depicted in Appendix Figures A4.1-4.3, which show the same trends.
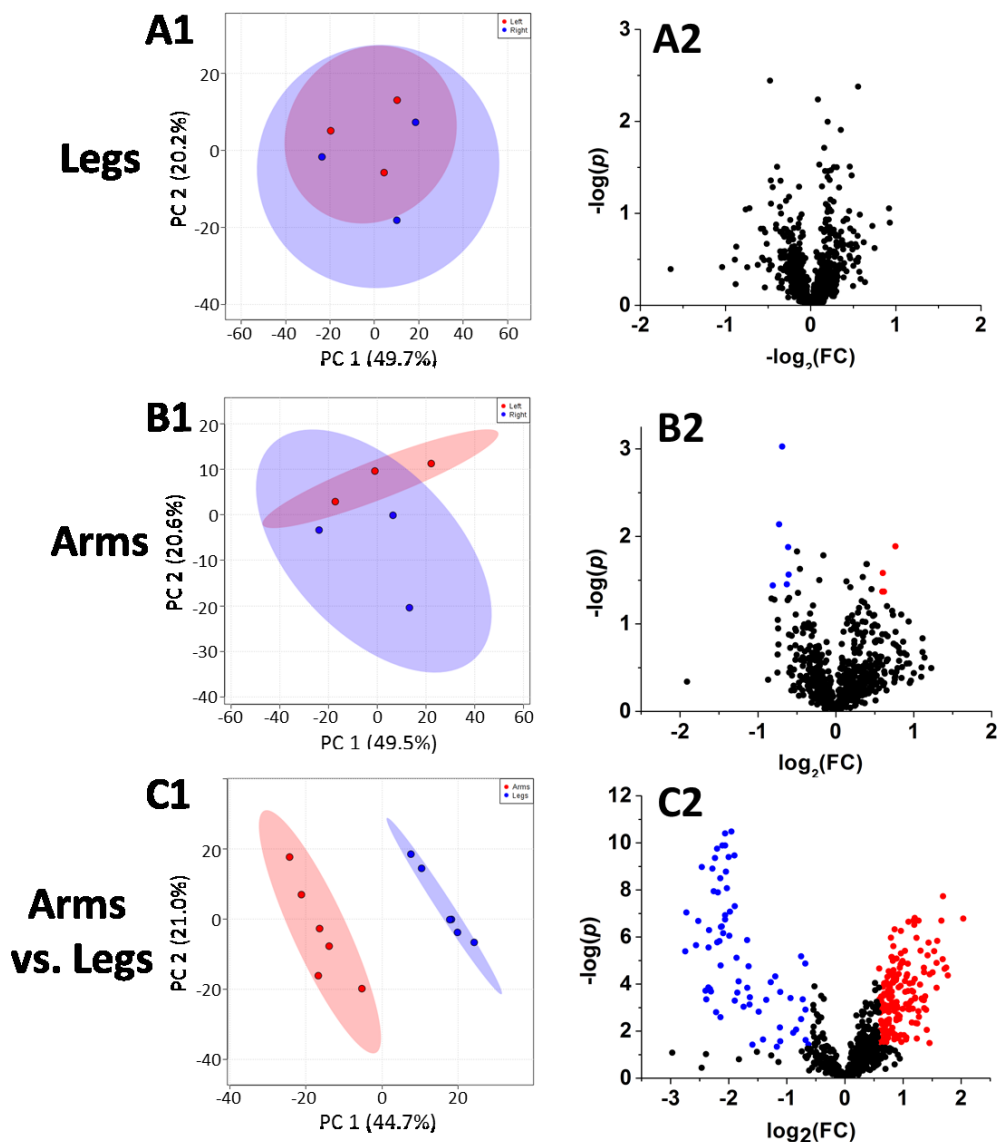
Figure 4.5. PCA score plots comparing left vs. right legs (A1), left vs. right arms (B1), and arms vs. legs (C1). Volcano plots comparing left vs. right legs (A2), left vs. right arms (B2), legs vs. arms (C2). Both sets of analyses show large sweat metabolome changes between arms and legs, and miniscule changes between left and right limbs. Cut-offs set to FC less than 0.67 or greater than 1.5, and p ≤ 0.05.

4.3.3 Sweat Metabolome Profiling Diseased and Healthy Areas of Lymphedema Patients.

Figure 4.6 depicts the results from lymphedema patients who have been successfully analyzed to this date. Multivariate and univariate analysis comparisons of diseased and healthy areas in unilateral arm patients appear similar to results seen between left and right forearms of healthy volunteers. However, large metabolome variation between diseased and healthy areas is observed for the patients with unilateral edema in the foot. It is interesting that metabolome variation between diseased and healthy areas is apparent in foot edema and not arm edema. One possible explanation is the pressure that is exerted on the sweat patch in the patient with foot edema while wearing their compression stocking and shoes. The compression sleeve worn by patients with upper body edemas is not as tight as the stockings worn by those affect by lower body edemas.

Data from the patient with unilateral foot edema produced a total of 85 metabolites with significantly differing levels between diseased and healthy areas (FC greater than 1.5 or less than 0.67 and $p \leq 0.05$.). DnsID search of these metabolites produced 6 matches based on accurate mass and retention time. A list of these identified metabolites is shown in Appendix Table A4.2. We were also able to match 24 of these significant metabolites to HMDB and 51 to EML libraries (See Supplementary Table S4.1). An interesting finding is the increased levels of glycylproline found in sweat collected from the diseased foot. Glycylproline is an end product of collagen breakdown, and increased levels of this metabolite has previously been found in the urine of patients with pressure sores.[18] Increased levels of glycylproline in diseased legs was also observed in the pilot study of lymphedema. Consistent trends observed for this metabolite in both studies generates confidence that the trend we are seeing is true. We postulate that tissue damage and increased collagen breakdown in the diseased legs of lymphedema patients may be generating the increased

glycylproline levels. We were unable to match the significant metabolites identified in the unilateral foot comparison with the unilateral arm comparisons.
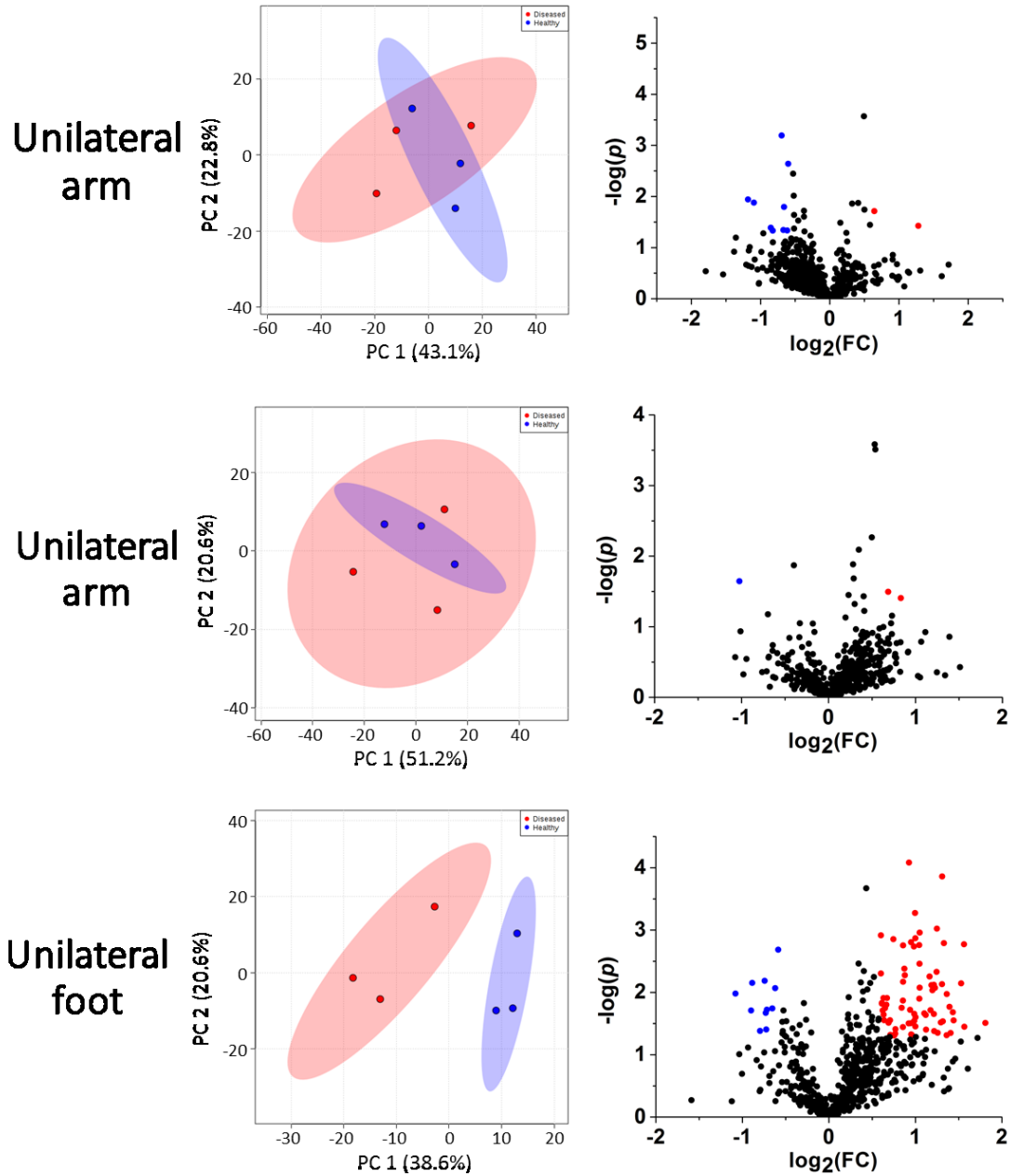
Figure 4.6. PCA score plots (left side) and volcano plots (right side) comparing diseased vs. healthy areas of 3 lymphedema patients. Very little differences are seen between diseased and healthy areas of unilateral arm patients, but large differences are seen between diseased and healthy areas of the unilateral foot patient. Cut-offs set to FC less than 0.67 or greater than 1.5, and p ≤ 0.05.

4.4 Conclusions

In this work, we profiled the sweat metabolome between diseased and healthy areas of lymphedema patients, and compared their results to the same areas of healthy people. Preliminary results show no significant differences in the sweat metabolome between the left and right limbs of healthy people, and larger differences between their arms and legs. Sweat metabolome differences between diseased and healthy areas of lymphedema patients with upper body edemas were not observed. However, large differences between diseased and healthy areas were observed in a patient with a lower body edema. Glycylproline was found to have increased levels in the diseased foot of this patients compared to their healthy foot. Increased levels for this metabolite was also found in diseased areas in the lymphedema pilot study. Based on the limited data available for this expanded study of lymphedema, it is difficult to make any definitive conclusions until sweat kits from more patients have been analyzed. Future work will confirm if increased levels of glycylproline is found in diseased areas of other patients with lower body edemas, and whether it may serve as a possible biomarker of lymphedema.

4.5 Literature Cited

1) Warren, A. G.; Brorson, H.; Borud, L. J.; Slavin, S. A. *Ann. Plast. Surg.* **2007**, *59*, 464-472.

2) Ly, C.; Kataru, R.; Mehrara, B. *Int. J. Mol. Sci.* **2017**, *18*, 171.

3) Schünemann, H.; Willich, N. *Deut. Med. Wochenschr.* **1997**, *122*, 536-541.

4) Petrek, J. A.; Senie, R. T.; Peters, M.; Rosen, P. P. *Cancer* **2001**, *92*, 1368-1377.

5) Querci della Rovere, G.; Ahmad, I.; Singh, P.; Ashley, S.; Daniels, I. R.; Mortimer, P. *Ann. Roy. Coll. Surg.* **2003**, *85*, 158-161.

6) Ozaslan, C.; Kuru, B. *Am. J. Surg.* **2004**, *187*, 69-72.

7) Hinrichs, C. S.; Watroba, N. L.; Rezaishiraz, H.; Giese, W.; Hurd, T.; Fassl, K. A.; Edge, S. B. *Ann. Surg. Oncol.* **2004**, *11*, 573.

8) Hooton, K.; Li, L. *Anal. Chem.* **2017**, *89*, 7847-7851.

9) Wu, Y.; Li, L. *Anal. Chem.* **2012**, *84*, 10723-10731.

10) Zhou, R.; Tseng, C.-L.; Huan, T.; Li, L. *Anal. Chem.* **2014**, *86*, 4675-4679.

11) Huan, T.; Li, L. *Anal. Chem.* **2015**, *87*, 1306-1313.

12) Huan, T.; Li, L. *Anal. Chem.* **2015**, *87*, 7011-7016.

13) Xia, J.; Wishart, D. S. *Curr. Protoc. Bioinformatics* **2016**, 14.10. 11-14.10. 91.

14) Huan, T.; Wu, Y.; Tang, C.; Lin, G.; Li, L. *Anal. Chem.* **2015**, *87*, 9838-9845.

15) Li, L.; Li, R.; Zhou, J.; Zuniga, A.; Stanislaus, A. E.; Wu, Y.; Huan, T.; Zheng, J.; Shi, Y.; Wishart, D. S. *Anal. Chem.* **2013**, *85*, 3401-3408.

16) Walsh, M. C.; Brennan, L.; Malthouse, J. P. G.; Roche, H. M.; Gibney, M. J. *Am. J. Clin. Nutr.* **2006**, *84*, 531-539.

17) Slupsky, C. M.; Rankin, K. N.; Wagner, J.; Fu, H.; Chang, D.; Weljie, A. M.; Saude, E. J.; Lix, B.; Adamko, D. J.; Shah, S. *Anal. Chem.* **2007**, *79*, 6995-7004.

18) Le, J.; Perier, C.; Peyroche, S.; Rascle, F.; Blanchon, M.; Gonthier, R.; Frey, J.; Chamson, A. *Amino Acids* **1999**, *17*, 315-322.

Chapter 5: Conclusions and Future Work

5.1 Thesis Summary

Human sweat can be noninvasively collected and used as a media for diagnosis of certain diseases as well as for drug detection. However, because of very low concentrations of endogenous metabolites present in sweat, metabolomic analysis of sweat with high coverage is difficult, making it less widely used for metabolomics research. In Chapter 2, a high-performance method for profiling the human sweat submetabolome based on chemical isotope labeling (CIL) liquid chromatography–mass spectrometry (LC–MS) is reported. Sweat was collected using a gauze sponge style occlusive patch, then differential 12C- and 13C-dansylation labeling was used to target the amine/phenol submetabolome. Over 2707 unique metabolites were detected across 54 sweat samples collected from six individuals with an average of 2002 ± 165 metabolites detected per sample from a total of 108 LC–MS runs. Using a dansyl standard library, we were able to identify 83 metabolites with high confidence; many of them have never been reported to be present in sweat. Using accurate mass search against human metabolome libraries, we putatively identified an additional 2411 metabolites. Uni- and multivariate analyses of these metabolites showed significant differences in the sweat submetabolomes between male and female, as well as between early and late exercise. These results demonstrate that the CIL LC–MS method described can be used to profile the human sweat submetabolome with high metabolomic coverage and high quantification accuracy to reveal metabolic differences in different sweat samples, thereby allowing the use of sweat as another human biofluid for comprehensive and quantitative metabolomics research.

In Chapter 3, we report a simple and inexpensive method for sweat collection over a defined period (e.g., 24 h) based on the use of a nonocclusive style sweat patch adhered to a skin.

This method was combined with differential chemical isotope labeling (CIL) LC–MS for mapping the metabolome profiles of sweat samples collected from skins of the left forearm, lower back, and neck of 20 healthy volunteers. Three 24-h sweat samples were collected at three different days from each subject for examining day-to-day metabolome variations. A total of 342 LC–MS runs were carried out (two runs were discarded due to instrumental issue), resulting in the detection and relative quantification of 3140 sweat metabolites with 84 metabolites identified and 2716 metabolites mass-matched to metabolome databases. Multivariate and univariate analyses of the metabolome data revealed a location-dependence characteristic of the sweat metabolome, offering a possibility of mapping the sweat metabolic differences according to skin locations. Significant differences in male and female sweat metabolomes could be detected, demonstrating the possibility of using the sweat metabolome to reveal biological variations among different comparative groups. Thus, the combination of noninvasive sweat collection and CIL LC–MS is a robust analytical tool for sweat metabolomics with potential applications including daily monitoring of the sweat metabolome as health indicators, discovering sweat-based disease biomarkers, and metabolomic mapping of sweat collected from different areas of skin with and without injuries or diseases.

In Chapter 4, we design a non-occlusive sweat collection kit and implement its use in a clinical study of lymphedema. By implementing the sweat collection kit, patient volunteers are able to collect their own sweat samples in the comfort of their own home, eliminating the numerous meetings between the volunteer and the analyst required for sample collection in previous studies. Preliminary results reveal metabolome changes in diseased vs. healthy areas of lymphedema patients that are not present between the same areas of healthy individuals. This project is still

ongoing at the time of this thesis submission. The results presented at this time represent our current interpretations of the data, which may be subject to change in the future.

5.2 Future Work

Patient volunteers for the clinical study of lymphedema are still being recruited in order to increase the population size and statistical reliability of the results in Chapter 4. We will also investigate if similar trends are observed between bilateral and unilateral patients, as well as between primary and secondary lymphedema.

Since sweat collection offers the benefit of non-invasive, frequent sample collection, other diseases and conditions that require frequent biospecimen collection may benefit using sweat collection as an alternative. Sweat also has the benefit of localized sample collection, meaning this sweat metabolomics workflow can be applied to profile metabolome between diseased vs. healthy areas of other conditions affecting the skin such as melanomas and atopic dermatisis.

There still remains the issue of sufficient sample amount collected for some individuals who do not sweat a lot. These individuals do not provide enough sweat for analysis even after the 24-hour collection period with the non-occlusive sweat patch. With the current workflow, these samples (conc. < 0.1 mM) always generate fewer peak pair numbers than the more concentrated samples (> 0.1mM) even after sample concentration normalization procedures and injecting the same molar amount onto the mass spectrometer. As a result, the pre-analytical variation of these dilute samples makes the data interpretation difficult when comparing them to more concentrated samples. Potential solutions to this issue include convincing sample collection volunteers to exercise more or use a sauna/steam room at a gym. The importance of being physically active while wearing the patch is already communicated to these volunteers before their first sample

collections, however we cannot be sure whether or not they follow our instructions. Another solution is to design some sort of compressive wrap around the sample collection areas in order to promote sweating. Lymphedema patients often wear compression stockings/bandages around their affected limbs in order to delay the onset of swelling. It has been noticed that samples collected from these areas are often more concentrated than samples collected from their non-wrapped, unaffected limbs.

The non-occlusive sweat collection kit is made from inexpensive materials found around a common analytical laboratory. If this kit needs to be commercialized in the future, this kit can be made to look more professional by including a custom designed box/label, and a proper sample collection tube holder that secures the samples so they do not fall out of the tray if the kit box is inverted.

Sweat metabolomics is a highly untapped field with the potential to uncover disease biomarkers that have not been detected in other biospecimens. Sweats ability to be collected non-invasively and frequently suggests potential future applications that involve continuous monitoring of health state and personalized medicine. I hope the techniques used in this thesis will be used to discover these application in the future, as this work is merely a stepping stone to reaching the full potential of sweat metabolomics research.

Bibliography

1) Dettmer, K.; Aronov, P. A.; Hammock, B. D. *Mass Spectrom. Rev.* **2007**, *26*, 51-78.

2) Courant, F.; Antignac, J. P.; Dervilly-Pinel, G.; Le Bizec, B. *Proteomics* **2014**, *14*, 2369-2388.

3) Mena-Bravo, A.; De Castro, M. L. *J. Pharmaceut. Biomed.* **2014**, *90*, 139-147.

4) Emwas, A.-H. M.; Salek, R. M.; Griffin, J. L.; Merzaban, J. *Metabolomics* **2013**, *9*, 1048-1072.

5) Hussain, J. N.; Mantri, N.; Cohen, M. M. *Clin. Biochem. Rev.* **2017**, *38*, 13.

6) Vulimiri, S. V.; Berger, A.; Sonawane, B. *Mutat. Res. Genet. Toxicol. Environ. Mutagen.* **2011**, *722*, 147-153.

7) Martínez-López, S.; Sarriá, B.; Gómez-Juaristi, M.; Goya, L.; Mateos, R.; Bravo-Clemente, L. *Food Res.Int.* **2014**, *63*, 446-455.

8) Wishart, D. S.; Jewison, T.; Guo, A. C.; Wilson, M.; Knox, C.; Liu, Y.; Djoumbou, Y.; Mandal, R.; Aziat, F.; Dong, E. *Nucleic Acids Res.* **2012**, *41*, D801-D807.

9) Guo, K.; Li, L. *Anal. Chem.* **2009**, *81*, 3919-3932.

10) Guo, K.; Li, L. *Anal. Chem.* **2010**, *82*, 8789-8793.

11) Zhao, S.; Dawe, M.; Guo, K.; Li, L. *Anal. Chem.* **2017**.

12) Huan, T.; Tang, C.; Li, R.; Shi, Y.; Lin, G.; Li, L. *Anal. Chem.* **2015**, *87*, 10619-10626.

13) Li, L.; Li, R.; Zhou, J.; Zuniga, A.; Stanislaus, A. E.; Wu, Y.; Huan, T.; Zheng, J.; Shi, Y.; Wishart, D. S. *Anal. Chem.* **2013**, *85*, 3401-3408.

14) Sato, K.; Kang, W. H.; Saga, K.; Sato, K. T. *J. Am. Acad. Dermatol.* **1989**, *20*, 537-563.

15) Hölzle, E. In *Hyperhidrosis and Botulinum Toxin in Dermatology*; Karger Publishers, 2002, pp 10-22.

16) Uno, H. *J. Invest. Dermatol.* **1977**, *69*, 112-120.

17) Wilke, K.; Martin, A.; Terstegen, L.; Biel, S. *Int. J. Cosmetic Sci.* **2007**, *29*, 169-179.

18) Morgan, R.; Patterson, M.; Nimmo, M. *Acta Physiol.* **2004**, *182*, 37-43.

19) Mitsubayashi, K.; Suzuki, M.; Tamiya, E.; Karube, I. *Anal. Chim. Acta* **1994**, *289*, 27-34.

20) Patterson, M. J.; Galloway, S. D.; Nimmo, M. A. *Exp. Physiol.* **2000**, *85*, 869-875.

21) Hooton, K.; Han, W.; Li, L. *Anal. Chem.* **2016**, *88*, 7378-7386.

22) Hooton, K.; Li, L. *Anal. Chem.* **2017**.

23) Sato, K.; Leidal, R.; Sato, F. *Am. J. Physiol-Reg. I.* **1987**, *252*, R166-R180.

24) Ready, M.; Quinton, P. *J. Membrane Biol.* **1994**, *140*, 57-67.

25) LeGrys, V. A. *Arch. Pathol. Lab. Med.* **2001**, *125*, 1420-1424.

26) Kintz, P. *Ther. Drug Monit.* **1996**, *18*, 450-455.

27) Huestis, M. A.; Oyler, J. M.; Cone, E. J.; Wstadik, A. T.; Schoendorfer, D.; Joseph, R. E. *J. Chromatogr. B* **1999**, *733*, 247-264.

28) Quattrini, C.; Jeziorska, M.; Tavakoli, M.; Begum, P.; Boulton, A.; Malik, R. *Diabetologia* **2008**, *51*, 1046-1050.

29) Shirreffs, S.; Maughan, R. *J. Appl. Physiol.* **1997**, *82*, 336-341.

30) Jadoon, S.; Karim, S.; Akram, M. R.; Kalsoom Khan, A.; Zia, M. A.; Siddiqi, A. R.; Murtaza, G. *Int. J. Anal. Chem.* **2015**, *2015*.

31) Appenzeller, B. M.; Schummer, C.; Rodrigues, S. B.; Wennig, R. *J. Chromatogr. B* **2007**, *852*, 333-337.

32) Kutyshenko, V. P.; Molchanov, M.; Beskaravayny, P.; Uversky, V. N.; Timchenko, M. A. *PLoS One* **2011**, *6*, e28824.

33) Calderón-Santiago, M.; Priego-Capote, F.; Jurado-Gámez, B.; de Castro, M. L. *J. Chromatogr. A* **2014**, *1333*, 70-78.

34) Calderón-Santiago, M.; Priego-Capote, F.; Turck, N.; Robin, X.; Jurado-Gámez, B.; Sanchez, J. C.; De Castro, M. D. L. *Anal. Bioanal. Chem.* **2015**, *407*, 5381-5392.

35) DeMarco, M. L.; Dietzen, D. J.; Brown, S. M. *Clin. Biochem.* **2015**, *48*, 443-447.

36) Myint, K. T.; Aoshima, K.; Tanaka, S.; Nakamura, T.; Oda, Y. *Anal. Chem.* **2009**, *81*, 1121-1129.

37) Sato, K.; Kang, W. H.; Saga, K.; Sato, K. T. *J. Am. Acad. Dermatol.* **1989**, 20, 537– 563

38) Raiszadeh, M. M.; Ross, M. M.; Russo, P. S.; Schaepper, M. A.; Zhou, W.; Deng, J.; Ng, D.; Dickson, A.;Dickson, C.; Strom, M.*J. Proteome Res.* **2012**, 11, 2127– 2139

39) Mena-Bravo, A.; Luque de Castro, M. D. *J. Pharm. Biomed. Anal.* **2014**, 90, 139– 147

40) Bandodkar, A. J.; Wang, J. *Trends Biotechnol.* **2014**, 32, 363– 371

41) Gao, W.; Emaminejad, S.; Nyein, H. Y. Y.; Challa, S.; Chen, K.; Peck, A.; Fahad, H. M.; Ota, H.; Shiraki, H.;Kiriya, D.*Nature* **2016**, 529, 509– 514

42) Farrell, P. M.; Rosenstein, B. J.; White, T. B.; Accurso, F. J.; Castellani, C.; Cutting, G. R.; Durie, P. R.;Legrys, V. A.; Massie, J.; Parad, R. B.*J. Pediatr.* **2008**, 153, S4– S14

43) Collie, J. T. B.; Massie, R. J.; Jones, O. A. H.; LeGrys, V. A.; Greaves, R. F. *Pediatr Pulmonol* **2014**, 49,106– 117

44) De Giovanni, N.; Fucci, N. *Curr. Med. Chem.* **2013**, 20, 545– 561

45) Kutyshenko, V. P.; Molchanov, M.; Beskaravayny, P.; Uversky, V. N.; Timchenko, M. A. *PLoS One* **2011**, 6,e28824

46) Harker, M.; Coulson, H.; Fairweather, I.; Taylor, D.; Daykin, C. A. *Metabolomics* **2006**, 2, 105– 112

47) Mark, H.; Harding, C. R. *Int. J. Cosmet. Sci.* **2013**, 35, 163– 168

48) Nunome, Y.; Tsuda, T.; Kitagawa, K. *Anal. Sci.* **2010**, 26, 917– 919

49) Calderon-Santiago, M.; Priego-Capote, F.; Jurado-Gamez, B.; Luque de Castro, M. D. *J. Chromatogr., A* **2014**, 1333, 70– 78

50) Calderon-Santiago, M.; Priego-Capote, F.; Turck, N.; Robin, X.; Jurado-Gamez, B.; Sanchez, J. C.;Luque de Castro, M. D. *Anal. Bioanal. Chem.* **2015**, 407, 5381– 5392

51) Dutkiewicz, E. P.; Lin, J. D.; Tseng, T. W.; Wang, Y. S.; Urban, P. L. *Anal. Chem.* **2014**, 86, 2337– 2344

52) Soini, H. A.; Bruce, K. E.; Klouckova, I.; Brereton, R. G.; Penn, D. J.; Novotny, M. V. *Anal. Chem.* **2006**, 78,7161– 7168

53) Xu, Y.; Gong, F.; Dixon, S. J.; Brereton, R. G.; Soini, H. A.; Novotny, M. V.; Oberzaucher, E.; Grammer, K.;Penn, D. J. *Anal. Chem.* **2007**, 79, 5633– 5641

54) Guo, K.; Li, L. *Anal. Chem.* **2009**, 81, 3919– 3932

55) Guo, K.; Li, L. *Anal. Chem.* **2010**, 82, 8789– 8793

56) Zhou, R.; Huan, T.; Li, L. *Anal. Chim. Acta* **2015**, 881, 107– 116

57) Peng, J.; Li, L. *Anal. Chim. Acta* **2013**, 803, 97– 105

58) Guo, K.; Bamforth, F.; Li, L. *J. Am. Soc. Mass Spectrom.* **2011**, 22, 339– 347

59) Peng, J.; Chen, Y. T.; Chen, C. L.; Li, L. *Anal. Chem.* **2014**, 86, 6540– 6547

60) Zheng, J.; Dixon, R. A.; Li, L. *Anal. Chem.* **2012**, 84, 10802– 10811

61) Xu, W.; Chen, D.; Wang, N.; Zhang, T.; Zhou, R.; Huan, T.; Lu, Y.; Su, X.; Xie, Q.; Li, L.*Anal. Chem.***2015**, 87, 829– 836

62) Li, Z. D.; Tatlay, J.; Li, L. *Anal. Chem.* **2015**, 87, 11468– 11474

63) Verde, T.; Shephard, R. J.; Corey, P.; Moore, R. *J. Appl. Physiol.* **1982**, 53, 1540– 1545

64) Wu, Y.; Li, L. *Anal. Chem.* **2012**, 84, 10723– 10731

65) Zhou, R.; Tseng, C. L.; Huan, T.; Li, L. *Anal. Chem.* **2014**, 86, 4675– 4679

66) Huan, T.; Li, L. *Anal. Chem.* **2015**, 87, 1306– 1313

67) Huan, T.; Li, L. *Anal. Chem.* **2015**, 87, 7011– 7016

68) Gentleman, R. C.; Carey, V. J.; Bates, D. M.; Bolstad, B.; Dettling, M.; Dudoit, S.; Ellis, B.; Gautier, L.;Ge, Y. C.; Gentry, J.*Genome Biol.* **2004**, 5, R80

69) Huan, T.; Wu, Y. M.; Tang, C. Q.; Lin, G. H.; Li, L. *Anal. Chem.* **2015**, 87, 9838– 9845

70) Li, L.; Li, R. H.; Zhou, J. J.; Zuniga, A.; Stanislaus, A. E.; Wu, Y. M.; Huan, T.; Zheng, J. M.; Shi, Y.;Wishart, D. S.*Anal. Chem.* **2013**, 85, 3401– 3408

71) McLean, C.; Graham, T. E. *J. Appl. Physiol.* **2002**, 93, 1471– 1478

72) Mangos, J. *Am. J. Physiol.* **1973**, 224, 1235– 1240

73) Han, W.; Li, L. *Metabolomics* **2015**, 11, 1733– 1742

74) Kim, K.; Mall, C.; Taylor, S. L.; Hitchcock, S.; Zhang, C.; Wettersten, H. I.; Jones, A. D.; Chapman, A.;Weiss, R. H. *PLoS One* **2014**, 9, e86223

75) Slupsky, C. M.; Rankin, K. N.; Wagner, J.; Fu, H.; Chang, D.; Weljie, A. M.; Saude, E. J.; Lix, B.;Adamko, D. J.; Shah, S.*Anal. Chem.* **2007**, 79, 6995– 7004

76) Kochhar, S.; Jacobs, D. M.; Ramadan, Z.; Berruex, F.; Fuerholz, A.; Fay, L. B. *Anal. Biochem.* **2006**, 352,274– 281

77) Hodson, M. P.; Dear, G. J.; Roberts, A. D.; Haylock, C. L.; Ball, R. J.; Plumb, R. S.; Stumpf, C. L.;Griffin, J. L.; Haselden, J. N. *Anal. Biochem.* **2007**, 362, 182– 192

78) Plumb, R.; Granger, J.; Stumpf, C.; Wilson, I. D.; Evans, J. A.; Lenz, E. M. *Analyst* **2003**, 128, 819– 823

79) Dunn, W. B.; Lin, W.; Broadhurst, D.; Begley, P.; Brown, M.; Zelena, E.; Vaughan, A. A.; Halsall, A.; Harding, N.; Knowles, J. D.*Metabolomics* **2015**, 11, 9– 26

80) Spaapen, L. J.; Ketting, D.; Wadman, S. K.; Bruinvis, L.; Duran, M. *J. Inherited Metab. Dis.* **1987**, 10, 383–390

81) Iwaki, M.; Murakami, E.; Kikuchi, M.; Wada, A.; Ogiso, T.; Oda, Y.; Kubo, K.; Kakehi, K. *J. Chromatogr., Biomed. Appl.* **1998**, 716, 335– 342

82) Gronwald, W.; Klein, M. S.; Zeltner, R.; Schulze, B. D.; Reinhold, S. W.; Deutschmann, M.; Immervoll, A. K.;Boger, C. A.; Banas, B.; Eckardt, K. U.*Kidney Int.* **2011**, 79, 1244– 1253

83) Gupta, A.; Dwivedi, M.; Nagana Gowda, G. A.; Ayyagari, A.; Mahdi, A. A.; Bhandari, M.; Khetrapal, C. L.*NMR Biomed.* **2005**, 18, 293– 299

84) Li, M.; Wang, B.; Zhang, M.; Rantalainen, M.; Wang, S.; Zhou, H.; Zhang, Y.; Shen, J.; Pang, X.; Zhang, M.*Proc. Natl. Acad. Sci. U. S. A.* **2008**, 105, 2117– 2122

85) Nicholson, J. K.; Holmes, E.; Wilson, I. D. *Nat. Rev. Microbiol.* **2005**, 3, 431– 438

86) Lelo, A.; Miners, J. O.; Robson, R. A.; Birkett, D. J. *Br. J. Clin. Pharmacol.* **1986**, 22, 183– 186

87) Ou-Yang, D. S.; Huang, S. L.; Wang, W.; Xie, H. G.; Xu, Z. H.; Shu, Y.; Zhou, H. H. *Br. J. Clin. Pharmacol.***2000**, 49, 145– 151

88) De Feo, P.; Di Loreto, C.; Lucidi, P.; Murdolo, G.; Parlanti, N.; De Cicco, A.; Piccioni, F.; Santeusanio, F. *J. Endocrinol. Invest.* **2003**, 26, 851– 854

89) Haralambie, G.; Berg, A. *Eur. J. Appl. Physiol. Occup. Physiol.* **1976**, 36, 39– 48

90) Refsum, H. E.; Gjessing, L. R.; Strømme, S. B. *Scand. J. Clin. Lab. Invest.* **1979**, 39, 407– 413

91) Tunnicliff, G. *Gen. Pharmacol.* **1998**, 31, 503– 509

92) Mena-Bravo, A.; de Castro, M. D. L. *J. Pharm. Biomed. Anal.* **2014**, 90, 139– 147

93) Calderón-Santiago, M.; Priego-Capote, F.; Turck, N.; Robin, X.; Jurado-Gámez, B.; Sanchez, J. C.;Luque de Castro, M. D. *Anal. Bioanal. Chem.* **2015**, 407, 5381– 5392

94) Delgado-Povedano, M. M.; Calderón-Santiago, M.; Priego-Capote, F.; Luque de Castro, M. D. *Anal. Chim. Acta* **2016**, 905, 115– 125

95) Hooton, K.; Han, W.; Li, L. *Anal. Chem.* **2016**, 88, 7378– 7386

96) Dutkiewicz, E. P.; Chiu, H. Y.; Urban, P. L. *Anal. Chem.* **2017**, 89, 2664– 2670

97) Imani, S.; Bandodkar, A. J.; Mohan, A. M. V.; Kumar, R.; Yu, S. F.; Wang, J.; Mercier, P. P. *Nat. Commun.* **2016**, 7, 11650

98) Jia, W. Z.; Bandodkar, A. J.; Valdes-Ramirez, G.; Windmiller, J. R.; Yang, Z. J.; Ramirez, J.; Chan, G.;Wang, J. *Anal. Chem.* **2013**, 85, 6553– 6560

99) Polliack, A.; Taylor, R.; Bader, D. *J. Rehabil. Res. Dev.* **1993**, 30, 250– 259

100) Tur-Garcia, E. L.; Davis, F.; Collyer, S. D.; Holmes, J. L.; Barr, H.; Higson, S. P. J. *Sens. Actuators, B* **2017**,242, 502– 510

101) Farrell, P. M.; Rosenstein, B. J.; White, T. B.; Accurso, F. J.; Castellani, C.; Cutting, G. R.; Durie, P. R.;Legrys, V. A.; Massie, J.; Parad, R. B.*J. Pediatr.* **2008**, 153, S4– S14

102) Calderon-Santiago, M.; Priego-Capote, F.; Jurado-Gamez, B.; de Castro, M. D. L. *J. Chromatogr. A* **2014**,1333, 70– 78

103) Calderon-Santiago, M.; Priego-Capote, F.; Turck, N.; Robin, X.; Jurado-Gamez, B.; Sanchez, J. C.;de Castro, M. D. L. *Anal. Bioanal. Chem.* **2015**, 407, 5381– 5392

104) De Giovanni, N.; Fucci, N. *Curr. Med. Chem.* **2013**, 20, 545– 561

105) Huestis, M. A.; Oyler, J. M.; Cone, E. J.; Wstadik, A. T.; Schoendorfer, D.; Joseph, R. E., Jr *J. Chromatogr., Biomed. Appl.* **1999**, 733, 247– 264

106) Kintz, P.; Tracqui, A.; Mangin, P.; Edel, Y. *J. Anal. Toxicol.* **1996**, 20, 393– 397

107) Kintz, P.; Samyn, N. In *Handbook of Analytical Separations*; Maciej, J. B., Ed.; Elsevier Science B.V.: New York, **2000**; Vol. 2, pp 459– 488.

108) Barnes, A. J.; De Martinis, B. S.; Gorelick, D. A.; Goodwin, R. S.; Kolbrich, E. A.; Huestis, M. A. *Clin. Chem.***2009**, 55, 454– 462

109) Gambelunghe, C.; Fucci, N.; Aroni, K.; Bacci, M.; Marcelli, A.; Rossi, R. *Ther. Drug Monit.* **2016**, 38, 634–639

110) Guo, K.; Li, L. *Anal. Chem.* **2009**, 81, 3919– 3932

111) Huan, T.; Li, L. *Anal. Chem.* **2015**, 87, 7011– 7016

112) Wu, Y.; Li, L. *Anal. Chem.* **2012**, 84, 10723– 10731

113) Zhou, R.; Tseng, C. L.; Huan, T.; Li, L. *Anal. Chem.* **2014**, 86, 4675– 4679

114) Huan, T.; Li, L. *Anal. Chem.* **2015**, 87, 1306-1313

115) Huan, T.; Wu, Y.; Tang, C.; Lin, G.; Li, L. *Anal. Chem.* **2015**, 87, 9838– 9845

116) Li, L.; Li, R.; Zhou, J.; Zuniga, A.; Stanislaus, A. E.; Wu, Y.; Huan, T.; Zheng, J.; Shi, Y.; Wishart, D. S., et al. *Anal. Chem.* **2013**, 85, 3401-3408.

117) Warren, A. G.; Brorson, H.; Borud, L. J.; Slavin, S. A. *Ann. Plast. Surg.* **2007**, 59, 464-472.

118) Ly, C.; Kataru, R.; Mehrara, B. *Int. J. Mol. Sci.* **2017**, 18, 171.

119) Schünemann, H.; Willich, N. *Deut. Med. Wochenschr.* **1997**, 122, 536-541.

120) Petrek, J. A.; Senie, R. T.; Peters, M.; Rosen, P. P. *Cancer* **2001**, 92, 1368-1377.

121) Querci della Rovere, G.; Ahmad, I.; Singh, P.; Ashley, S.; Daniels, I. R.; Mortimer, P. *Ann. Roy. Coll. Surg.* **2003**, 85, 158-161.

122) Ozaslan, C.; Kuru, B. *Am. J. Surg.* **2004**, 187, 69-72.

123) Hinrichs, C. S.; Watroba, N. L.; Rezaishiraz, H.; Giese, W.; Hurd, T.; Fassl, K. A.; Edge, S. B. *Ann. Surg. Oncol.* **2004**, 11, 573.

124) Hooton, K.; Li, L. *Anal. Chem.* **2017**, 89, 7847-7851.

125) Wu, Y.; Li, L. *Anal. Chem.* **2012**, 84, 10723-10731.

126) Zhou, R.; Tseng, C.-L.; Huan, T.; Li, L. *Anal. Chem.* **2014**, 86, 4675-4679.

127) Huan, T.; Li, L. *Anal. Chem.* **2015**, 87, 1306-1313.

128) Huan, T.; Li, L. *Anal. Chem.* **2015**, 87, 7011-7016.

129) Xia, J.; Wishart, D. S. *Curr. Protoc. Bioinformatics* **2016**, 14.10. 11-14.10. 91.

130) Huan, T.; Wu, Y.; Tang, C.; Lin, G.; Li, L. *Anal. Chem*. **2015**, 87, 9838-9845.

131) Li, L.; Li, R.; Zhou, J.; Zuniga, A.; Stanislaus, A. E.; Wu, Y.; Huan, T.; Zheng, J.; Shi, Y.; Wishart, D. S. *Anal. Chem.* **2013**, 85, 3401-3408.

132) Walsh, M. C.; Brennan, L.; Malthouse, J. P. G.; Roche, H. M.; Gibney, M. J. *Am. J. Clin. Nutr*.**2006**, 84, 531-539.

133) Slupsky, C. M.; Rankin, K. N.; Wagner, J.; Fu, H.; Chang, D.; Weljie, A. M.; Saude, E. J.; Lix, B.; Adamko, D. J.; Shah, S. *Anal. Chem.* **2007**, 79, 6995-7004.

134) Le, J.; Perier, C.; Peyroche, S.; Rascle, F.; Blanchon, M.; Gonthier, R.; Frey, J.; Chamson, A. *Amino Acids* **1999**, 17, 315-322.

Appendix

Chapter 2: Comprehensive and Quantitative Profiling of the Human Sweat Submetabolome Using High-Performance Chemical Isotope Labeling LC-MS

DAY 1
10-20min
20-30min
30-40min

DAY 2
10-20min
20-30min
30-40min

DAY 3
10-20min
20-30min
30-40min
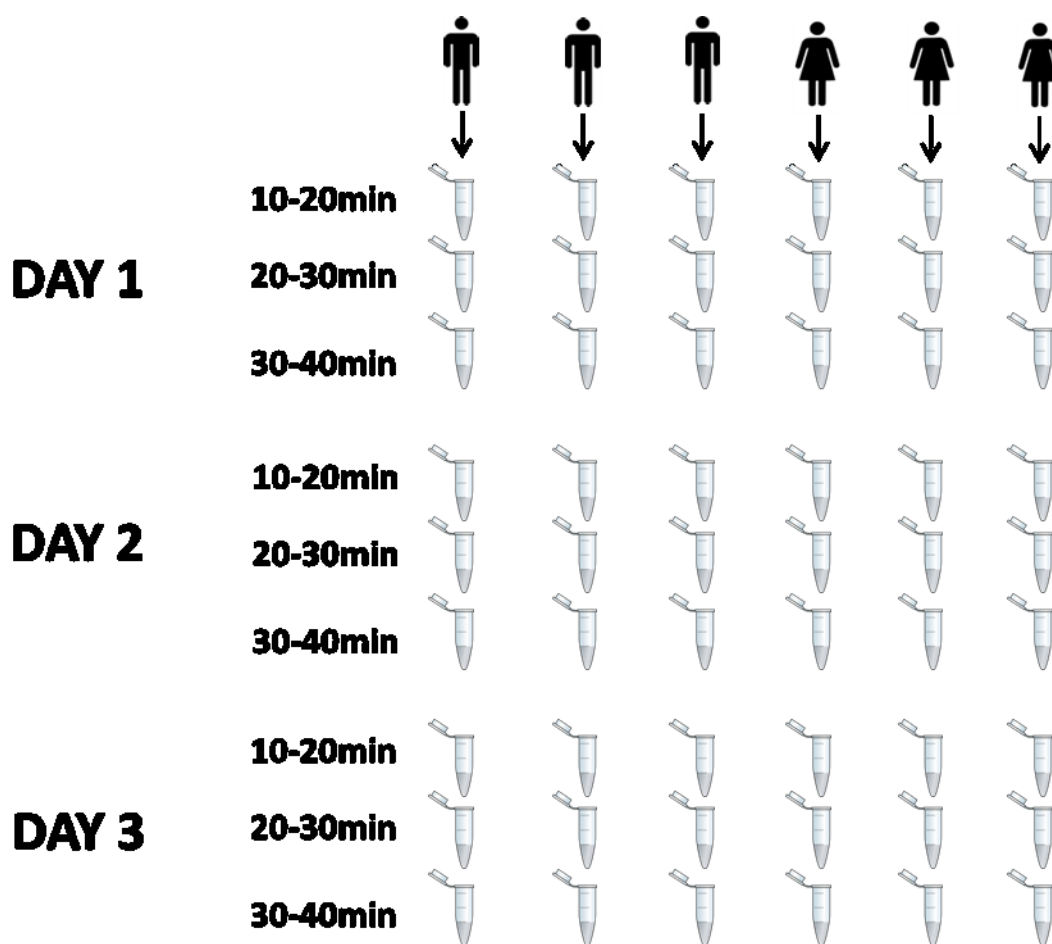
Appendix Figure A2.1. Diagram of sweat samples collected from the 3 male and 3 female volunteers. On each day, 3 sweat samples are taken from each volunteer. One during 10-20 minutes of exercise, one during 20-30 minutes of exercise, and one during 30-40 minutes of exercise. A total of 54 sweat samples were collected.
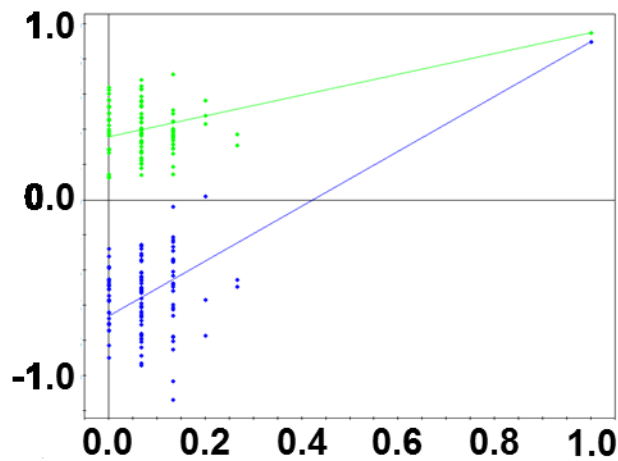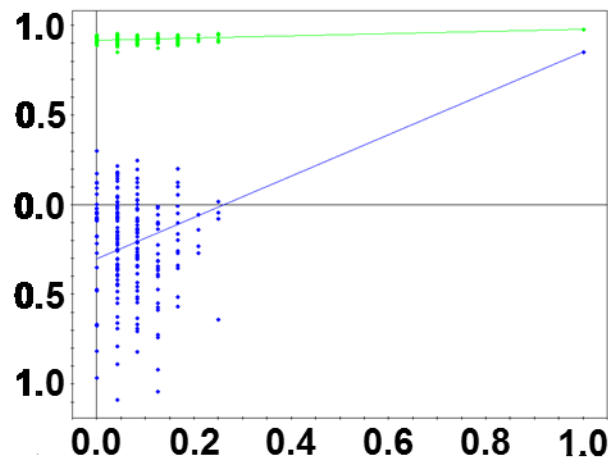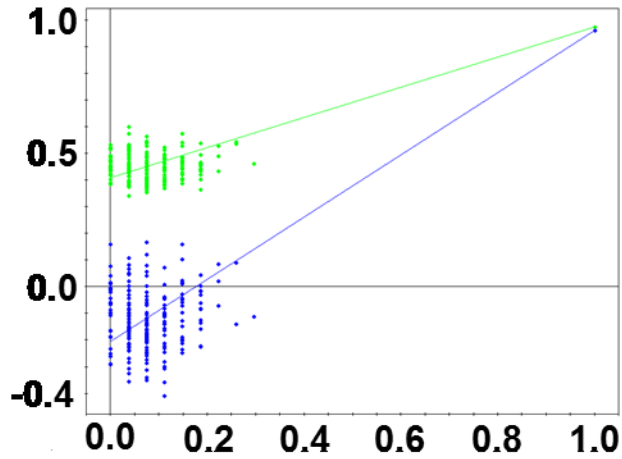
Appendix Figure A2.2. Permutations test results from (top) male vs. female, (middle) T1 vs. T2. vs. T3, (bottom) individual comparison PLS-DA models. (A) Intercepts: R2 = 0.0, 0.408, Q2 = 0.0, -0.207; (B) Intercepts: R2 = 0.0, 0.918, Q2 = 0.0, -0.305; (C) Intercepts: R2 = 0.0, 0.359, Q2 = 0.0, -0.662

Appendix Table A2.1. Metabolites positively identified using the dansyl standards library based on accurate mass and retention time matches.

Compound Name	HMDB No.	Dansylated Mass + H (Da)	Monoisotopic Mass (Da)	Calibrated RT (min)
O-Phosphoethanolamine	HMDB00224	375.0774	141.0191	1.81
Taurine	HMDB00251	359.0730	125.0147	2.16
L-Arginine	HMDB00517	408.1700	174.1117	2.36
Guanidine	HMDB01842	293.1067	59.0483	2.80
Homo-L-arginine	HMDB00670	422.1856	188.1273	2.81
L-Asparagine	HMDB00168	366.1118	132.0535	2.88
L-Glutamine	HMDB00641	380.1275	146.0691	3.20
Gamma Glutamylglutamic acid	HMDB11737	510.1541	276.0958	3.30
Methionine Sulfoxide	HMDB02005	399.1043	165.0460	3.58
Citrulline	HMDB00904	409.1540	175.0957	3.62
Methionine Sulfoxide – Isomer	HMDB02005	399.1043	165.0460	4.04
L-Homoserine	HMDB00719	353.1166	119.0582	4.06
L-Serine	HMDB00187	339.1009	105.0426	4.35
L-Glutamic Acid	HMDB00148	381.1115	147.0532	4.89
L-Aspartic Acid	HMDB00191	367.0958	133.0375	5.00
L-Threonine	HMDB00167	353.1166	119.0582	5.83
N6-Acetyl-L-Lysine	HMDB00206	422.1744	188.1161	6.04
Glycine	HMDB00123	309.0903	75.0320	6.56
Glycylproline	HMDB00721	406.1431	172.0848	7.19
5-Aminolevulinic acid	HMDB01149	365.1166	131.0582	7.45
L-Alanine	HMDB00161	323.1060	89.0477	7.54
Gamma-Aminobutyric acid	HMDB00112	337.1216	103.0633	7.77
Uridine	HMDB00296	478.1279	244.0695	7.81
4-Aminohippuric acid	HMDB01867	428.1275	194.0691	8.44
3-Aminoisobutanoic acid	HMDB03911	337.1216	103.0633	8.63
Uridine - H2O	HMDB00296	460.1173	244.0695	8.67
5-Aminopentanoic acid	HMDB03355	351.1373	117.0790	8.76
5-Hydroxymethyluracil	HMDB00469	376.0962	142.0378	8.81
Serinyl-Leucine	HMDB29043	452.1850	218.1267	8.89

Glycyl-Valine	HMDB28854	408.1588	174.1004	8.94
L-Alpha-aminobutyric acid	HMDB00452	337.1216	103.0633	9.14
L-Glutamic Acid - H2O	HMDB00148	363.1009	147.0532	9.38
Phenylalanyl-Glycine	HMDB28995	456.1588	222.1004	9.41
L-Aspartyl-L-phenylalanine	HMDB00706	514.1642	280.1059	10.11
L-Proline	HMDB00162	349.1216	115.0633	10.15
Phenylalanyl-Alanine	HMDB28988	470.1744	236.1161	10.58
Glycyl-Isoleucine	HMDB28844	422.1744	188.1161	10.78
L-Valine	HMDB00883	351.1373	117.0790	10.81
L-Methionine	HMDB00696	383.1094	149.0510	10.87
Glycyl-L-Leucine	HMDB00759	422.1744	188.1161	11.07
Imidazoleacetic acid	HMDB02024	360.1012	126.0429	11.15
Alanyl-Leucine	HMDB28691	436.1901	202.1317	11.36
Uracil	HMDB00300	346.0856	112.0273	11.40
Glycyl-Tryptophan	HMDB28852	495.1697	261.1113	11.42
L-Tryptophan	HMDB00929	438.1482	204.0899	11.44
Glycyl-Phenylalanine	HMDB28848	456.1588	222.1004	11.85
Alanyl-Phenylalanine	HMDB28694	470.1744	236.1161	12.10
6-Hydroxynicotinic acid	HMDB02658	373.0853	139.0269	12.50
L-Phenylalanine	HMDB00159	399.1373	165.0790	12.72
L-Isoleucine	HMDB00172	365.1529	131.0946	13.02
Leucyl-Proline	HMDB28937	462.2057	228.1474	13.05
Gamma-Aminobutyric acid - H2O	HMDB00112	319.1144	103.0633	13.27
L-leucine	HMDB00687	365.1529	131.0946	13.32
Urocanic acid	HMDB00301	372.1012	138.0429	13.51
Phenylalanyl-Valine	HMDB29008	498.2057	264.1474	13.69
5-Hydroxylysine	HMDB00450	315.1085	162.1004	13.93
L-Cystine	HMDB00192	354.0702	240.0238	14.06
Hydroxyphenyllactici acid	HMDB00755	416.1162	182.0579	14.41
Theophylline	HMDB01889	414.1230	180.0647	15.47
Phenyl-Leucine	N/A	512.2214	278.1631	15.87
Ornithine	HMDB00214	300.1033	132.0899	16.30

Leucyl-phenylalanine	HMDB13243	512.2214	278.1630	16.62
Histidinyl-Alanine	HMDB28878	460.1649	226.1066	16.76
p-Hydroxyphenylacetic acid	HMDB00020	386.1057	152.0473	16.95
Aniline	HMDB03012	327.1162	93.0578	17.29
L-Lysine	HMDB00182	307.1111	146.1055	17.39
Alanyl-Histidine	HMDB28689	460.1649	226.1066	17.69
4-Hydroxybenzoic acid	HMDB00500	372.0900	138.0317	17.72
Indole-3-carboxylic acid	HMDB03320	395.1060	161.0477	19.27
Tyrosyl-Glycine	HMDB29105	353.1060	238.0954	20.02
Tyrosyl-Alanine	HMDB29098	360.1138	252.1110	20.87
1,4-diaminobutane	HMDB01414	278.1083	88.1000	21.16
Glycyl-Tyrosine	HMDB28853	353.1060	238.0954	21.48
3-Hydroxymandelic acid – COOH	HMDB00750	356.0951	168.0423	21.51
Alanyl-Tyrosine	HMDB28699	360.1138	252.1110	21.79
L-Tyrosine	HMDB00158	324.5953	181.0739	22.68
Histamine	HMDB00870	578.1901	111.0796	22.72
Phenol	HMDB00228	328.1002	94.0419	23.23
Leucyl-Tyrosine	HMDB28941	381.1373	294.1580	23.82
Phenylalanyl-Tyrosine	HMDB29007	398.1295	328.1423	23.99
Protocatechuic acid	HMDB01856	311.0716	154.0266	24.55
p-Cresol	HMDB01858	342.1158	108.0575	24.55
Tyramine	HMDB00306	302.6004	137.0841	25.79

Appendix Table A2.2. Metabolites positively identified using the dansyl standards library based on accurate mass and retention time matches in the gender comparison.

Compound Name	HMDB No.	Dansylated Mass + H (Da)	Monoisotopic Mass (Da)	Calibrated RT (min)
O-Phosphoethanolamine	HMDB00224	375.0774	141.0191	1.81
L-Glutamic Acid	HMDB00148	381.1115	147.0532	4.89
Glycyl-Valine	HMDB28854	408.1588	174.1004	8.94
L-Glutamic Acid - H2O	HMDB00148	363.1009	147.0532	9.38
6-Hydroxynicotinic acid	HMDB02658	373.0853	139.0269	12.5
Leucyl-Proline	HMDB28937	462.2057	228.1474	13.05
Urocanic acid	HMDB00301	372.1012	138.0429	13.51
Hydroxyphenyllactici acid	HMDB00755	416.1162	182.0579	14.41
Theophylline	HMDB01889	414.1230	180.0647	15.47
Ornithine	HMDB00214	300.1033	132.0899	16.3
Aniline	HMDB03012	327.1162	93.0578	17.29
1,4-diaminobutane	HMDB01414	278.1083	88.1000	21.16
Glycyl-Tyrosine	HMDB28853	353.1060	238.0954	21.48
Alanyl-Tyrosine	HMDB28699	360.1138	252.1110	21.79

Appendix Table A2.3. Metabolites positively identified using the dansyl standards library based on accurate mass and retention time matches in the exercise time comparison.

Compound Name	HMDB No.	Dansylated Mass + H (Da)	Monoisotopic Mass (Da)	Calibrated RT (min)
L-Arginine	HMDB00517	408.1700	174.1117	2.36
Guanidine	HMDB01842	293.1067	59.0483	2.80
L-Asparagine	HMDB00168	366.1118	132.0535	2.88
Methionine Sulfoxide	HMDB02005	399.1043	165.0460	3.58
Citrulline	HMDB00904	409.1540	175.0957	3.62
Methionine Sulfoxide – Isomer	HMDB02005	399.1043	165.0460	4.04
L-Glutamic Acid	HMDB00148	381.1115	147.0532	4.89
L-Threonine	HMDB00167	353.1166	119.0582	5.83
Glycylproline	HMDB00721	406.1431	172.0848	7.19
5-Aminolevulinic acid	HMDB01149	365.1166	131.0582	7.45
Glycyl-Valine	HMDB28854	408.1588	174.1004	8.94
L-Valine	HMDB00883	351.1373	117.0790	10.81
Glycyl-L-Leucine	HMDB00759	422.1744	188.1161	11.07
Imidazoleacetic acid	HMDB02024	360.1012	126.0429	11.15
6-Hydroxynicotinic acid	HMDB02658	373.0853	139.0269	12.50
L-Phenylalanine	HMDB00159	399.1373	165.0790	12.72
L-Isoleucine	HMDB00172	365.1529	131.0946	13.02
Leucyl-Proline	HMDB28937	462.2057	228.1474	13.05
L-leucine	HMDB00687	365.1529	131.0946	13.32
Ornithine	HMDB00214	300.1033	132.0899	16.30
Histidinyl-Alanine	HMDB28878	460.1649	226.1066	16.76
L-Lysine	HMDB00182	307.1111	146.1055	17.39

Alanyl-Histidine	HMDB28689	460.1649	226.1066	17.69
L-Tyrosine	HMDB00158	324.5953	181.0739	22.68
Histamine	HMDB00870	578.1901	111.0796	22.72

Chapter 3: Non-occlusive Sweat Collection Combined with Chemical Isotope Labeling LC-MS for Human Sweat Metabolomics and Mapping the Sweat Metabolomes at Different Skin Locations
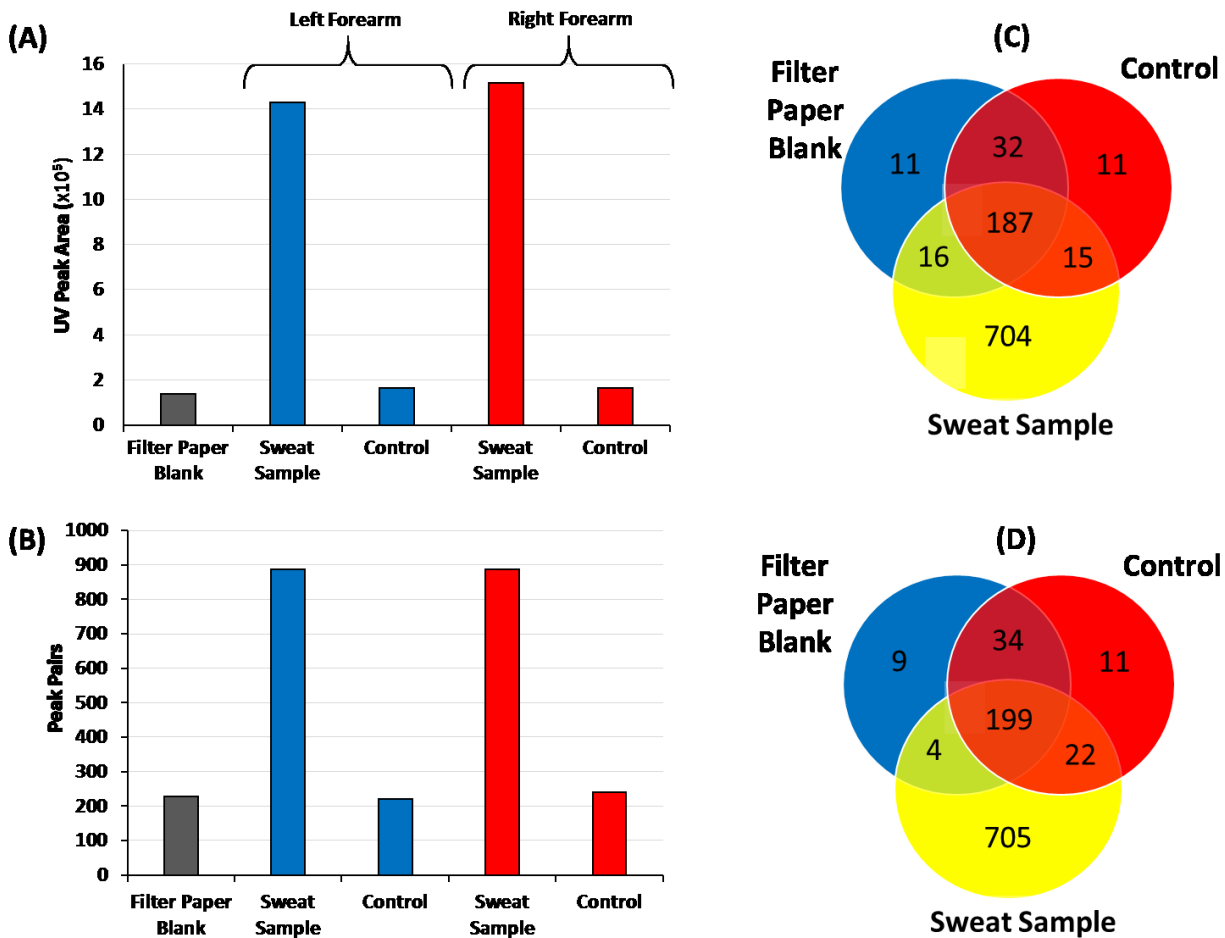
Appendix Figure A3.1. (A) UV peak and (B) peak pair number of sweat and control samples to test for environmental contamination. Venn diagrams of peak pairs detected for (C) left and (D) right forearm experiments.

Appendix Table A3.1. Metabolites positively identified using the dansyl standards library based on accurate mass and retention time matches.

Compound Name	HMDB No.	Dansylated Mass + H (Da)	Monoisotopic Mass (Da)	Calibrated RT (min)
O-Phosphoethanolamine	HMDB00224	375.0774	141.0191	1.90
Taurine	HMDB00251	359.0730	125.0147	2.36
L-Arginine	HMDB00517	408.1700	174.1117	2.45
Homo-L-arginine	HMDB00670	422.1856	188.1273	2.86
Symmetric dimethylarginine	HMDB03334	436.2013	202.1430	3.02
L-Asparagine	HMDB00168	366.1118	132.0535	3.21
L-Glutamine	HMDB00641	380.1275	146.0691	3.52
Citrulline	HMDB00904	409.1540	175.0957	3.64
Methionine Sulfoxide	HMDB02005	399.1043	165.0460	3.66
Methionine Sulfoxide - Isomer	HMDB02005	399.1043	165.0460	4.16
L-Serine	HMDB00187	339.1009	105.0426	4.40
L-Glutamic Acid	HMDB00148	381.1115	147.0532	4.90
L-Aspartic Acid	HMDB00191	367.0958	133.0375	5.00
Trans-4-Hydroxyl-L-Proline	HMDB00725	365.1166	131.0582	5.22
N6-Acetyl-L-Lysine	HMDB00206	422.1744	188.1161	5.56
Ethanolamine	HMDB00149	295.1111	61.0528	6.16
Glycine	HMDB00123	309.0903	75.0320	6.59
N-Alpha-acetyllysine	HMDB00446	422.1744	188.1161	6.71
Glycylproline	HMDB00721	406.1431	172.0848	7.02
N-Acetylputrescine	HMDB02064	364.1689	130.1106	7.03
L-Alanine	HMDB00161	323.1060	89.0477	7.59
Gamma-Aminobutyric acid	HMDB00112	337.1216	103.0633	7.74

3-Aminoisobutanoic acid	HMDB03911	337.1216	103.0633	8.69
Serinyl-Leucine	HMDB29043	452.1850	218.1267	8.71
5-Aminopentanoic acid	HMDB03355	351.1373	117.0790	8.73
5-Hydroxymethyluracil	HMDB00469	376.0962	142.0378	8.99
Serinyl-Leucine	HMDB29043	452.1850	218.1267	9.13
L or D-Alpha-aminobutyric acid	HMDB00452	337.1216	103.0633	9.20
L-Glutamic Acid - H2O	HMDB00148	363.1009	147.0532	9.26
Phenylalanyl-Glycine	HMDB28995	456.1588	222.1004	9.40
Methylcysteine	HMDB02108	369.0937	135.0354	9.54
Serinyl-Phenylalanine	HMDB29046	486.1693	252.1110	9.58
L-Aspartyl-L-phenylalanine	HMDB00706	514.1642	280.1059	9.75
Threoninyl-Leucine	HMDB29065	466.2006	232.1423	10.06
L-Proline	HMDB00162	349.1216	115.0633	10.19
Phenylalanyl-Alanine	HMDB28988	470.1744	236.1161	10.60
Imidazoleacetic acid	HMDB02024	360.1012	126.0429	10.89
L-Methionine	HMDB00696	383.1094	149.0510	10.92
L-Valine	HMDB00883	351.1373	117.0790	10.99
Alanyl-Leucine	HMDB28691	436.1901	202.1317	11.08
Glycyl-Tryptophan	HMDB28852	495.1697	261.1113	11.11
Uracil	HMDB00300	346.0856	112.0273	11.25
Alanyl-Leucine	HMDB28691	436.1901	202.1317	11.39
L-Tryptophan	HMDB00929	438.1482	204.0899	11.49
Glycyl-Phenylalanine	HMDB28848	456.1588	222.1004	11.62
Alanyl-Phenylalanine	HMDB28694	470.1744	236.1161	11.94

Diaminopimelic acid	HMDB01370	329.1060	190.0954	12.47
L-Phenylalanine	HMDB00159	399.1373	165.0790	12.77
Diaminopimelic acid - Isomer	HMDB01370	329.1060	190.0954	12.91
3-Hydroxymandelic acid	HMDB00750	402.1006	168.0423	12.93
Leucyl-Proline	HMDB28937	462.2057	228.1474	12.95
L-Isoleucine	HMDB00172	365.1529	131.0946	13.07
Urocanic acid	HMDB00301	372.1012	138.0429	13.24
L-leucine	HMDB00687	365.1529	131.0946	13.33
Alpha-Aspartyl-lysine	HMDB04987	364.6246	261.1325	13.56
5-Hydroxylysine	HMDB00450	315.1085	162.1004	13.91
Hydroxyphenyllactic acid	HMDB00755	416.1162	182.0579	14.15
L-Cystine	HMDB00192	354.0702	240.0238	14.18
5-Hydroxyindoleacetic acid	HMDB00763	425.1166	191.0582	15.18
Theophylline	HMDB01889	414.1230	180.0647	15.38
Phenyl-Leucine	N/A	512.2214	278.1631	15.82
Acetaminophen	HMDB01859	385.1216	151.0633	16.16
Ornithine	HMDB00214	300.1033	132.0899	16.40
Leucyl-phenylalanine	HMDB13243	512.2214	278.1630	16.51
3-Hydroxyphenylacetic acid	HMDB00440	386.1057	152.0473	16.72
Gentisic acid	HMDB00152	388.0849	154.0266	17.05
Aniline	HMDB03012	327.1162	93.0578	17.37
L-Lysine	HMDB00182	307.1111	146.1055	17.47
4-Hydroxybenzoic acid	HMDB00500	372.0900	138.0317	17.49
Alanyl-Histidine	HMDB28689	460.1649	226.1066	17.67

L-Histidine	HMDB00177	389.1278	155.0695	18.18
Tyrosyl-Glycine	HMDB29105	353.1060	238.0954	19.89
Tyrosyl-Alanine	HMDB29098	360.1138	252.1110	20.78
1,4-diaminobutane	HMDB01414	278.1083	88.1000	21.09
Glycyl-Tyrosine	HMDB28853	353.1060	238.0954	21.36
3-Hydroxymandelic acid - COOH	HMDB00750	356.0951	168.0423	21.56
Alanyl-Tyrosine	HMDB28699	360.1138	252.1110	21.74
Cadaverine	HMDB02322	285.1162	102.1157	22.38
L-Tyrosine	HMDB00158	324.5953	181.0739	22.66
Tyrosyl-Valine	HMDB29118	374.1295	280.1423	22.84
4-Nitrophenol	HMDB01232	373.0853	139.0269	23.46
Tyrosyl-Leucine	HMDB29109	381.1373	294.1580	23.80
Phenylalanyl-Tyrosine	HMDB29007	398.1295	328.1423	23.99
Tyramine	HMDB00306	302.6004	137.0841	25.80
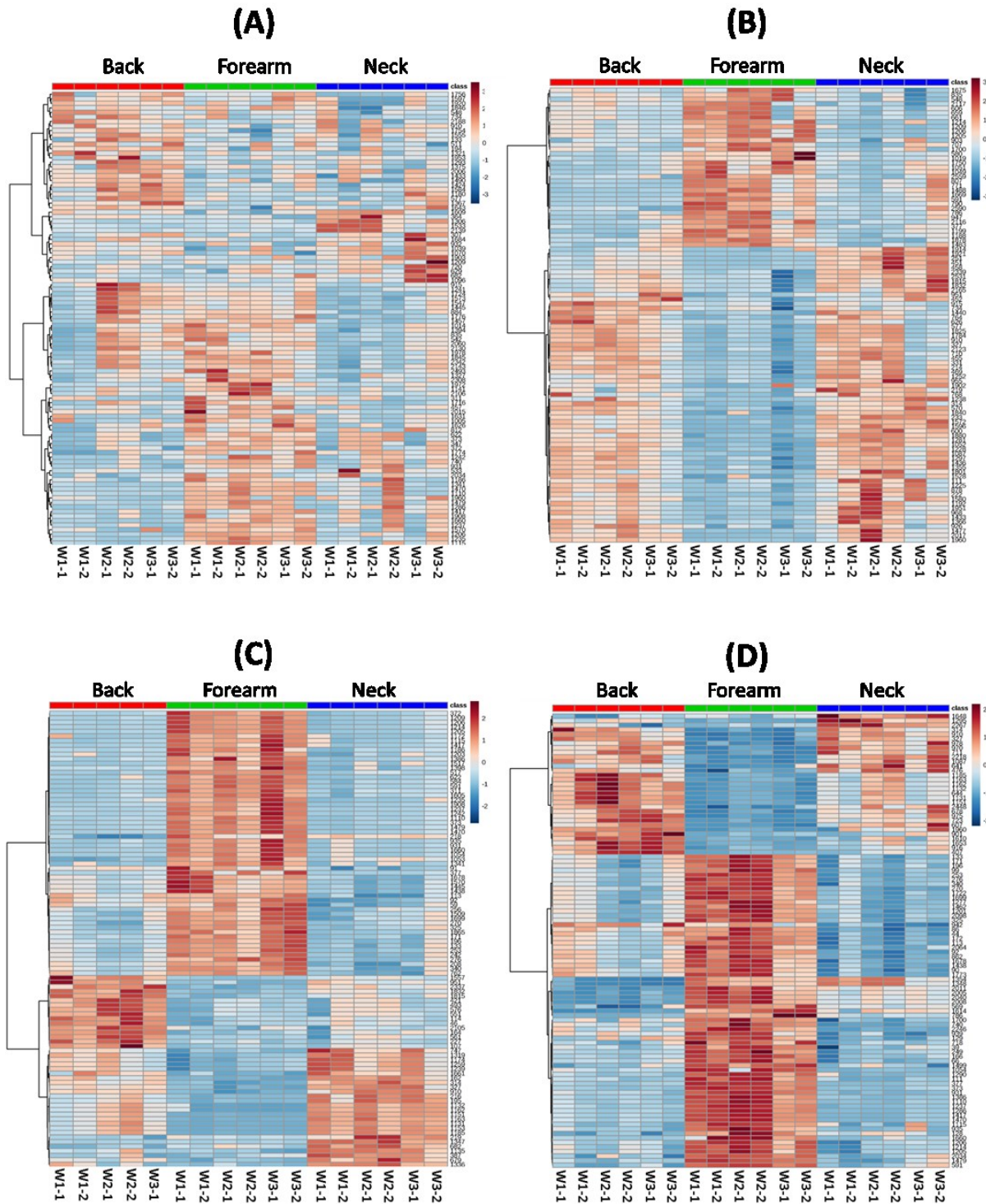
Appendix Figure A3.2. Heat maps showing the top 100 significant metabolites: (A) subject #1, (B) subject #2, (C) subject #3, (D) subject #4. The bottom axis, Wx-y, refers to the replicate sample spot y collected from week x (e.g., W1-1 refers to the replicate sample spot 1 collected in week 1, while W1-2 refers to the replicate sample spot 2 collected in week 1).

Appendix Figure A3.3. Heat maps showing the top 100 significant metabolites: (A) subject #5, (B) subject #6, (C) subject #7, (D) subject #8.

Appendix Figure A3.4. Heat maps showing the top 100 significant metabolites: (A) subject #9, (B) subject #10, (C) subject #11, (D) subject #12.
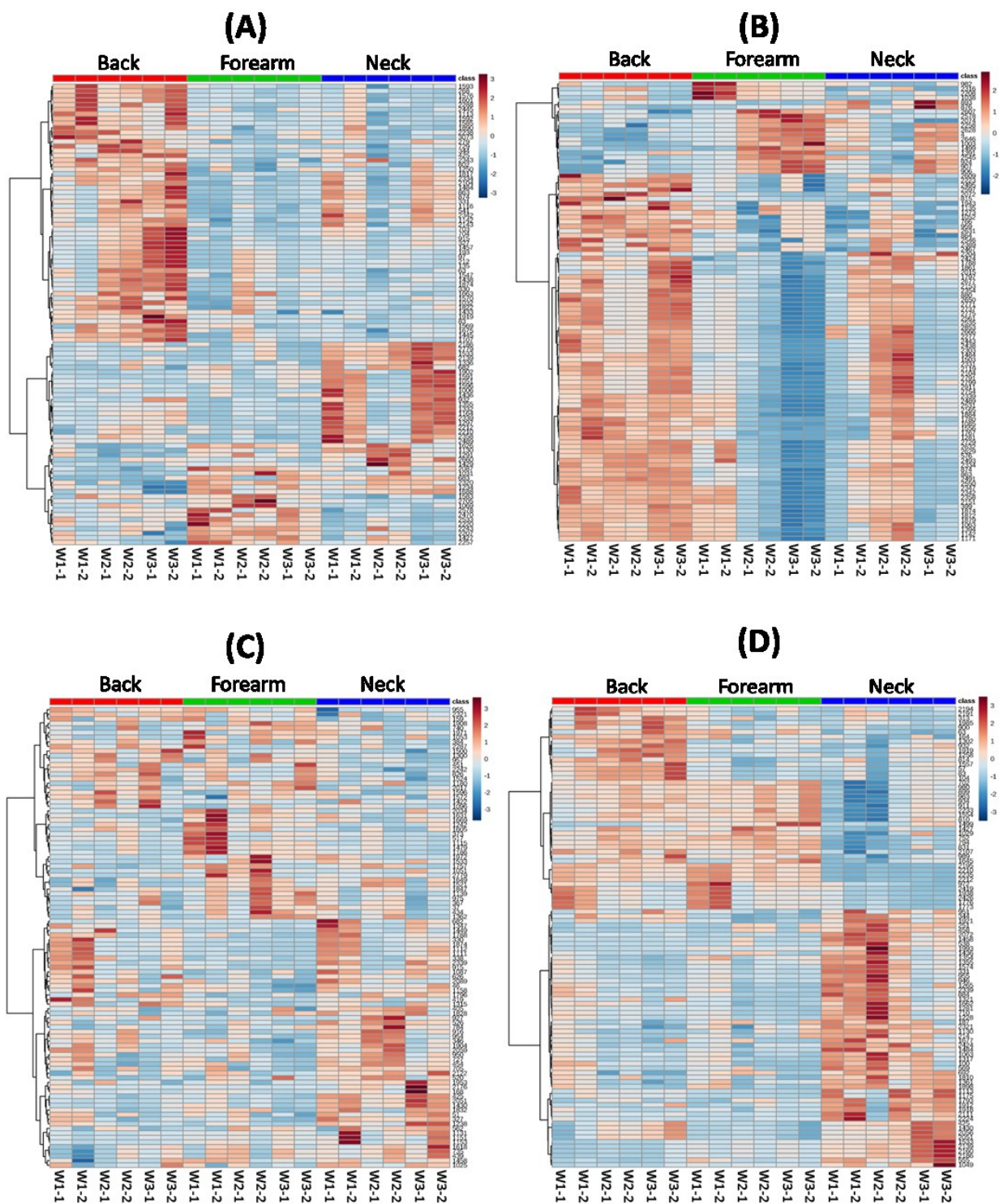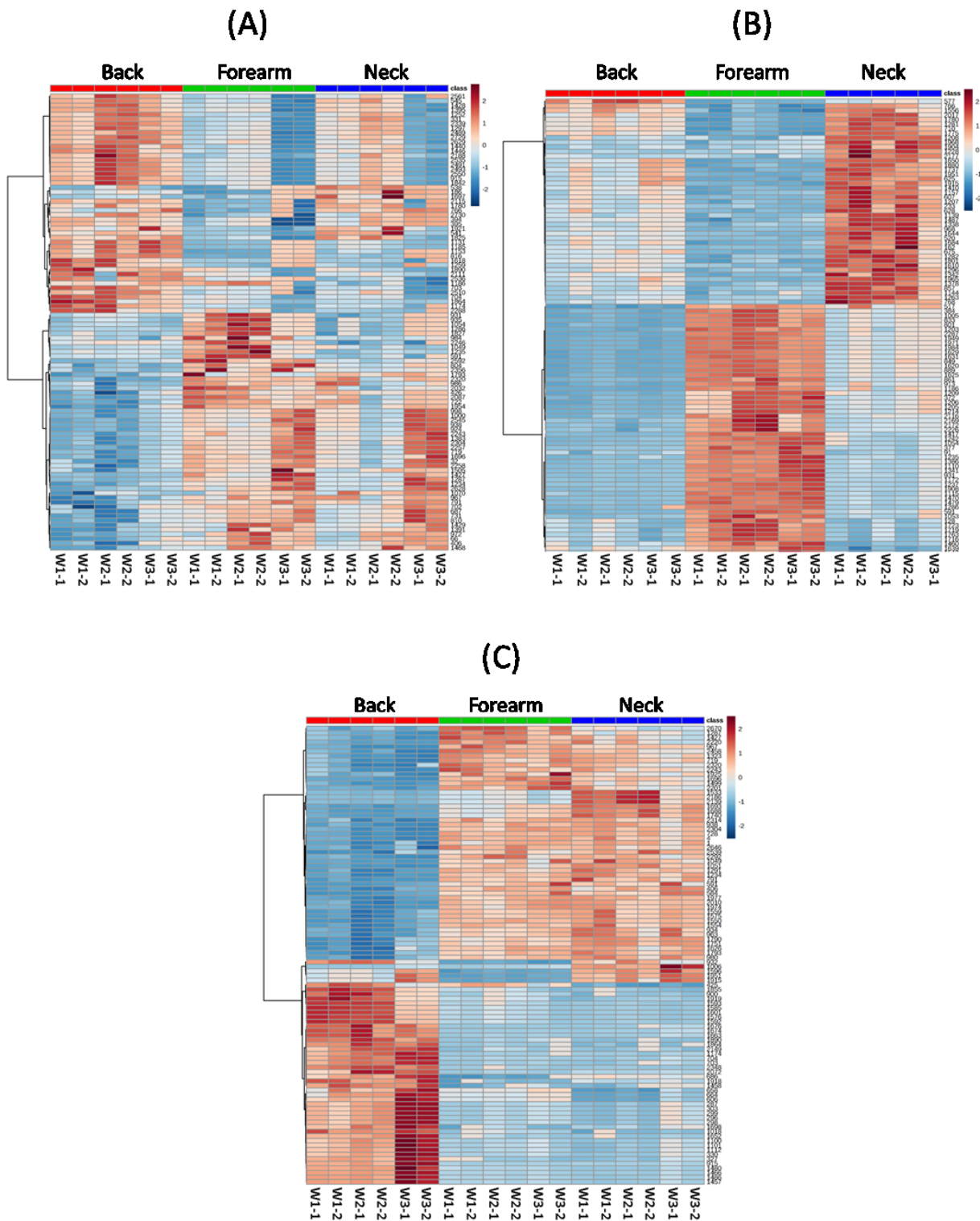
Appendix Figure A3.5. Heat maps showing the top 100 significant metabolites: (A) subject #13, (B) subject #14, (C) subject #15, (D) subject #16.
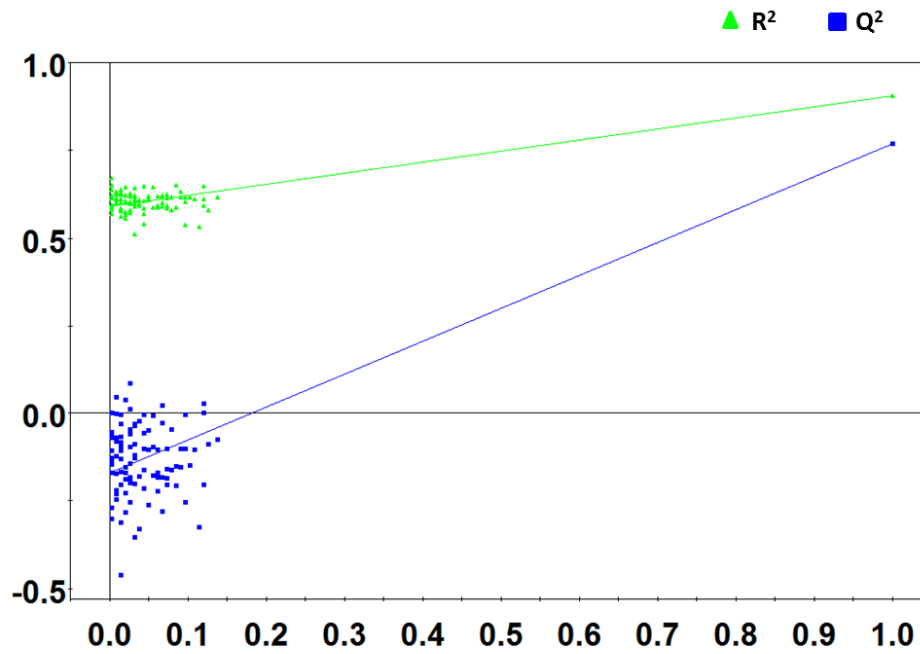
Appendix Figure A3.6. Heat maps showing the top 100 significant metabolites: (A) subject #17, (B) subject #18, (C) subject #19.

Appendix Figure A3.7. Permutations test for male vs. female (all collection areas). R2X = 0.590, R2Y = 0.905, Q2 = 0.770
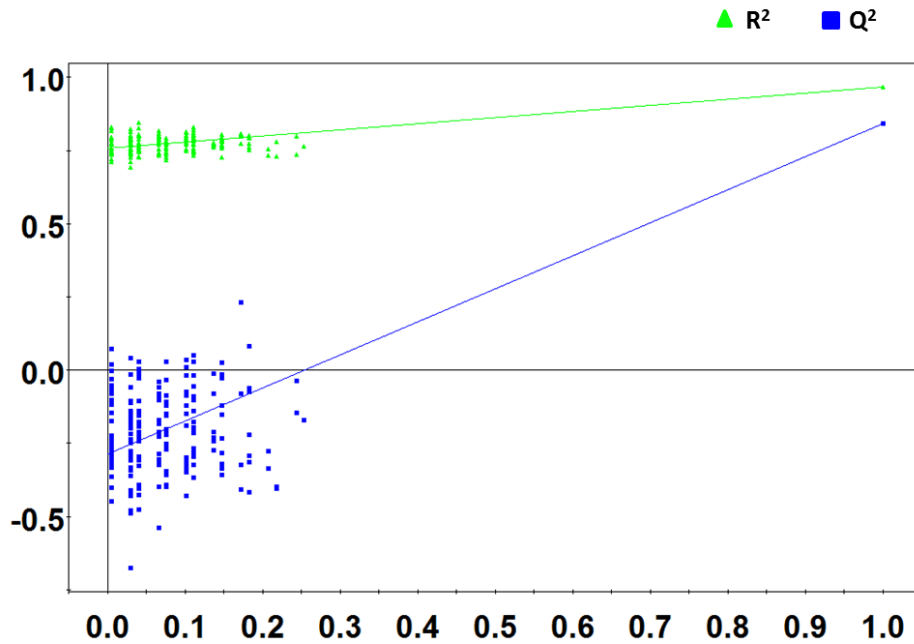
Appendix Figure A3.8. Permutations test for male vs. female (Lower Back). R2X = 0.582, R2Y = 0.965, Q2 = 0.844
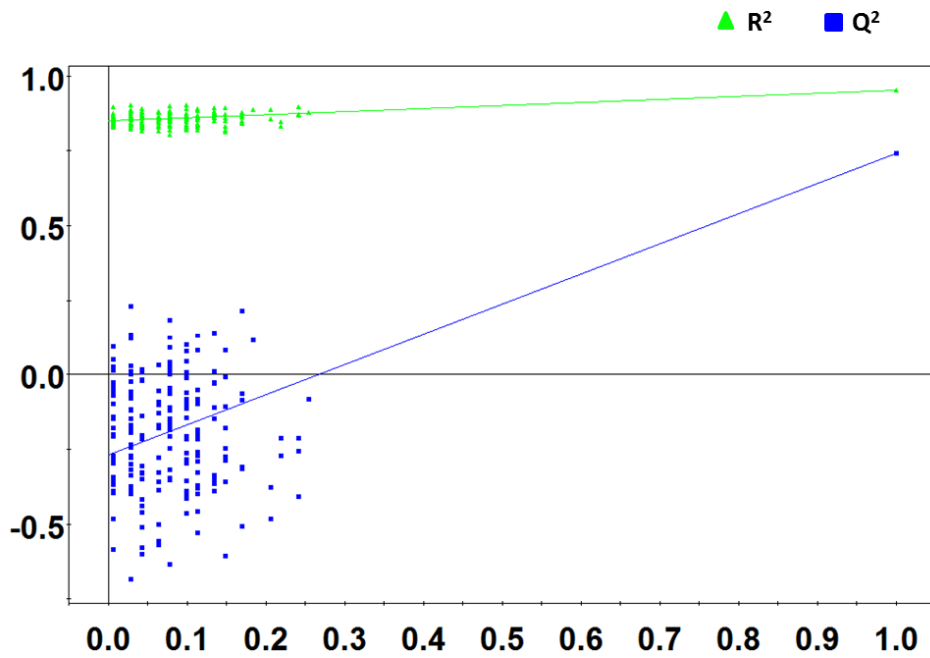
Appendix Figure A3.9. Permutations test for male vs. female (Neck). R2X = 0.626, R2Y = 0.951, Q2 = 0.740
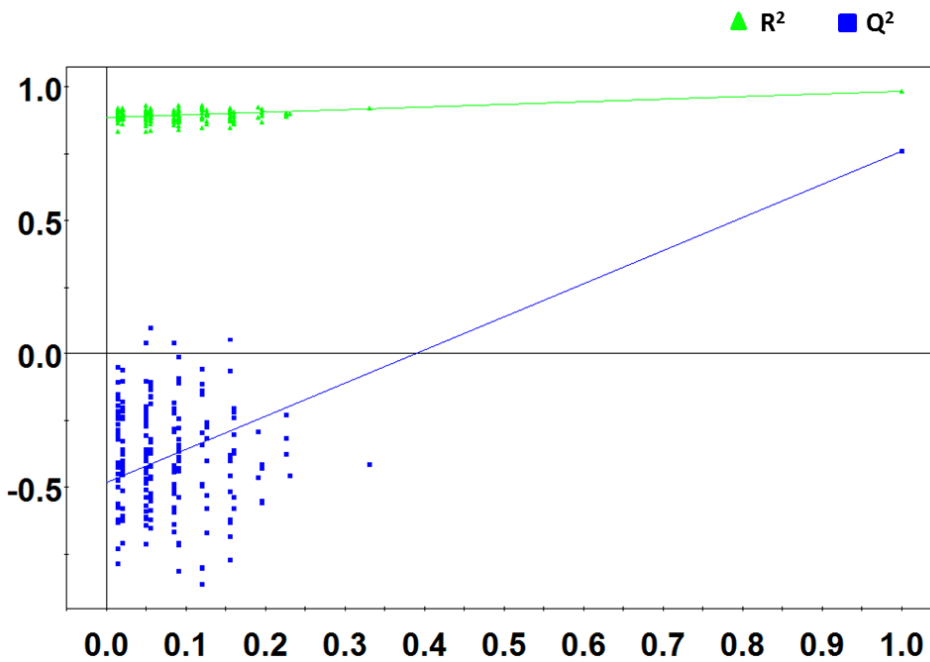
Appendix Figure A3.10. Permutations test for male vs. female (Left Forearm). R2X = 0.683, R2Y = 0.983, Q2 = 0.759
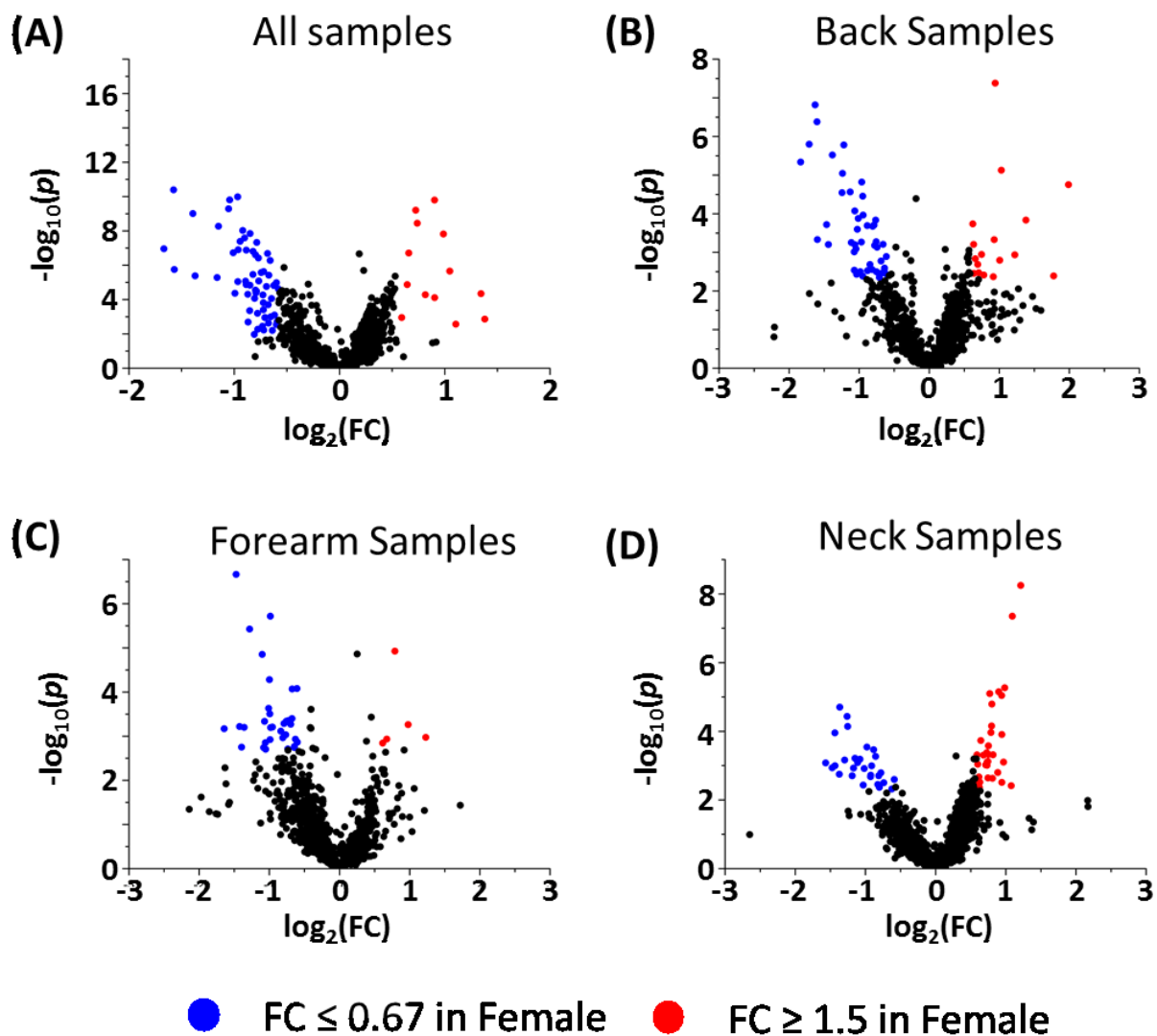
Appendix Figure A3.11. Volcano plots comparing sexes using (A) all samples, (B) lower back samples, (C) left forearm samples, and (D) neck samples. Metabolites meeting the criteria of 0.67 ≥ fold change ≥ 1.5 and q ≤ 0.05 are highlighted.

Chapter 4: Metabolic Profiling of Sweat Collected from Edema Affected and Healthy Areas of Lymphedema Patients Using A Non-Occlusive Sample Collection Kit and Chemical Isotope Labeling LC-MS

Appendix Table A4.1. List of positively identified metabolites in samples collected using the non-occlusive sweat patch kit using DnsID.

Compound Name	HMDB No.	Dansylated Mass (Da)	Monoisotopic mass (Da)	RT (min)
Taurine	HMDB00251	359.0730	125.0147	2.24
L-Arginine	HMDB00517	408.1700	174.1117	2.44
L-Asparagine	HMDB00168	366.1118	132.0535	3.00
L-Glutamine	HMDB00641	380.1275	146.0691	3.32
Citrulline	HMDB00904	409.1540	175.0957	3.74
Methionine Sulfoxide - Isomer	HMDB02005_2	399.1043	165.0460	4.20
L-Serine	HMDB00187	339.1009	105.0426	4.40
L-Glutamic Acid	HMDB00148	381.1115	147.0532	5.05
L-Aspartic Acid	HMDB00191	367.0958	133.0375	5.16
L-Threonine	HMDB00167	353.1166	119.0582	5.79
Ammonia	HMDB00051	251.0849	17.0266	5.82
Ethanolamine	HMDB00149	295.1111	61.0528	6.00
Glycine	HMDB00123	309.0903	75.0320	6.59
Glycylproline	HMDB00721	406.1431	172.0848	7.17
Beta-Alanine	HMDB00056	323.1060	89.0477	7.24
L-Alanine	HMDB00161	323.1060	89.0477	7.57
Gamma-Aminobutyric acid	HMDB00112	337.1216	103.0633	7.79
Uridine	HMDB00296	478.1279	244.0695	7.84
Uridine - H2O	HMDB00296_2	460.1173	244.0695	8.67

3-Aminoisobutanoic acid	HMDB03911	337.1216	103.0633	8.67
5-Aminopentanoic acid	HMDB03355	351.1373	117.0790	8.68
5-Hydroxymethyluracil	HMDB00469	376.0962	142.0378	8.87
Serinyl-Leucine	HMDB29043	452.1850	218.1267	8.90
2-Aminoisobutyric acid	HMDB01906	337.1216	103.0633	8.91
Xanthine	HMDB00292	386.0917	152.0334	8.95
L-Alpha-aminobutyric acid	HMDB00452	337.1216	103.0633	9.13
Glycyl-Valine	HMDB28854	408.1588	174.1004	9.19
Serinyl-Phenylalanine	HMDB29046	486.1693	252.1110	9.38
Phenylalanyl-Glycine	HMDB28995	456.1588	222.1004	9.43
L-Glutamic Acid - H2O	HMDB00148_2	363.1009	147.0532	9.46
Hypoxanthine - Isomer	HMDB00157_3	370.0968	136.0385	9.65
Methylamine	HMDB00164	265.1005	31.0422	9.82
Threoninyl-Leucine	HMDB29065	466.2006	232.1423	10.18
L-Proline	HMDB00162	349.1216	115.0633	10.18
Glycyl-Isoleucine	HMDB28844	422.1744	188.1161	10.78
L-Valine	HMDB00883	351.1373	117.0790	10.81
L-Methionine	HMDB00696	383.1094	149.0510	10.89
Imidazoleacetic acid	HMDB02024	360.1012	126.0429	11.12
Glycyl-L-Leucine	HMDB00759	422.1744	188.1161	11.22
Uracil	HMDB00300	346.0856	112.0273	11.34
Alanyl-Leucine	HMDB28691	436.1901	202.1317	11.36
L-Tryptophan	HMDB00929	438.1482	204.0899	11.44
Glycyl-Phenylalanine	HMDB28848	456.1588	222.1004	11.65
Alanyl-Phenylalanine	HMDB28694	470.1744	236.1161	12.11

L-Phenylalanine	HMDB00159	399.1373	165.0790	12.74
3-Hydroxymandelic acid	HMDB00750	402.1006	168.0423	12.94
Leucyl-Proline	HMDB28937	462.2057	228.1474	12.99
L-Isoleucine	HMDB00172	365.1529	131.0946	13.06
L-Alloisoleucine	HMDB00557	365.1529	131.0946	13.20
L-leucine	HMDB00687	365.1529	131.0946	13.36
Urocanic acid	HMDB00301	372.1012	138.0429	13.52
Phenylalanyl-Valine	HMDB29008	498.2057	264.1474	13.62
2-Hydroxyphenethlamine - Isomer	HMDB01065_2	371.1424	137.0841	13.77
L-Cystine	HMDB00192	354.0702	240.0238	14.11
Hydroxyphenyllactic acid	HMDB00755	416.1162	182.0579	14.39
5-Hydroxyindoleacetic acid	HMDB00763	425.1166	191.0582	15.09
Theophylline	HMDB01889	414.1230	180.0647	15.42
Ornithine	HMDB00214	300.1033	132.0899	16.58
Leucyl-phenylalanine	HMDB13243	512.2214	278.1630	16.59
Histidinyl-Alanine	HMDB28878	460.1649	226.1066	16.69
3-Hydroxyphenylacetic acid	HMDB00440	386.1057	152.0473	16.72
p-Hydroxyphenylacetic acid	HMDB00020	386.1057	152.0473	16.91
Vanillic acid	HMDB00484	402.1006	168.0423	17.34
L-Lysine	HMDB00182	307.1111	146.1055	17.47
4-Hydroxybenzoic acid	HMDB00500	372.0900	138.0317	17.57
Alanyl-Histidine	HMDB28689	460.1649	226.1066	17.62
L-Histidine	HMDB00177	389.1278	155.0695	18.09
Indole-3-carboxylic acid	HMDB03320	395.1060	161.0477	19.27

Pseudoephedrine	HMDB01943	399.1737	165.1154	19.38
Tyrosyl-Glycine	HMDB29105	353.1060	238.0954	20.19
Tyrosyl-Alanine	HMDB29098	360.1138	252.1110	20.86
Glycyl-Tyrosine	HMDB28853	353.1060	238.0954	21.63
3-Hydroxymandelic acid - COOH	HMDB00750_2	356.0951	168.0423	21.64
Alanyl-Tyrosine	HMDB28699	360.1138	252.1110	21.85
L-Tyrosine	HMDB00158	324.5953	181.0739	22.65
Tyrosyl-Valine	HMDB29118	374.1295	280.1423	22.83
Phenol	HMDB00228	328.1002	94.0419	23.16
4-Nitrophenol	HMDB01232	373.0853	139.0269	23.45
Tyrosyl-Leucine	HMDB29109	381.1373	294.1580	23.77
Phenylalanyl-Tyrosine	HMDB29007	398.1295	328.1423	24.22
4-Ethylphenol	HMDB29306	356.1315	122.0732	25.63
Pyrocatechol	HMDB00957	289.0767	110.0368	26.70
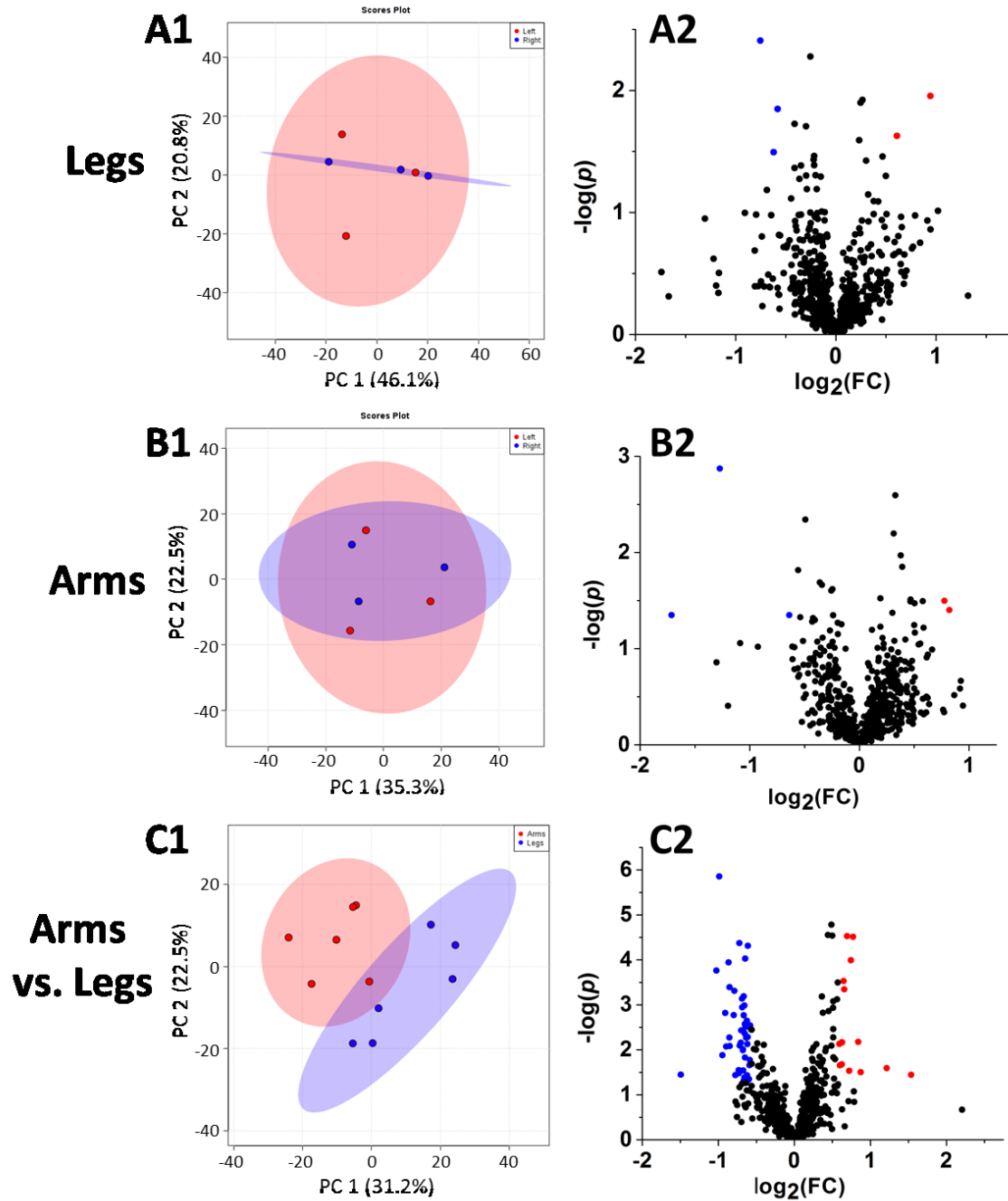
Appendix Figure A4.1. PCA score plots comparing left vs. right legs (A1), left vs. right arms (B1), and arms vs. legs (C1). Volcano plots comparing left vs. right legs (A2), left vs. right arms (B2), and arms vs. legs (C2). Both sets of analyses show large sweat metabolome changes between arms and legs, and miniscule changes between left and right limbs. Cut-offs set to FC less than 0.67 or greater than 1.5, and $p \leq 0.05$.
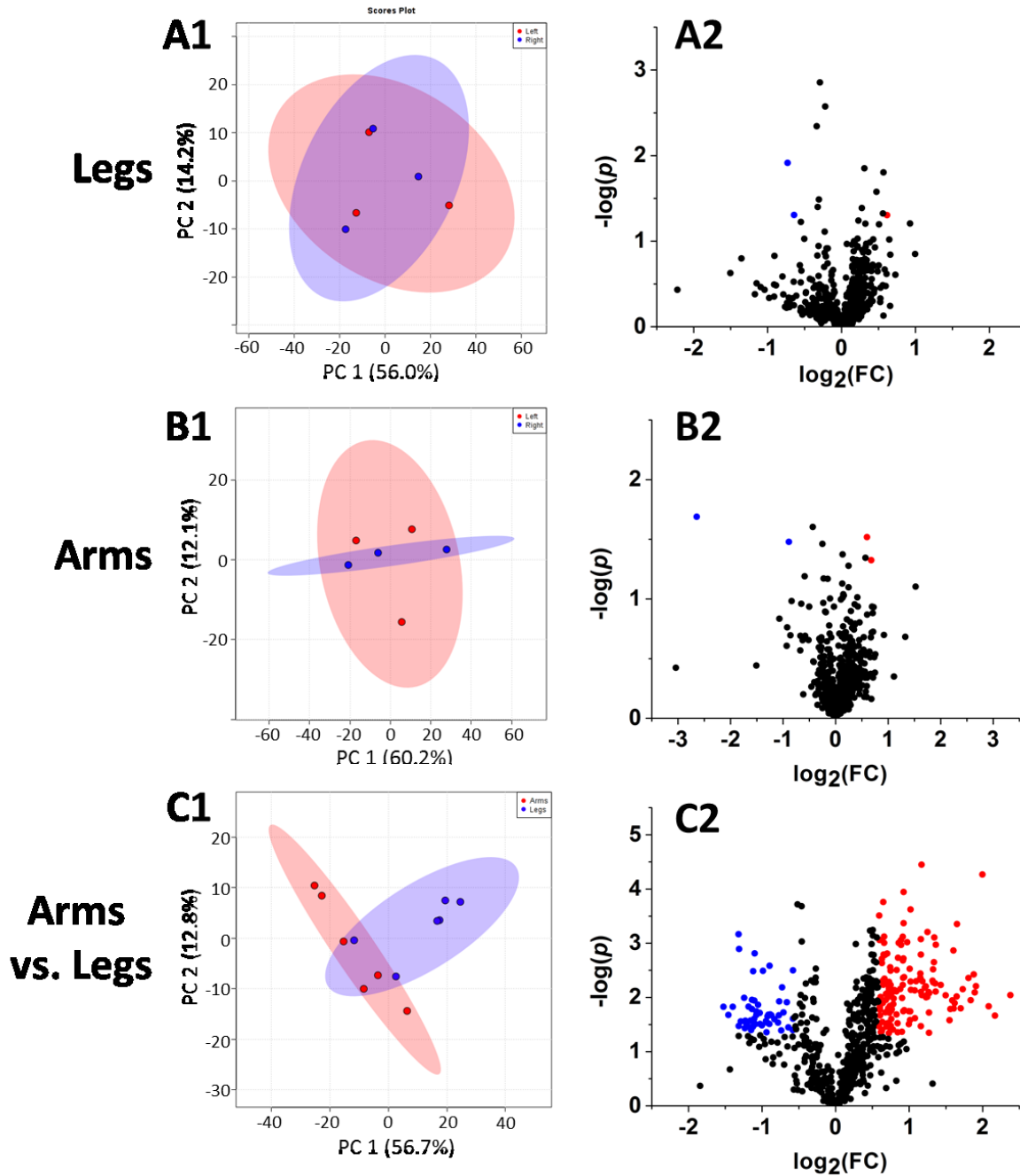
Appendix Figure A4.2. PCA score plots comparing left vs. right legs (A1), left vs. right arms (B1), and arms vs. legs (C1). Volcano plots comparing left vs. right legs (A2), left vs. right arms (B2), and arms vs. legs (C2). Both sets of analyses show large sweat metabolome changes between arms and legs, and miniscule changes between left and right limbs. Cut-offs set to FC less than 0.67 or greater than 1.5, and p ≤ 0.05.
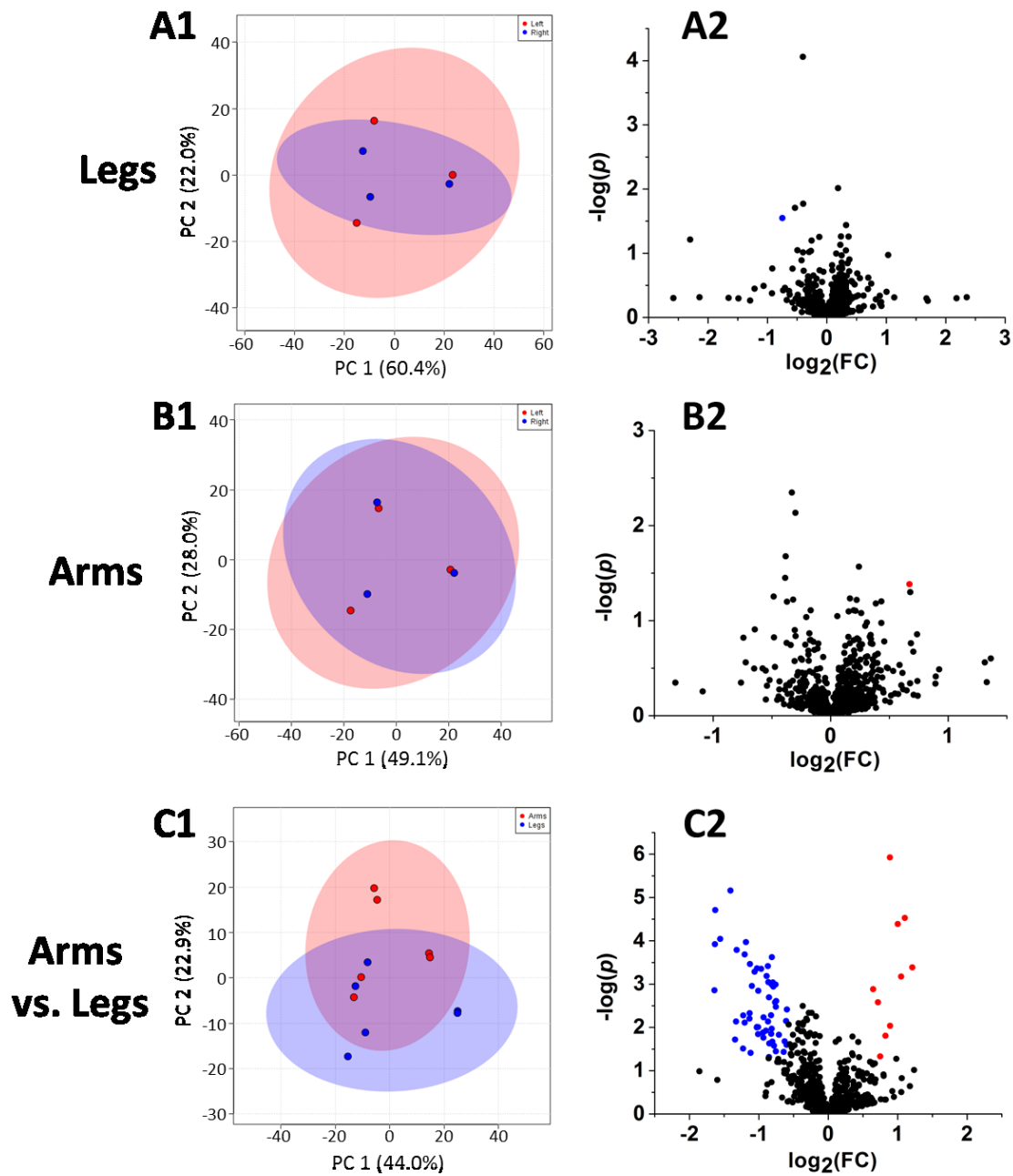
Appendix Figure A4.3. PCA score plots comparing left vs. right legs (A1), left vs. right arms (B1), and arms vs. legs (C1). Volcano plots comparing left vs. right legs (A2), left vs. right arms (B2), and arms vs. legs (C2). Both sets of analyses show large sweat metabolome changes between arms and legs, and miniscule changes between left and right limbs. Cut-offs set to FC less than 0.67 or greater than 1.5, and $p \leq 0.05$.

Appendix Table A4.2. DnsID library search results of metabolites with significantly differing levels between diseased and healthy areas in a patient with unilateral foot edema.

Compound Name	Dansylated Mass + H (Da)	Monoisotopic Mass (Da)	Average Ratio (Healthy)	Average Ratio (Diseased)	FC (D/H)	*p*-value
Glutamine	380.1275	146.0691	0.22	0.34	1.58	1.58E-02
Glycylproline	406.1431	172.0848	0.57	1.35	2.38	9.50E-04
Uridine - H2O	460.1173	244.0695	0.49	0.82	1.69	4.91E-02
Alanyl-Leucine	436.1901	202.1317	0.76	1.27	1.68	1.40E-03
Phenol	328.1002	94.0419	0.42	0.75	1.79	1.77E-02
4-Ethylphenol	356.1315	122.0732	0.24	0.55	2.29	9.24E-03